February 17, 2016

This is in response to your letter to the Naval Research Laboratory (NRL) dated
January 27, 2016 citing the Freedom of Information Act (FOIA), and requesting
copies of the following NRL reports:
1. Chubb, T. A. and Chubb, S. R.; Fusion Reactions in Deuteraded Palladium. The Why of Cold
Fusion Heat. 1996
2. Chambers, G. P., Hubler, G. K., Kucherov, Y.; Glow Discharge in Deuterium. 1995
3. Dominguez, D. D., Hagans, P. L., Imamm M. A.; A Summary of NRL Research on
Anomalous Effects in Deuterated Palladium Electrochemical Systems. 1996

We have conducted a database search using the criteria you provided at the NRL Technical
Library; we were unable to locate any responsive documents matching #1 and #2. Document #3
is provided as a .pdf document. Fees related to this request have been waived.

If you believe an adequate search for responsive records was not accomplished, you may file an
appeal in writing to: Department of the Navy, Office of the General Counsel, 1000 Navy
Pentagon, Washington, DC 20350-1000.

The appeal must be postmarked within 60 days from the date of this letter to be considered.
Your appeal should contain a copy of this letter along with a statement explaining why you
believe an adequate search had not been conducted. It is recommended that the letter of appeal
and the envelope both bear the notation "Freedom of Information Act Appeal."

Should you have any questions regarding the foregoing, please contact me at 202-767-2541.

Sincerely,

RICHARD L. THOMPSON
Freedom of Information Act Officer
By direction of the Commanding Officer

Enclosure

Naval Research Laboratory

Washington, DC 20375-5320

NRL/MR/6170--96-7803

A Summary of NRL Research on Anomalous Effects in Deuterated Palladium Electrochemical Systems

DAWN D. DOMINGUEZ
PATRICK L. HAGANS

Surface Chemistry Branch
Chemistry Division

M. ASHRAF IMAM

Physical Metallurgy Branch
Materials Science and Technology Division

January 9, 1996

DISTRIBUTION STATEMENT ___A___ APPLIES.
Further distribution authorized by_____
___UNLIMITED_____only.

PER Codes 6170 + 6350
Russell Imam
RS. 5596.3/280 9/14/09

New Energy Times

REPORT DOCUMENTATION PAGE		Form Approved OMB No. 0704-0188

Public reporting burden for this collection of information is estimated to average 1 hour per response, including the time for reviewing instructions, searching existing data sources, gathering and maintaining the data needed, and completing and reviewing the collection of information. Send comments regarding this burden estimate or any other aspect of this collection of information, including suggestions for reducing this burden, to Washington Headquarters Services, Directorate for Information Operations and Reports, 1215 Jefferson Davis Highway, Suite 1204, Arlington, VA 22202-4302, and to the Office of Management and Budget, Paperwork Reduction Project (0704-0188), Washington, DC 20503.

1. AGENCY USE ONLY (Leave Blank)	2. REPORT DATE January 9, 1996	3. REPORT TYPE AND DATES COVERED 01/92-06/95	
4. TITLE AND SUBTITLE A summary of NRL Research on Anomalous Effects in Deuterated Palladium Electrochemical Systems			5. FUNDING NUMBERS PE - 61153N
6. AUTHOR(S) Dawn D. Dominguez, Patrick L. Hagans, and M. Ashraf Imam			
7. PERFORMING ORGANIZATION NAME(S) AND ADDRESS(ES) Naval Research Laboratory Washington, DC 20375-5320			8. PERFORMING ORGANIZATION REPORT NUMBER NRL/MR/6170–96-7803
9. SPONSORING/MONITORING AGENCY NAME(S) AND ADDRESS(ES) Office of Naval Research 800 North Quincy Street Arlington, VA 22217-5660	DISTRIBUTION STATEMENT _A_ APPLIES. Further distribution authorized by _UNLIMITED_ only.		10. SPONSORING/MONITORING AGENCY REPORT NUMBER
11. SUPPLEMENTARY NOTES			
12a. DISTRIBUTION/AVAILABILITY STATEMENT Approved for Public Release Distribution Unlimited			12b. DISTRIBUTION CODE

13. ABSTRACT (Maximum 200 words)

Claims of excess power produced in electrochemical cells have been made by many investigators including those from two Navy laboratories. The excess power reportedly occurs in palladium electrodes highly loaded with deuterium. Other anomalous effects such helium—4, tritium and low energy radiation production have also been reported. This report summarizes the experimental results from a number of electrochemical loading/calorimetric experiments on palladium electrodes run at NRL. The experiments were carried out with the purpose of replicating the published excess power results obtained at the other Navy laboratories and with the goal of identifying the experimental conditions necessary to produce anomalous effects. Most of the experiments described were attempts to electrolytically load pure palladium or palladium alloy cathodes with deuterium (or hydrogen) and then to measure the power produced in the electrolytic cells. Loading was monitored in situ by measuring the change in the axial resistance of the cathode and comparing the measure values with the known relationship between resistance and the D(H)/Pd atomic ratios. While attaining high levels of deuterium loading in palladium cathodes was difficult we found that using materials with a large grain microstructure facilitated the loading. Calorimetric measurements on the highly loaded cathodes were initially made in isoperibol calorimeters that had a sensitivity of $\pm 10\%$. No excess power (≥ 200 mW) and no radiation above the background were measured in any of the experiments described. Highly sensitive heat conduction calorimeters were evaluated for their use with the electrochemical cells. Results showed that measurements at the ± 10 mW level were possible in the heat conduction calorimeters when data were collected frequently and signal averaging was used. Another experiment that was investigated was the electrochemical codeposition of palladium and deuterium on cathodes. Again, no radiation above background levels was detected in these experiments.

14. SUBJECT TERMS Anomalous effects Deuterated palladium			15. NUMBER OF PAGES 141
			16. PRICE CODE
17. SECURITY CLASSIFICATION OF REPORT UNCLASSIFIED	18. SECURITY CLASSIFICATION OF THIS PAGE UNCLASSIFIED	19. SECURITY CLASSIFICATION OF ABSTRACT UNCLASSIFIED	20. LIMITATION OF ABSTRACT SAR

CONTENTS

FIGURES

Fig. 45 - XPS survey spectra obtained at various total sputter times from a metallic gray area of a palladium/0.18 wt.% boron rod (#94081801) cathode which produced excess heat at NAWC

Fig. 46 - As in Figure 45 but taken from a black colored area of the electrode

Fig. 47 - Fig. 47 - Changes in the excess power calculated for a reference cell as a function of input power. Top curve: using a calibration constant of 9.5 watts/volt from 0-9 watts input power. Bottom curve: using 9.5 watts/volt for input powers from 0-50 mW and 9.3 watts/volt for input powers from 50 mW - 9 watts

EXECUTIVE SUMMARY

INTRODUCTION

Anomalous effects, which include excess power, the production of helium-4, tritium and low energy radiation, have been reported in deuterated palladium systems. Some of these reports originated at Navy laboratories. The ONR-sponsored Navy Program to investigate Anomalous Effects in Deuterated Systems was conceived to corroborate the experimental results from the Navy laboratories. The Naval Research Laboratory (NRL) participation in the Program had four main objectives. They were to (1) replicate experimental procedures provided by NAWC and NRaD to verify the results, (2) develop and employ the diagnostic capabilities available at the Laboratory to measure radiation, tritium and helium, (3) ascertain what, if any, correlations existed between the reaction products identified and the experimental variables, and (4) produce and supply well characterized palladium cathode materials with known, controlled processing history.

These objectives have been accomplished and the results of the NRL effort is described in this report. The report summarizes the experimental results from a large number of carefully controlled electrochemical loading/calorimetric experiments on palladium and palladium alloy electrodes carried out at NRL. In some experiments palladium and deuterium were codeposited on cathodes. In others, deuterium was electrolytically loaded into palladium cathodes while loading was determined *in situ*. Radiation measurements were made during both types of electrochemical experiments. Calorimetric measurements were made during the latter.

CONCLUSIONS

The following conclusions are the result of the careful and well-controlled experiments carried out by the authors:

(1) Loading palladium cathodes into the β-phase with deuterium is facilitated by using material with a large grain microstructure;

(2) Most palladium cathodes with elongated or small grains didn't load deuterium into the β-phase;

(3) Hardly any grain growth occurred on annealing high purity (99.99% or better) palladium cathodes at 1100°C for 20 hours whereas lower purity (99.9%) materials readily grew large grains;

(4) Transmission electron microscopy and x-ray diffraction studies identified two distinct phases in the palladium/0.62 weight percent boron alloy; the lattice parameters for the different phases were measured;

(5) Prolonged electrolysis at high current density in basic solution resulted in the formation of a relatively thick layer on the cathode (> 1000Å) composed of a varied elemental composition with very little or no Pd identifiable on the surface. Twenty different elements have been identified from XPS analysis of over 30 different electrode surfaces. Cationic, anionic and organic species in the electrolyte have been detected as part of these surface overlayers. The anodes remained relatively film-free;

(6) Longer electrolysis times ($\sim$ 1000 hrs.) produced thicker films on NRL Pd cathodes compared to shorter times (< 500 hrs.). In addition, the thicker films contained larger quantities of both Cu and Pt

relative to Pd and in general higher loadings were obtained with these films present. This suggests that thicker films may help block the egress of D from the Pd lattice;

(7) Thinner films where Pd was present at or near the surface were found on excess heat producing electrodes obtained from SRI and NAWC (exceptions are where large quantities of certain species were added to the electrolyte to help or initiate excess heat formation). Very little copper was found in these films but appreciable amounts of Pt were present. Thin films without Cu may be necessary for excess power measurement;

(8) The source of some elements found in the cathode overlayer may be bulk diffusion of impurities such as Pt and Cu caused by the severe lattice distortion produced by absorption of large quantities of D or H;

(9) High sensitivity heat-conduction calorimeters are capable of accurately measuring ± 10 mW of excess power in electrochemical cells at high input power provided that calibration constants are known to at least one part in 10^3, and that cell voltage and sensor voltage measurements are made frequently and treated with appropriate statistics;

(10) No excess power > 200 mW was measured in any electrolytic cells containing NRL palladium and palladium/10% silver cathodes in NRL isoperibol calorimeters;

(11) No anomalous radiation was detected with either germanium or sodium iodide gamma-ray detectors during any electrochemical experiments with deuterium or hydrogen-loaded palladium or palladium/10% silver cathodes;

(12) The palladium/deuterium codeposition experiment is inherently irreproducible;

(13) No anomalous radiation was detected during the palladium/deuterium codeposition experiment with either a germanium gamma-ray detector or an x-ray detector.

A SUMMARY OF NRL RESEARCH ON ANOMALOUS EFFECTS IN DEUTERATED PALLADIUM ELECTROCHEMICAL SYSTEMS

INTRODUCTION

This report has been prepared to summarize information from a large quantity of unpublished data derived from experiments carried out at The Naval Research Laboratory (NRL) concerning the "Cold Fusion" phenomenon. The work at NRL was done between 1 January 1992 and 30 June 1995 as part of the Office of Naval Research (ONR)-sponsored Navy Program to understand anomalous effects in electrochemically loaded materials. Other participants in the Navy Program included NAWC (Naval Air Warfare Center Weapons Division, NAWC, CA) and NCCOSC-NRaD (Naval Command, Control and Ocean Surveillance Center - Naval Research and Development, San Diego, CA); these laboratories already had work ongoing in the area when the Navy Program began in 1992. Miles et al. [1] at NAWC had reported calorimetric evidence for excess power from the conventional Pons and Fleischmann-type electrochemical experiment. They also reported [2,3] a correlation between the generation of excess power and the production of helium-4, as well as some evidence for low energy radiation (dental film exposure). Szpak et al. [4,5] at NRaD had published an experimental approach in which palladium was electrodeposited in the presence of evolving deuterium (a codeposition experiment). Evidence for radiation (photographic film exposure), tritium production and temperature increases were reported from their experiments.

The goal of the Navy Program was for the three Navy laboratories to collaborate in reproducing the reported effects. More specifically, NAWC and NRaD were to establish reliable procedures for producing anomalous effects and then attempt to enhance the effects. NRL's objective was to (1) replicate experimental procedures provided by NAWC and NRaD to verify the results, (2) develop and employ the diagnostic capabilities available at the Laboratory to measure radiation, tritium and helium, (3) ascertain what, if any, correlations existed between the reaction products identified and the experimental variables, and (4) produce and supply well characterized palladium cathode materials with known, controlled processing history.

Dr. Dawn Dominguez (Code 6170 - Solid-Liquid Interface Section, Surface Chemistry Branch) was identified as the principle investigator of the Program at NRL. She was the person responsible for carrying out the electrochemical experiments that would, hopefully, reproduce the results obtained at NAWC and NRaD. Other Chemistry Division (Code 6100) personnel associated with the Program included Drs. Patrick Hagans (starting in May 1993), Debra Rolison, William O'Grady, David Venezky and James Murday.

NRL had several means for measuring radiation during these experiments. These included a liquid nitrogen-cooled germanium gamma-ray detector and a sodium iodide gamma-ray detector that were capable of radiation spectroscopy within the range of 50 keV-14 MeV. Geiger-Mueller α-β-γ detectors of the type used by Dr. Melvin Miles (NAWC) as safety monitors were also available. An x-ray detector for the 4-80 keV range was also used. The germanium, sodium iodide and x-ray detectors used at NRL

were at least as sensitive as the GM detector and photographic/dental films used at NAWC and NRaD. The main advantage of the NRL detectors was their energy resolution capability that allowed identification of any radiation detected. NRL personnel associated with the radiation measurements included Drs. Steven King, Gary Phillips and David Nagel from Code 6600.

Scintillation counters for tritium measurements were also available at NRL. One counter was located in Health Physics (Code 1244) and the second was located in The Biomolecular Engineering Division (Code 6900). Because NRL decided to postpone tritium measurements until excess power had been measured, neither of these instruments was used in the Navy Program.

Helium measurements were to be made at NRL by Dr. Jeff Wyatt (Code 6110) *after* excess power was obtained in the Pons and Fleischmann-type electrochemical experiment. The measurements were to have been made on a mass spectrometer that could easily distinguish between deuterium and helium-4 in the gas phase. The instrument could also separate helium-3 and helium-4 isotopes and could have potentially been used to look for evidence of enhanced isotopic ratios of other elements. Neither helium nor other isotope measurements were made since *no excess power was measured at The Naval Research Laboratory.*

Processing and characterization of cathode materials was carried out by Dr. M.A. Imam of the Materials Science Division (Code 6323) at NRL. Processing included choosing an appropriate starting material and then arc melting, swaging, machining and annealing the material to produce a cathode material with homogeneous composition, controlled microstructure and minimal defects. Johnson Matthey palladium sponge (supposedly 99.999% purity) was selected as the starting material for cathode preparation. Arc melting was carried out in a water-cooled copper hearth. Extreme care was taken throughout the processing to minimize contamination of the cathode material with impurities. Dry machining was used to avoid contacting the cathode material with oil or water. Annealing was done in a vacuum of 10^{-5} torr or better. All annealed samples were cooled slowly in a furnace to room temperature. Characterization of the bulk palladium before and after processing was done by Glow-Discharge Mass Spectroscopic (GDMS) Analyses (Shiva Technologies, Inc., Syracuse, NY). The GDMS results will be shown later in the report. X-ray photoelectron (XPS) spectroscopy was also used to examine the surface and near-surface before electrolysis. Other characterization methods used on the processed material included optical microscopy, x-ray diffraction, transmission electron microscopy and microhardness measurements. GDMS and XPS analyses were also used to characterized several cathodes at the completion of the electrolysis experiments.

ONR played a lead role throughout the duration of the Anomalous Effects Program. Specifically, Dr. Robert Nowak was the ONR Scientific Officer in charge of coordinating the Program; he actively guided discussions that determined the roles of the individual laboratories in the Program. In addition, scientific results were informally presented to Dr. Nowak in a series of frequent meetings at NRL and he participated in group discussions that influenced the course of NRL's research. Scientific results were formally presented to managements of ONR (Dr. Frederick Saalfeld) and NRL (Drs. Timothy Coffey and Bhakta Rath) approximately every six months. NRL and NAWC also provided a series of written reports on a regular basis to ONR that summarized the status of the Program.

Support for the Anomalous Effects Program was provided by The Office of Naval Research. The Naval Research Laboratory (NRL), Washington, DC provided additional support for all three authors.

PALLADIUM/DEUTERIUM CODEPOSITION EXPERIMENT

In March 1989 Fleischmann and Pons announced/reported [6] that electrochemically induced nuclear fusion of deuterium compressed into palladium cathodes produced excess enthalpy as well as neutrons and tritium. Following the announcement, many attempts were made to reproduce the experiments that generated the anomalous effects; the results have been conflicting. At least part of the difficulty in reproducing the experiments was that many variables are encountered in the palladium-deuterium system, and their relative importance and interdependence are not known. This was exacerbated by the long charging times (i.e., weeks) required to load the cathodes with deuterium to the β-phase (D/Pd > 0.7) and long times (i.e., months) required to produce excess heat.

An alternate experimental approach for producing deuterium-loaded palladium was reported by Szpak et al. [4,5]. In this approach, palladium from a D_2O electrolyte was deposited on a copper cathode in the presence of evolving deuterium. A significant advantage of the Pd/D codeposition experiment over the more conventional loading experiment was that the codeposition experiment was much quicker to carry out (i.e., hours for the deposition and days to produce anomalous effects). Anomalous effects, which included excess enthalpy, and the production of tritium and some form of radiation, were initially reported using this approach at NRaD. Subsequently, NAWC reported [7] the production of radiation in similar experiments and data published by Hodko and Bockris [8] seemed to support the tritium results.

This section of the report describes the efforts made at the NRL to reproduce the Pd/D codeposition experiments carried out at NRaD and at NAWC, and to corroborate their results. Measurement of excess enthalpy is controversial in the Pd/D codeposition experiment because catalytic recombination of the evolved gases (D_2 and O_2) occurs readily and is exothermic. Tritium measurements are controversial because the separation factor is not accurately known. (The separation of tritium and deuterium on palladium during electrolysis results in tritium enrichment in the electrolyte by a factor within the range of 1.7-2.2) [8]. As a result, NRL focussed on reproducing the reported anomalous radiation, and detecting and analyzing the radiation generated using germanium gamma-ray and beryllium x-ray radiation detectors.

Electrochemical Cell/Calorimeter Design

All experiments described in this report were carried out in open electrochemical cells with no recombination catalyst. The electrolytic cell used at NRL for the codeposition experiment was essentially identical to the cell used at NAWC. It was constructed from a borosilicate-glass test tube (I.D. = 1.6 cm, L = 15 cm) and a rubber stopper that was wrapped with Teflon tape. Pons and Fleischmann recommended [9,10] that long, thin cells be used for good thermal mixing from the gas evolution. Two symmetrical coil anodes were used. One was made from 0.1 cm diameter platinum wire (99.9% purity) and the second was made from 0.1 cm diameter platinum-20% rhodium thermocouple wire from NAWC. The anodes had eight windings in a length of 2-2.5 cm and the diameter of the windings was about 1.5 cm. Most of the cathodes (d = 0.635 cm, L = 1.2-1.5 cm) were center-bored and soldered to a stainless steel rod (d = 0.16 cm). The solder joint was covered with epoxy and Teflon tape. In a few NRL experiments, the cathode was a 0.2 cm diameter, 15 cm long silver rod. Cathode and anode leads extended through the rubber stopper. The leads were isolated with heat shrinkable Teflon tubing inside the cell. A Teflon cruciform was used to center the cathode inside the test tube. The rubber stopper was fitted with a Y-shaped glass tube with one end covered by a rubber septum for injection of the appropriate solutions and the other end attached to a silicone oil bubbler via Teflon tubing. (A thick-walled rubber vacuum tubing was used at NAWC.) The stopper was sealed to the cell with silicone rubber.

Isoperibol calorimeters of the type used at NAWC were initially constructed for the NRL codeposition experiments. A drawing of a typical electrolytic cell/calorimeter setup is shown in Figure 1. The calorimeters have been described in the literature [1,11]. Briefly, the calorimeters were made from a 16 oz polyethylene bottle (O.D.=7.0 cm) in which a large borosilicate-glass tube (I.D.=3.1 cm) was centered. The area between the glass tube and the polyethylene bottle was packed with vermiculite and Styrofoam insulation. The top of the calorimeter assembly was sealed with parafilm and silicone rubber. The electrochemical cell was centered within the large glass tube of the calorimeter and the area between the cell and the calorimeter was filled with water that served as a heat-transfer medium. Two thermistor thermometers (YSI Incorp., Model 731) calibrated to within $\pm 0.01\,°C$ (with $\pm 0.15\,°C$ accuracy and a 9 second time constant) were inserted into thin-walled glass tubes (d=0.4 cm) and these were placed in the water gap between the cell and the calorimeter. The thermistors were positioned about 2 cm and 4 cm from the bottom of the cell. The calorimeter/electrolytic cell assembly was suspended in a circulating constant temperature bath (Techne, Model B-26 bath, Model TE-8A circulator) set at $27.00 \pm 0.01\,°C$. A 100 Ω platinum RTD (resistance temperature device) was used to monitor the water bath temperature.

The calorimeters and constant temperature bath were never used in the NRL codeposition experiments because NAWC reported that catalytic recombination of deuterium or hydrogen and oxygen occurred frequently in the experiments and heat released from this reaction complicated the calorimetry. In addition, control radiation measurements showed that the cell, calorimeter and bath effectively stopped x-rays with energies of less than 50 keV and, that gamma-ray transmission in the 270-1330 keV range was severely attenuated. As such, the calorimetric work was de-emphasized during the codeposition experiments in favor of the radiation measurements.

Preparation of Cell Components/Solutions/Electrodes

At NRL, glass and Teflon cell components were first cleaned with a soap and water wash. After rinsing and drying, the components were placed in an acid bath (HNO_3/H_2SO_4), rinsed with triply distilled water and oven dried before using. NAWC followed the soap and water wash and distilled water rinse with an acetone rinse before drying the glassware in a vacuum oven. NRL chose to eliminate the acetone rinse to avoid introducing organics into the electrolytic cell.

Solutions of 0.3 M LiCl in D_2O and 0.050 M $PdCl_2$ in 0.3 M LiCl/D_2O (0.050 M Li_2PdCl_4) were needed for the codeposition experiment. Deuterium oxide (99.9% D, chemical purity 98+%) was purchased from Cambridge Isotope Laboratory (DLM-4, lot BG-1242) in 100 g bottles. On receipt, the unopened bottles of D_2O were stored in a glove box under a nitrogen atmosphere. Lithium chloride used was obtained from three sources - (1) Aldrich anhydrous 99% #21,323-3, lot 2808BL, (2) Johnson Matthey 976216, lot S96256R (this was determined to be a hydrated form of lithium chloride), and (3) Johnson Matthey ultra dry 99.999% #13584, lot F05316. Palladium chloride was purchased from (1) Johnson Matthey 99.9% #11034, lot F11A33 and (2) Alfa Products 60.0% Pd #58109, lot 042583. Both lithium chloride and palladium chloride were stored in the glove box. When needed, the as-received LiCl and $PdCl_2$ salts were weighed out and dissolved in D_2O or 0.3 M LiCl/D_2O, respectively, in the glove box. The latter resulted in a 0.050 M Li_2PdCl_4 stock solution that was stored in the glove box along with the 0.3M LiCl solution. The Li_2PdCl_4 stock solution was made up in a septum-sealed vial so that it could be removed from the glove box to make additions to the cell while it was running.

No attempt was made by the Navy laboratories to use reagents from the same source or with identical lot numbers in the codeposition experiments. However, in several instances, Dr. Ben Bush (NAWC) prepared the solutions needed for the codeposition experiment at NAWC using their procedures
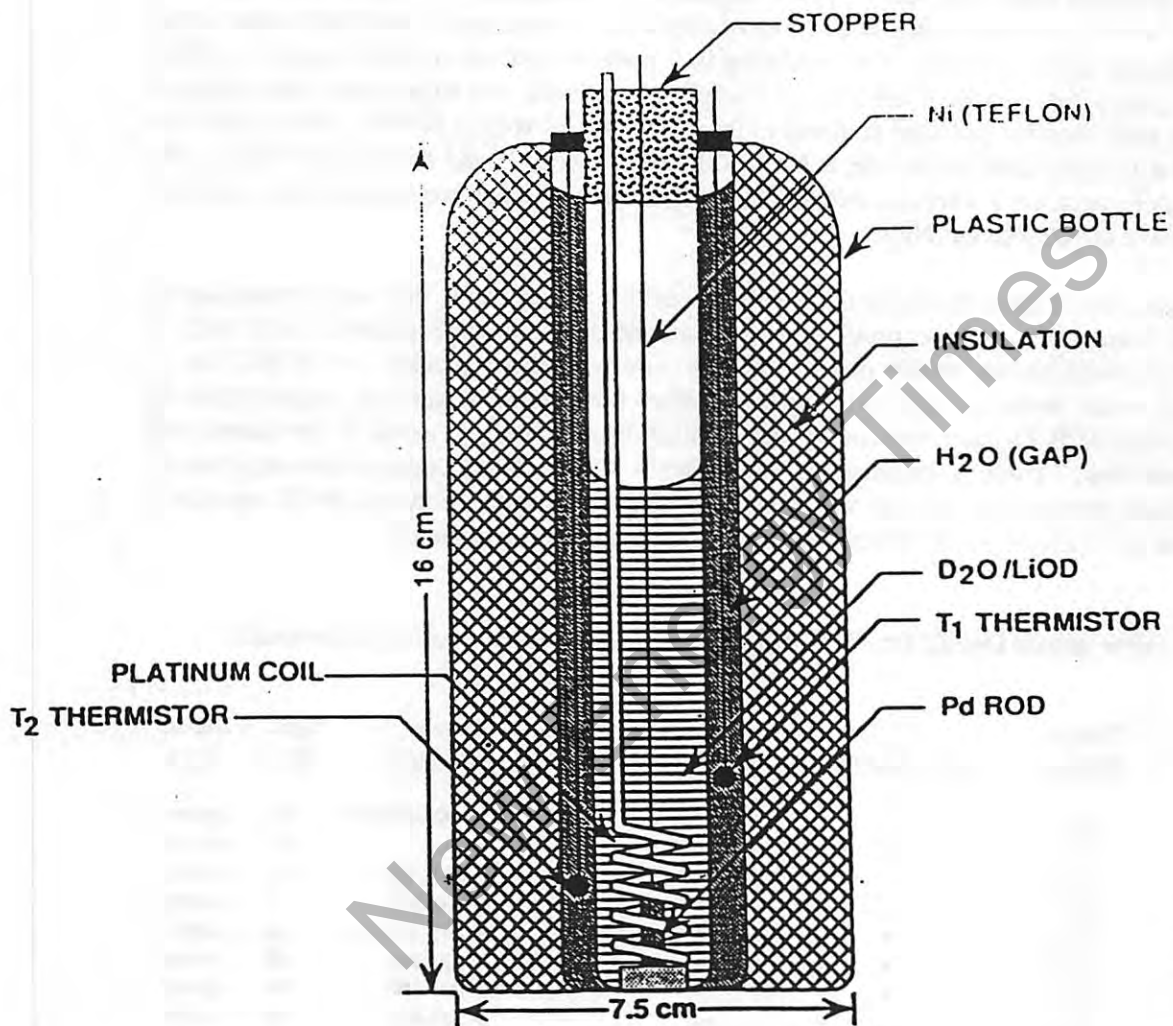
Fig. 1 - Electrochemical calorimetric cell design (from reference 1)

and shipped them to NRL in sealed ampoules. Cells that had solutions made at NAWC are indicated in Table 1. At NAWC, no glove box was used to store reagents, or to mix or store their solutions. However, their LiCl was dried before use by dissolving the salt in D_2O and evaporating the D_2O on the Schlenk line. This process was repeated several times to get rid of any absorbed H_2O. NRaD stored and weighed their reagents in a glove box with an argon atmosphere but, they made their solutions on the benchtop and used them immediately.

Nineteen different cells were run in NRL codeposition experiments. Of these, 17 took place in heavy water (see Table 1) and two in light water. The two light water experiments and the first two heavy water experiments had silver cathodes. The remaining heavy water experiments had copper or silver-plated copper or gold-plated copper (Cu/Ni/Ag or Cu/Ni/Au) cathodes. All except the silver cathodes were machined to have rounded ends and soldered to the stainless steel rods at NAWC. The solder joint was also covered with epoxy and Teflon tape at NAWC. In experiments #3 and #5-10 (see Table 1), two nearly identical calorimetric cells were connected electrically in series. Cells were run under galvanostatic control, as they were at NAWC and NRaD.

Before using any of the cathodes in the NRL codeposition experiments, they were treated in one of several ways. Sometimes, new or previously-used cathode surfaces were polished (600 grit) or roughened (180 grit) with silicon carbide paper. Some of these were then "pickled" in 1M HCl for 30 minutes to remove oxide, boiled in H_2O and wiped dry. Other times, cathode surfaces were cleaned via a chemical etch (NH_4OH/H_2O_2) and then rinsed with distilled water and wiped dried. A few times, both pretreatments were used. Table 1 summarizes some details of the NRL codeposition experiments including the cathode preparation. Anodes were generally cleaned by immersion in a 50-50 mixture of concentrated nitric and sulfuric acids, rinsed with triply distilled water and dried.

Table 1 - Experimental Details for NRL Palladium/Deuterium Codeposition Experiments

Exp't No.	Solution Source	Cathode Material	SiC	HCl	Etch	Cathodic Protection	DCl Addition	Current Steps(mA)	Time (Hrs.)	Deposit Type
1	NRL	Ag	–	–	•	•	–	6-100-300-500	40	mossy
2	NRL	Ag	–	–	•	•	–	6-500	46	mossy
3A	NAWC	Cu-A	•	–	•	•	–	6-100-300	20	mossy
3B	NRL	Ag	•	–	•	•	–	6-100-300	20	mossy
4	NAWC	Cu-A	•	•	–	•	–	6-100-300-500	39	metallic
5A	NAWC	Cu-A	•	•	–	–	•	6-100-300	69	mossy
5B	NAWC	Cu-B	•	•	–	–	•	6-100-300	69	mossy
6A	NRL	Cu-C	•	•	–	–	–	6-300-500	69	mossy
6B	NRL	Cu/Ni/Ag-D	–	–	•	–	–	6-300-500	69	mossy
7A	NRL	Cu-A	•	•	–	–	–	6-300-R-300	72	mossy
7B	NRL	Cu/Ni/Au	–	–	•	–	–	6-300-R-300	72	mossy
8A	NRL	Cu-C	•	•	–	•	•	6-20-100-300	67	mossy
8B	NRL	Cu-D	•	•	–	•	•	6-20-100-300	67	mossy
9A	NRL	Cu-C	•	•	–	•	–	6-100-300-R-300	66	metallic
9B	NRL	Cu-D	•	•	–	•	•	6-100-300-R-300	66	metallic
10A	NRL	Cu-B	•	•	–	•	–	6-100-20-100-300	64	mossy
10B	NRL	Cu-E	•	•	–	•	–	6-100-20-100-300	64	mossy

At NAWC, new or previously-used copper cathodes were treated with a wire brush in addition to the SiC paper to polish the electrode surface. Then, the electrode was "pickled" in HCl, boiled in water, rinsed with acetone and dried in a vacuum oven (70-80°C) until ready to use. The wire brush treatment was repeated after oven drying. Researchers at NAWC thought the wire brush might have been inadvertently contaminated with silver-tin solder (5%/95%). As a result, wire brushing the cathode may have "tinned" the surface. NRL did not attempt to reproduce this surface treatment. NAWC anodes were cleaned with soap and water, rinsed and, heated to red hot with a flame.

Cell Assembly/Operation

The cells for the two light water codeposition experiments were assembled on the benchtop with care to avoid excessive handling of the cell components after they were cleaned. Clean, latex gloves were used in the assembly of each new cell. Cell assembly for most of D_2O experiments (11 out of 17) was done in the glove box. Cells for the other D_2O experiments were assembled on the benchtop. In all of the assemblies, the cathode was centered in the cell 2 cm above the bottom of the test tube and the Teflon cruciform that aided the centering was located 2-3 cm above the top of the cathode so that it would be out of the current path. The anode was positioned so that its ends extended above and below the cathode by 0.5 cm. Good cathode-anode symmetry was important for uniform current distribution across the cathode.

After aligning the electrodes and assembling the cells, one of two procedures was followed. The first originated at NRaD and the second was a modified procedure that was used frequently at NAWC. In the first procedure, the assembled cell was attached to the oil bubbler in the hood and 10 mL of the 0.050 M Li_2PdCl_4 was injected into the cell without any prior addition of LiCl. Then, the experiment was started with 6 mA of current applied galvanostatically to the cell for 10-15 hours. The current density on the cathode was about 1.5-2 mA cm^{-2}. (Note - NRaD begins their experiments under galvanostatic control at a current density of about 4 mA cm^{-2} for around 12 hours. They then transfer to potentiostatic control for the remainder of the experiment.) In the modified procedure, 5 mL of 0.3 M LiCl was pipetted into a cell. The cell was then set up in the hood and attached to an oil bubbler. Immediately following, 6 mA of current was applied galvanostatically to the cell for 15-90 minutes. D_2 liberated during this step was thought by NAWC to cathodically protect the cathode from dissolving into the electrolyte. Then, while the applied current was still at 6 mA, 5 mL of 0.050 M Li_2PdCl_4 was injected into the cell via a syringe. In both procedures the current was generally left at 6 mA for 10-15 hours after the addition of the Li_2PdCl_4. During this time, the initially dark colored solution turned clear as palladium and deuterium were deposited. The current was then increased to 300 or 500 mA in one or more steps in attempts to generate some anomalous radiation. The modified procedure, which included the cathodic protection step, was used in 9 out of 17 heavy water cells and both light water cells.

When using the second procedure, the cell voltage usually dropped on injection of the Li_2PdCl_4. Researchers at NAWC postulated that the voltage drop occurred because the solution became acidic from the reaction of $PdCl_2$ with evolved D_2 to form Pd and DCl. (A voltage drop was also observed if DCl was deliberately added to the solution.) In attempts to slow the deposition, NAWC researchers sometimes added a small amount of DCl (40 μL of 38% DCl) along with the 0.050 M Li_2PdCl_4 to acidify the contents of the cell. NRL replicated this addition in a couple of experiments. Specifically, in NRL experiment #5, the DCl was added to both cells at the start of the experiment and in NRL experiments #8 and 9B, the DCl was added after the cathodic protection step (See Table 1).

Detectors for the radiation measurements were also set up in the hood, as close to the electrolytic cells as possible. The x-ray detector was usually positioned 10-20 cm above the top of a single cell and,

above and between a pair of cells that were centered about 15-20 cm apart. The germanium gamma-ray detector was also located 10-20 cm above the cells and 10-20 cm off to one side. Cells for the two light water experiments and for the first four heavy water experiments were held inside calorimeters though no calorimetric measurements were made, and the calorimeters were suspended in the water bath. In these cases, the calorimeters were simply intended to contain the cells in case of an explosion. In later experiments, after it was determined that the calorimeter and bath severely attenuated the x-ray and gamma ray transmission, cells were clamped directly in front of the germanium detector. No calorimeters nor water baths were used in the later experiments.

Experimental Results

Details of the codeposition experimental setups and results can be found in the NRL laboratory notebook # N-7661 assigned to Dr. Dawn Dominguez. The notebook covers the time from 2-10-92 to 9-30-92.

Two different types of palladium deposits were noted in the NRL Pd/D codeposition experiments. One type has been described as a mossy or dendritic deposit. Another has been described as a dense, bright or metallic deposit. The latter was generally the more adherent. NRaD reported that the dense deposit was responsible for the 2-4°C temperature increase of the cathode above that of the electrolyte, and for the production of tritium and some low energy form of radiation that was detected with photographic film. NAWC found that the cathodes with bright deposits generated the most radiation based on the response of a Geiger-Mueller detector. NAWC also noted that the bright palladium deposit was found in the pits on the cathode surface rather than on the flats.

In the NRL experiments, metallic deposits were found on the cathodes from 3 out of 17 Pd/D codeposition experiments. The metallic deposit on the copper electrode from experiment #4 was dense at the top of the cathode (i.e., no copper was visible through the film) but, somewhat less dense at the bottom of the cathode. The nonuniformity of the coating was probably due to gradients in current density. When the electrode was shown to Dr. Mel Miles (NAWC), he commented that the deposit was the best he had seen. The metallic deposit on one copper cathode from experiment #9 was located primarily on the bottom of the electrode with a small amount visible on the sides. The second copper cathode from experiment #9 had a very uniform metallic deposit all over the electrode surface. This dense deposit looked even better than the one from experiment #4. The metallic deposit was likely palladium metal in combination with palladium deuteride, although no analysis was done to confirm this suspicion. It should be noted that although experiments #1 and 4 had identical current-time profiles (see Table 1), the depositions were carried out on different substrates.

Cathodes from the other NRL Pd/D codeposition experiments generally had black, mossy deposits on their surfaces. Some deposits were uniform and some were blotchy. The deposits were thought to be β-PdD. Besides the deposits found on the cathode, there was often a reddish-brown or black precipitate on the bottom of the cell, on the anode, and floating on the electrolyte surface. The precipitates and floating deposit were likely the result of dendrites that formed on the cathode surface and then flaked off. On one occasion, both cells in experiment #6 experienced dendritic shorts between the anode and cathode.

The three NRL experiments that led to metallic deposits on the cathodes were all treated with SiC paper and "pickled" in 1 M HCl. None were treated with the chemical etch, NH_4OH/H_2O_2. All three underwent the cathodic protection step. Only one of the three was acidified with DCl. Four other cathodes

from experiments #8 and #10 received the same treatments, but none of the four formed metallic deposits. As such, no definite correlation between cathode treatment and type of palladium deposit was found.

Other specifics about some NRL experiments should also be mentioned. First, in experiments #1 and 2, the lithium chloride used was not anhydrous (Johnson Matthey 976216). There was also a problem getting a good seal between the stopper and the cell in these experiments. Second, in experiment #7B there was a loud bang shortly after the cell current was cut off, and the cell was shattered. The explosion likely resulted when deuterium contacted palladium particles on the cell wall above the electrolyte. As the palladium particles dried, a small spark could have been produced that ignited the deuterium in the headspace. NAWC had a couple of small explosions under similar conditions, but their cells didn't shatter. In experiments #7 and 9, when the cell current was at 300 mA, the direction of the current was reversed to -300 mA in attempts to redissolve deposited palladium into the electrolyte and then redeposit it on the cathode when the current direction was returned to normal. Since this procedure was followed in both experiments #7 and 9, it could not account for the different types of deposits produced.
Experiment #9 had a different current-time profile than experiment #7 (see Table 1).

Background radiation measurements were made at NRL with both the germanium gamma-ray and the x-ray detectors. These measurements were made in the hood with no cells in place, with deuterium cells assembled and electrically connected, and with light water cells running. The background with the germanium detector and with the x-ray detector was 54 cps and 0.065 cps, respectively. This was approximately half the background radiation measured at NAWC. (Their gamma ray and x-ray backgrounds were 114 cps and 0.117 cps, respectively. The higher background was due, in part, to higher potassium levels at NAWC.) The observed run-to-run variability at NRL was 0.6% (6σ) in the germanium detector. Radiation measurements at NRL were also made on all codeposition experiments in heavy water. However, there was no increase in total counts measured during the heavy water experiments compared to normal background variations. Also, no statistically significant (90% confidence level) new peaks were found in any of the runs.

Radiation measuring equipment (γ,x-ray) from NRL was also transferred to NAWC to use during their codeposition experiments. In addition, NRL researchers spent several weeks at NAWC setting up the equipment and training NAWC researchers to use the equipment. Radiation data acquired at NAWC was analyzed at NRL. Again, no changes were observed in the radiation data that correlated with a palladium/deuterium codeposition experiment.

At the completion of several NRL experiments, the electrolyte was decanted from the cell and the samples were sent to NRaD for tritium analysis along with samples of the D_2O and 0.3 M LiCl that were used. The experiments that had the electrolyte analyzed were #4, 6A, 6B, 7A, 8A and 8B from Table 1. All these, except #7A, showed an 8-10% increase in tritium content over the D_2O alone. Experiment #7A showed only 2% enrichment. NRaD and NAWC often noted similar small increases in the tritium content of the electrolyte that could be explained by the isotopic separation factor [8]. However, increases in the tritium concentration of more than 100% were measured in the electrolyte at NRaD. Increases of this magnitude are not predicted from the isotopic separation factor. Will et al. [12,13] also reported significant tritium enhancements (up to a factor of 52) in four out of four electrolytic cells where 0.2 cm diameter palladium (99.9%) wires were highly loaded with deuterium in 0.5 M D_2SO_4. They found that the tritium/deuterium ratio in the palladium cathodes was about 100 times larger than in the electrolyte or gas phase. They also determined that the tritium concentration was larger near the center of the palladium wire than at its ends.

Discussion

It is apparent that several different procedures were being tried at NAWC to generate radiation by the codeposition experiment. These procedures were not used in the initial experiments at NRaD nor NAWC. The procedures included variations in electrode pretreatment, introduction of a cathodic protection step, and adjustment of the electrolyte pH.

Initially, it was thought that a smooth electrode surface was desirable. What was noted at the end of a codeposition experiment was that the cathode was often pitted and that the desired dense or metallic deposit of palladium was found in the pits. Pit formation suggests that the current density may have initially been higher in those spots. However, when few cathodes developed the dense, bright deposits, NAWC decided to roughen the surface. At first, this was accomplished with coarser (180) SiC paper but, later, more aggressive abrasion (metal file, a saw, a drill or a punch) was used to roughen the electrode surface and to remove grain boundaries and oxides. The idea of the more aggressive abrasion was to produce a very rough surface with asperities in order to alter the current density distribution. Roughening the cathodes to this extent was not done at NRL. No cathode roughening was known to occur at NRaD.

The cathodic protection step was not used at NRaD. NAWC researchers introduced the step to prevent dissolution of the copper cathode in the electrolyte. Copper metal is very stable in concentrated base (pH 10-12), but its stability decreases dramatically as the pH is lowered. Without the step, some copper would likely dissolve and redeposit with palladium, but this doesn't appear to matter. Thus, the cathodic protection step probably has little value.

The adjustment of the electrolyte pH was another variable that NAWC attempted to control. First, a voltage drop was noted on the addition of the Li_2PdCl_4 solution presumably due to the reaction of $PdCl_2$ with evolved deuterium to form DCl. As a result, DCl was deliberately added to some solutions to make them acidic. Then, to avoid large changes in pH (pD) and decrease chlorine evolution, researchers at NAWC added 1 M LiOD after the cathodic protection step to neutralize the DCl produced. Finally, they attempted to carry out the codeposition in buffered solutions. None of these adjustments lead to the generation of radiation.

NRaD tried different substrates for the codeposition although copper foil was used initially. Other substrates that they found to work included nickel, silver, gold and platinum. Sometimes, silver or gold was plated onto copper with a nickel overlayer to prevent interdiffusion of silver (or gold) and copper. NRaD found the palladium or β-PdD deposit was more adherent on silver and gold than on copper. Both NRL and NAWC attempted a codeposition experiment on a silver-plated copper cathode and NRL tried a gold-plated copper cathode. However, no radiation above background was detected with these substrates at either laboratory and no excess enthalpy was measured at NAWC.

In April, Dr. Nowak (ONR) suggested that NAWC and NRaD each follow their own "best" recipes without deviation in five consecutive Pd/D codeposition experiments, and that they each provide their fully documented procedures, experimental results and interpretations to NRL and ONR by mid-May. NAWC reported that their highest level of radiation (65% above background or 73σ) was recorded during one of their five experiments. No radiation above background was observed in the other four experiments and no excess enthalpy was measured in any of the five experiments. NRaD reported a 20% increase in radiation over the background in two of their five Pd/D experiments, but no significant spectral differences were observed. No light water cells were running at either laboratory during these experiments.

In all, 36 different codeposition experiments were carried out at NAWC. These included two cells run with light water and 34 cells run with heavy water. Excess power (13% and 16%) was only seen in two heavy water cells out of 27 with calorimetric measurements as a diagnostic. Changes in the tritium content of the electrolyte was found to vary from -1-60% in 23 heavy water cells. Radiation levels above background were detected with Geiger-Mueller radiation monitors in 9 heavy water experiments where two cells were run in series. Three of these experiments produced radiation from 65 σ to 73 σ above background. Six other cells produced radiation from 4 σ to 39 σ above background. A light water experiment consisting of two cells showed a radiation level 13 σ above background. NRL germanium γ-ray and beryllium x-ray radiation detectors were in place and running during eight heavy water experiments where no radiation above background was detected. NAWC researchers postulate that Cl_2 contamination in the cell and exit gas tubing was responsible for the lack of reproducibility in the codeposition experiment by passivating the copper cathode and hindering palladium deposition.

Reasons for stopping the codeposition experiments at NRL included the following - (1) there were no positive results at NRL (i.e., no excess radiation was observed during heavy water experiments compared to normal background variations), (2) there were inconsistent results from NAWC, (3) essential control experiments had not been run at NRaD so positive results were suspect, (4) there was no prescription or recipe from either NRaD or NAWC to verify at NRL (both laboratories followed different procedures and both were still making frequent changes in experimental variables) and, (5) well-characterized palladium cathodes with known processing history became available at NRL. As such, the decision was made for NRL to attempt to replicate the excess heat, helium and, radiation claims of NAWC with the new NRL cathode materials.

11

CONVENTIONAL ELECTROCHEMICAL LOADING EXPERIMENT

In June 1992, Dr. Nowak (ONR) and NRL personnel agreed that NRL and NAWC would continue in the Navy Program with their focus on the conventional palladium-deuterium electrochemical loading experiment. The two laboratories were to collaborate closely with an emphasis on repeatably producing calorimetric evidence for anomalous behavior. In addition, NRL was to attempt to correlate excess power with deuterium loading and with any radiation (γ-ray, x-ray) measured while NAWC was to look for correlations between excess power and helium.

Work done at NRL was undertaken with the philosophy of conducting clean, careful, well-controlled experiments so that the results obtained would be both reproducible and publishable. Palladium and palladium alloys processed at NRL were to be used as cathodes so that the availabilty of consistent material would not be an issue. The cathode materials were to be well-characterized both chemically and metallurgically. The experiments were also to incorporate loading measurements and to include a large number of control cells.

Electrochemical Cell/Calorimeter Designs

Conventional electrochemical loading experiments were carried out at NRL using open electrochemical cells of the type described by Miles [1] with some modifications. The modified design included an *in situ* means to monitor the loading atomic ratios, specifically D/Pd and H/Pd, as reported by McKubre [14]. Briefly, loading was monitored by measuring the change in the axial resistance of the cathode. Resistance measurements were made by a standard four-point probe technique. To accommodate larger cathodes and platinum wires for the resistance measurements, a larger (2.5 cm diameter x 15 cm length) borosilicate-glass test tube was used as the electrolysis cell in the NRL-modified design. However, it was recognized that the larger diameter electrolytic cell could decrease the accuracy of the calorimetry by decreasing the efficiency of thermal mixing in the cell from the bubbling at the electrodes. The electrolyte volume in the NRL cells was 30 mL (nearly twice the volume of the NAWC cells).

The modified cell design also attempted to control the level of impurities introduced into the system so that the results would be more readily reproducible. To accomplish this, the obvious sources of volatile and/or soluble impurities that were present in NAWC cells were eliminated. More specifically, Teflon stoppers fitted with Viton o-rings sealed NRL cells in place of rubber stoppers, and spot-welding replaced solder and epoxy as a method of joining current leads to the cathodes. NRL Teflon cell tops were of two designs. In the first, the five wires from the electrolytic cell were bunched together and passed through a compression fitting for attachment to the electronics. In the second, the five wires were individually fed through Teflon screws that tightened on small, Viton o-rings. Both designs had Teflon tubing for exit gases and electrolyte addition. Teflon plugs were also used for centering the cathode in early experiments, but their use was ultimately discontinued.

The isoperibol calorimeter design that was used at NAWC was also modified for use in the NRL electrochemical loading experiment. The modified calorimeters were constructed from a 32 oz, wide mouth polyethylene bottle (O.D.=9.0 cm) and a larger diameter borosilicate-glass tube (I.D.=4.0 cm). The volume of the gap between the calorimeter and the electrolytic cell was 130 mL, but the H_2O level in the gap was kept 5 mL low to decrease the rate of evaporation. The volume of the gap in NAWC calorimeters was 68 mL, also kept 5 mL low. NRL calorimeters were immersed in a water bath maintained at $27.00 \pm 0.02\,^\circ$C. The NAWC constant temperature bath was maintained at $27.50 \pm 0.02\,^\circ$C. Other features of the calorimeters were identical to those described in the codeposition section of this report. Photographs of the NRL cell and isoperibol calorimeter are shown in Figure 2.
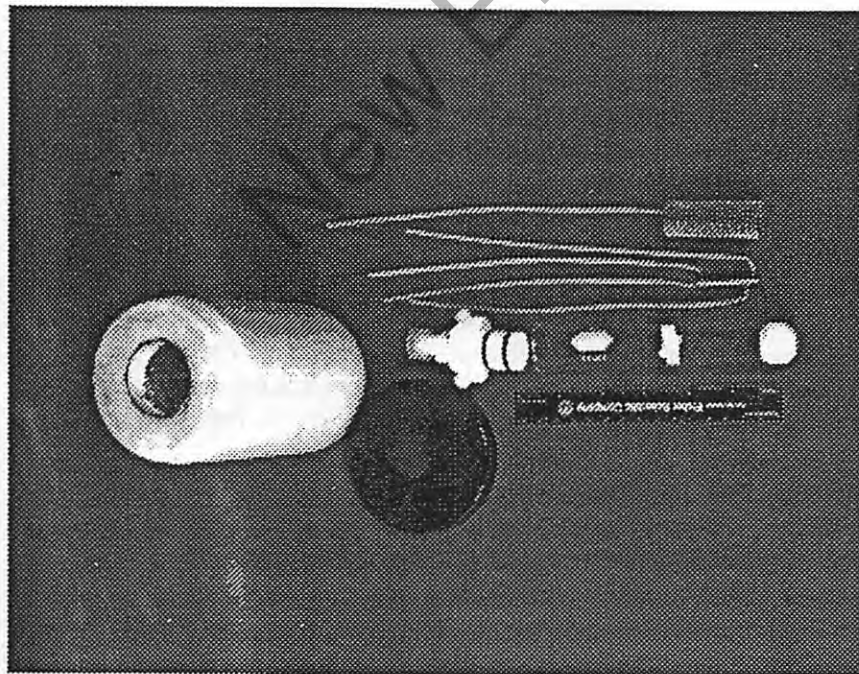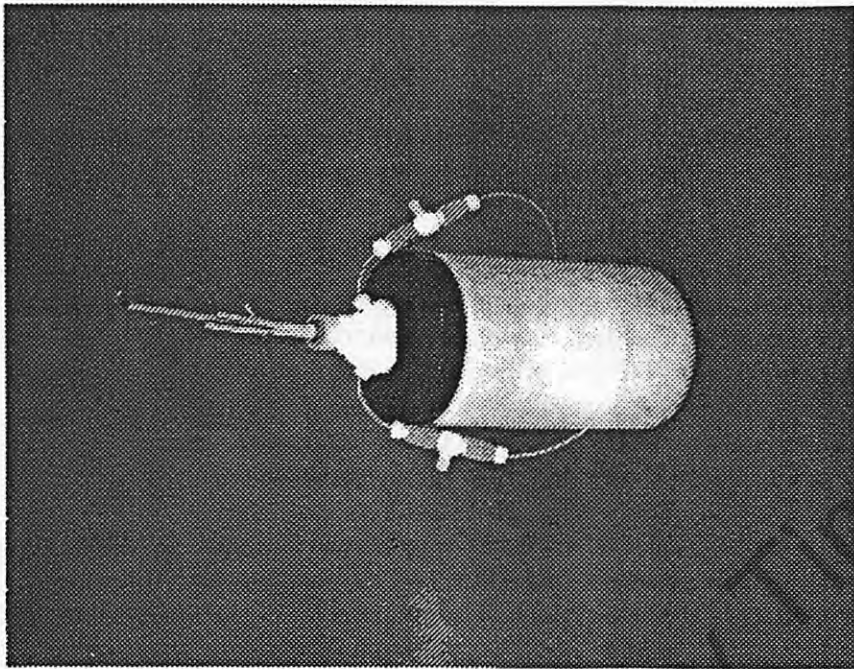
Fig. 2 - Photographs of (a) an NRL electrolytic cell and (b) an NRL isoperibol calorimeter

Heat measurements made in isoperibol calorimeters at NRL were compromised not only by larger electrolytic cells than NAWC, but also by the larger diameter calorimeters, resistance wires on the cathodes and room temperature fluctuations ($\pm$2-3°C). The increased diameter of the NRL calorimeters meant that more heat was lost from the top of the calorimeters. The resistance wires on the cathode were additional sources of heat loss from the calorimeter, and room temperature fluctuations of several degrees centigrade contributed to large measurement uncertainties ($\pm$200 mW at 2 watts input power) at NRL.

A custom-designed, multi-cell heat-conduction calorimeter (also called a Seebeck calorimeter) was acquired by NRL in October 1994 from Hart R & D, Inc., Mapleton, UT. The specifications for the design were that the calorimeters have (1) high measurement precision from 10 mW of output power with up to 20 W input power, (2) fast response, (3) linear output for ease of interpretation, and (4) long term (months) measurement stability.

A drawing of two cell positions in the multi-cell heat-conduction calorimeter is shown in Figure 3. As seen in the Figure, each calorimeter position consisted of two nested aluminum cans with heat flux sensors (Materials Electronic Products Corporation, Trenton, NJ) wired in series between the cans. The heat flux sensors are thermoelectric devices (TEDs) that produce an output voltage proportional to the temperature difference on their faces; the temperature difference is, in turn, proportional to the heat flow through the device. (The sensors or TEDs are also called Seebeck devices). The calorimeter accommodated four electrolytic cells in anodized aluminum cell holders. Wires exiting a cell were heat-sunk to an anodized aluminum plug that capped the cell holder and was located in the measurement area (area surrounded by heat flow sensors). A second anodized aluminum plug, located 1 cm above the first, was heat-sunk to a constant temperature environment provided by a 27.000$\pm$0.002°C water bath attached to an external circulator. Wires from the electrolytic cell passed through both anodized aluminum plugs and a Delrin top where external connections to the measurement instrumentation were made.

Preparation of Cell Components/Solutions/Electrodes

Glass and Teflon cell components were cleaned as described in the codeposition section of this report. Again, organics were avoided to eliminate contamination of the electrodes.

NRL researchers took the position that control of impurities in electrolytic cells was important for obtaining reproducible electrochemical experiments and for understanding the factors that affected the initiation and persistence of anomalous effects. As such, only high purity reagents were used in the NRL experiments, and cell components were cleaned and handled as they would be for ultra-high vacuum work. In addition, precautions were taken to minimize the exposure of all reagents to the ambient atmosphere to avoid contamination with light water. Unopened bottles of deuterium oxide (Cambridge Isotope Laboratories, 99.9% or Ontario Hydro, 99.93%) cans of lithium foil (Johnson Matthey, 99.9%), aluminum shot (Johnson Matthey, 99.999%) and deuterated hydrochloric and nitric acids were taken into a glove box with a boil-off nitrogen atmosphere for storage on receipt of the materials. Freshly prepared, 0.1 M LiOD electrolyte was made in the glove-box before each new electrochemical experiment in heavy water. Reagents for light water experiments were stored outside the glovebox on the benchtop.

Initially, no attempt was made by NRL or NAWC to use reagents from the same commercial source or with identical lot numbers. Then, in the summer of 1994, NRL agreed to purchase sufficient quantities of deuterium oxide, lithium foil and platinum wire with the same lot numbers and to distribute the materials to NAWC, the University of Utah, and Utah State researchers as the University groups became a part of the Navy Program.

14

Delrin Lid 17.75X13 IE
18.5X14.5 OD

Water level
1/2 inch below lid

Wires heat sinking

Test tube

Cell carrier

Cell holder

Heat flux sensor

Heat sinked to water

Water tight case

water bath case
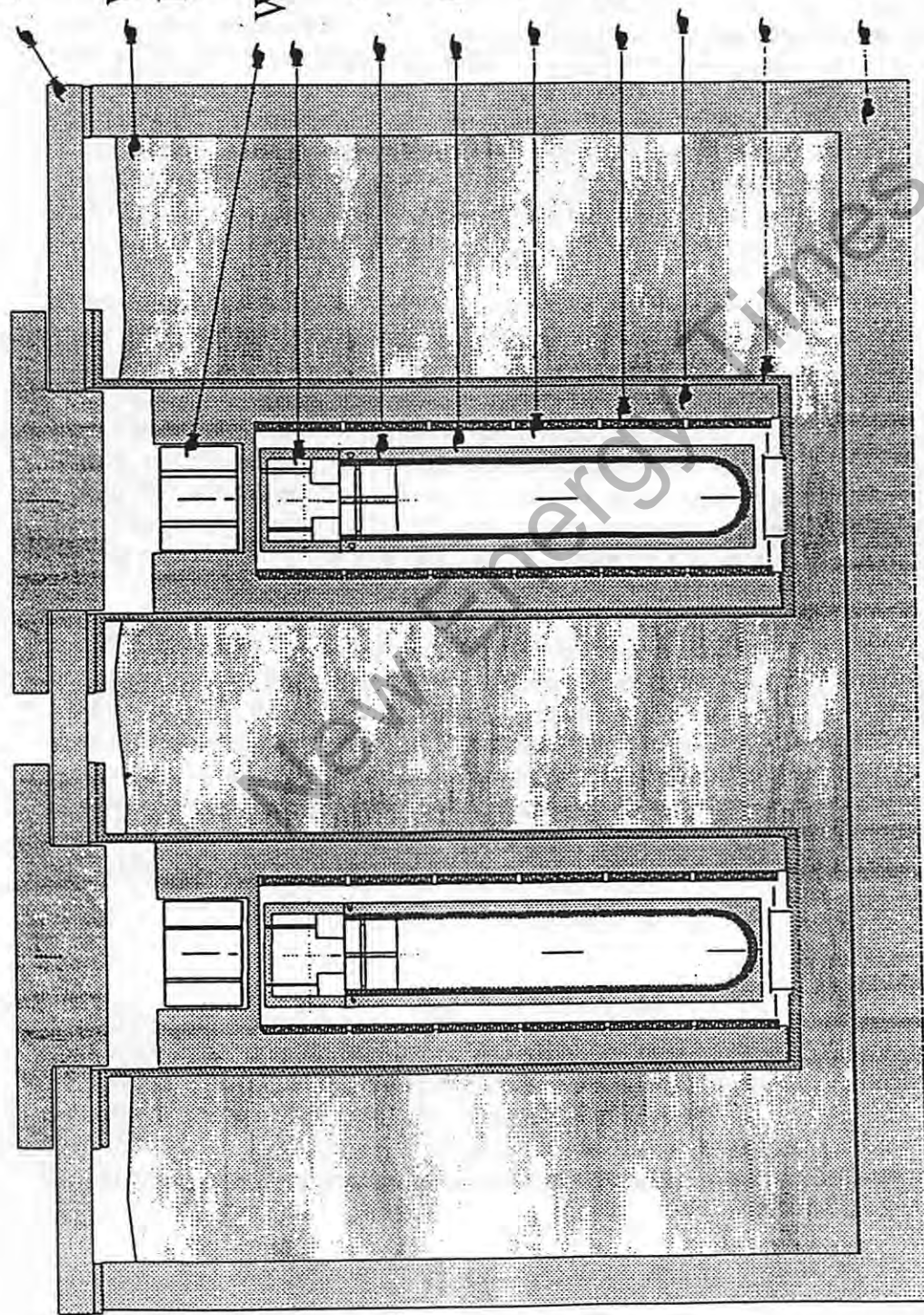
Fig. 3 - Front view of two cell positions in the custom-designed, multi-cell (4) heat-conduction calorimeter

15

Some cathodes used in the NRL electrochemical studies were materials prepared and characterized at NRL. Other cathodes were obtained commercially or provided to NRL from NAWC or SRI International (SRI, Menlo Park, CA). The NRL-processed cathode materials included palladium rods, palladium plates, rods of palladium/10% silver alloy, and rods with three compositions of palladium/boron alloy. Pure palladium sponge (Johnson Matthey, 99.999%) was used to produce the NRL cathodes. Palladium cathodes obtained from sources other than NRL were either 0.3 or 0.4 cm diameter rods or 0.1 cm diameter wire. The purity of all the materials varied from 99.9% to 99.997%.

Palladium rods were prepared at NRL by arc-melting the palladium sponge several times, forming a large rod and swaging to 0.4 cm diameter. For NRL cathodes, the swaged rods were cut into 3.5 cm lengths and machined to have rounded ends and four grooves to hold the platinum wires. NAWC cathodes were cut to 1.5-2.0 cm lengths and machined with only one groove. The specific designs of the cathodes for the two Navy laboratories are shown in Figure 4. Palladium plates (used at NRL only) were rolled after arc-melting, annealed, and rolled again to obtain a thickness of 0.07 cm. Rolled material was then cut into electrodes with 0.7 width x 3.5 cm length, and machined to have four grooves for resistance wires. Platinum (Johnson Matthey, 99.9%) contact wires for the resistance measurements were initially attached to the cathodes before annealing. But, because wires broke easily and often became detached, it became more feasible to first anneal the cathodes and then spot-weld the wires. A photograph of an NRL palladium rod cathode with resistance wires attached is shown in Figure 5.

When possible, palladium and/or palladium/silver electrodes were used to spot-weld the platinum wires to the palladium cathodes. This was done to avoid contaminating the cathode surface. Sometimes, when good spot-welds were not made with these electrodes, it was necessary to use copper/chromium spot-weld electrodes. A 30 second etch in either "heavy" or "light" aqua regia usually followed the spot-welding to remove contaminates from the cathode. Other NRL work [15] showed that the etch also increases the initial reactive surface area of the palladium and aids in the development of surface structures that form with D_2O or H_2O electrolysis. Cathodes were always rinsed in the isotopically appropriate water after an etch. The platinum wires attached to the cathodes were then covered with heat-shrinkable Teflon tubing to isolate them from the contact with the electrolyte and gases in the headspace of the cell.

Three types of cylindrical anodes were used in the NRL electrochemical experiments. These included anodes made from 0.1 cm diameter platinum wire (Johnson Matthey, 99.9%), platinum gauze (Johnson Matthey, 99.9%) and platinum-clad niobium mesh (Intrepid Industries, 99.99% platinum). Each NRL anode was also spot-welded to a 1.0 cm diameter platinum lead wire that was covered with heat-shrinkable Teflon tubing. NAWC used tightly-wound coils of 0.07 cm diameter platinum - 20% rhodium thermocouple wire and 0.1 cm diameter platinum wire as anodes. NRL anodes were generally 5 cm long with ends extending at least 0.5 cm above and below the cathode. Anodes were cleaned by immersion in a 50-50 mixture of concentrated nitric and sulfuric acids, rinsed with triply distilled water and dried.

Cell Assembly/Operation

Assembly of the electrolysis cells for the heavy water experiments was initially attempted in the glove-box with care to eliminate excessive handling of the cell components. Clean, latex gloves were placed over the butyl rubber glove-box gloves before the assembly of each new cell. Annealed cathodes with resistance wires attached were taken into the box and soaked in D_2O for 15-20 minutes to allow for hydrogen-deuterium exchange. The cathode and an acid-cleaned anode cage were then mounted in an acid-cleaned, D_2O-rinsed borosilicate-glass test tube. Freshly prepared electrolyte was added to the cell
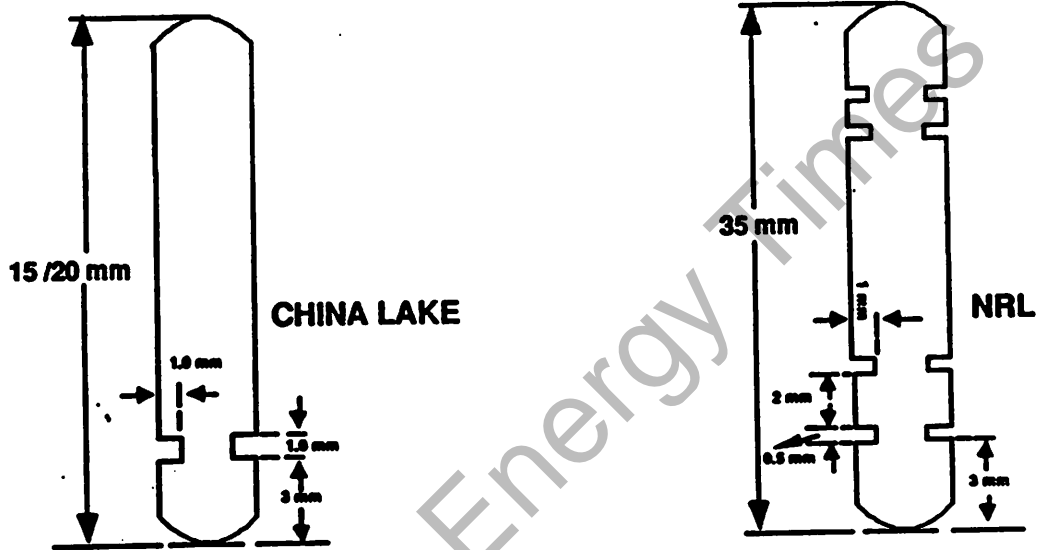
Fig. 4 - Specific designs of 0.4 cm diameter palladium rod cathodes prepared at NRL for experiments at NRL and NAWC
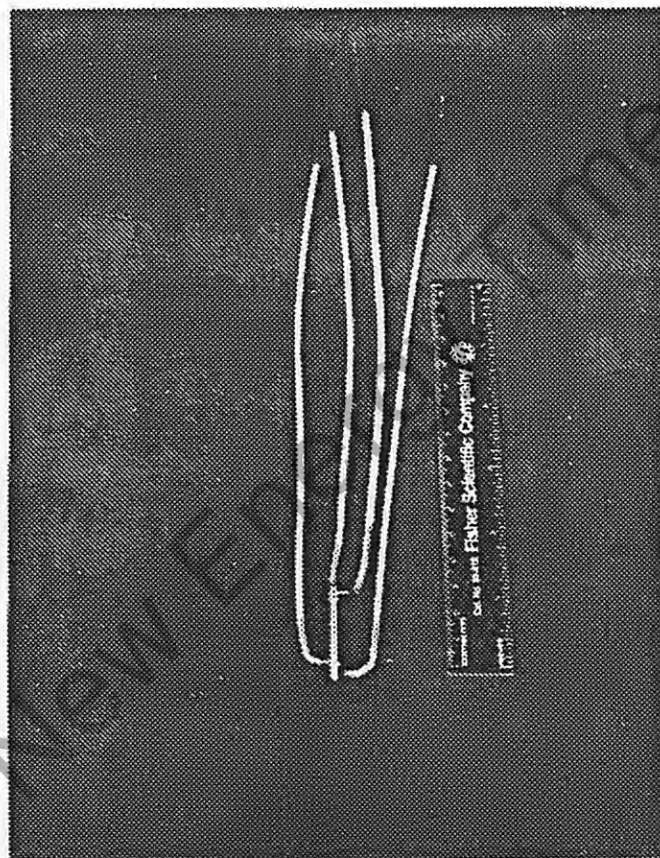
Fig. 5 - Photograph of an NRL 0.4 cm diameter palladium rod cathode with platinum resistance wires attached and covered with heat-shrinkable Teflon tubing

after it was sealed with the Teflon stopper. The sealed cell was then brought out of the box, installed in the calorimeter, and electrically connected for calorimetric cell calibration and electrode charging.

Cell assembly in the glove-box was awkward and cumbersome, however. As a result, most cells were ultimately assembled on the benchtop using clean, latex gloves to avoid excessive handling of the cell components. In addition, the cells were positioned in the calorimeters and electrical connections were made prior to the addition of electrolyte.

Two nearly identical calorimetric cells were usually connected electrically in series in each electrochemical loading experiment. One cell contained heavy water; the second cell, that contained light water, served as a control. Cells were run under galvanostatic control, as they were at NAWC (and, originally, at the University of Utah [16]). Electrode loading was started as soon as possible after electrolyte addition. Initial charging was usually done with current densities of 20-25 mA cm^{-2} on the cathodes. For 0.4 cm diameter rod electrodes (A=4.5 cm^2), initial charging took 2-3 days. Deuterium or hydrogen loading reached a D(H)/Pd atomic ratio of 0.70-0.75 during this time. The current density was then increased in 20-25 mA cm^{-2} steps every day or two to continue loading the cathode up to a D(H)/Pd ~ 1.00. Calorimetric measurements were begun once the current density on the cathode reached 100 mA cm^{-2}. At this current density, the electrochemical input power to a cell with a 0.4 cm diameter cathode was 1-2 watts. Most of the NRL calorimetric measurements were made at current densities of 100-200 mA cm^{-2}, but current densities were increased up to 300-450 mA cm^{-2} for short periods of time.

Current densities used at NRL during initial cathode charging and calorimetric measurements were comparable to those usually used at NAWC and SRI International (Menlo Park, CA). Fleischmann and Pons charged their electrodes at low to intermediate current densities (<100 mA cm^{-2}). They then increased the current density up to 2 A cm^{-2} for calorimetric measurements.

In NRL experiments, electrolyte was replenished with D$_2$O or H$_2$O before the total electrolyte volume in the cell was 5 mL below the starting level. This procedure kept the cathode and anode completely submerged beneath the solution level. The frequency of additions varied depending on the current applied to the cell and the cathode area. For 0.4 cm diameter palladium cathodes (A=4.5 cm^2) at low applied currents (<100 mA), additions were made every two or three days. At intermediate currents (100-500 mA), additions were made every 24 hours. At high currents (>500 mA), additions were made every 8-12 hours. Following an addition, the cell temperature was allowed to equilibrate for at least 3 hours (>6 thermal time constants) before continuing the calorimetric measurements. Some electrolyte additions contained small amounts (typically 120-275 ppm) of dissolved aluminum metal. Aluminum was added to facilitate the attainment and maintenance of high D(H)/Pd loadings as described by McKubre et al. [17].

Calibration of the calorimetric cells in isoperibol calorimeters was carried out electrolytically as described by Miles [1]. New isoperibol calorimeters were initially calibrated with 0.4 cm diameter palladium/10% silver or palladium rod cathodes in 0.1 M LiOH. Calibration cathodes had only one 0.1 cm diameter platinum wire attached for electrode charging and no wires for resistance measurements. Calibrations were typically carried out with input powers of 0.2-12 watts. Isoperibol calorimeters were recalibrated in situ during each new loading experiment assuming no excess power was produced. During the recalibrations, the cathodes had all four platinum wires for resistance measurements attached. Recalibrations were carried out in either LiOH or LiOD.

A typical calibration curve for an isoperibol calorimetric cell is shown in Figure 6. As seen in the figure, the results are linear over the power range used. Calorimetric cell constants were determined from the slope of the line of input power versus cell temperature measured by the two thermistors.
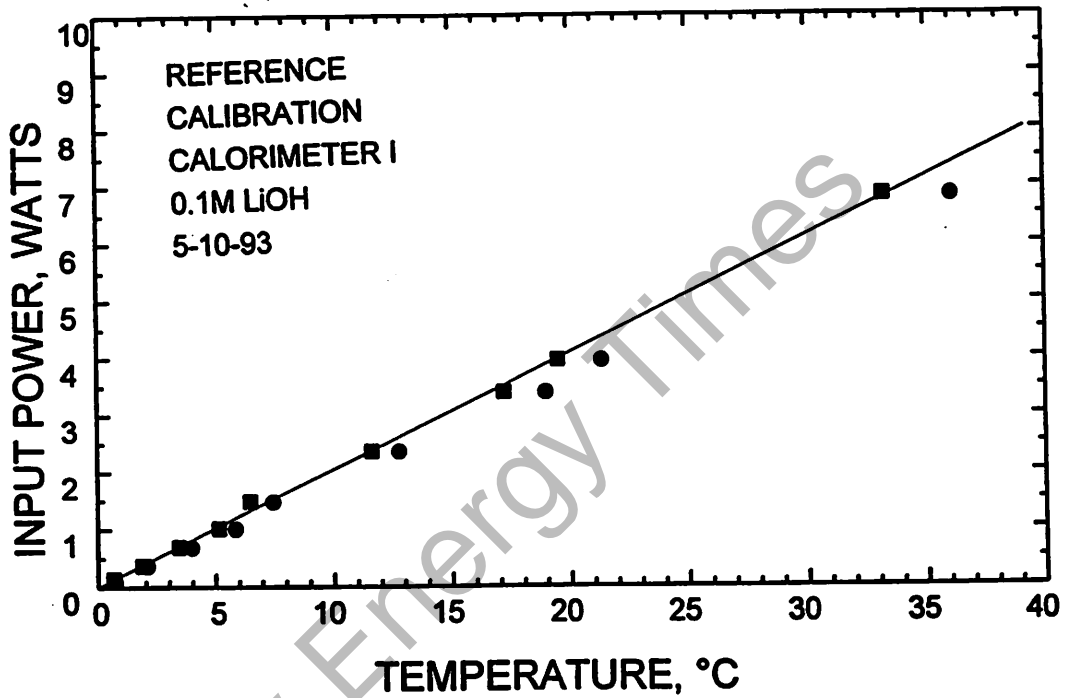
Fig. 6 - Calibration of an electrolytic cell filled with 0.1 M LiOH in an NRL isoperibol calorimeter. The thermistor positioned near the top (●) of the cathode tended to give a higher temperature reading than the thermistor positioned lower in the cell (■)

Typically, calibration constants for NRL isoperibol calorimetric cells with palladium rod cathodes were around 0.200 W/°C. Calibration constants for NAWC isoperibol calorimetric cells were about 0.140 W/°C [1]. NRL's larger calibration constant resulted from more heat loss from the calorimetric cells. The larger calibration constant meant less accurate calorimetry and larger measurement uncertainties.

The four positions in the heat-conduction calorimeter were initially calibrated using a 100 ohm resistance heater in three measurement configurations - (1) in the wall of the calorimeter, (2) in an empty cell, and (3) in a cell filled with electrolyte. Calibration constants of the four calorimeter positions were determined to be 9.5 ± 0.1 W/V using the three configurations. The baseline noise level of the calorimeter was determined to be ± 0.2 milliwatts.

The heat-conduction calorimeters were recalibrated to increase the accuracy of the calorimeter calibration constants, K. K values accurate to 1 part in 10^4 were needed to measure 10 mW excess power in an electrolytic cell with an electrochemical input power of 10 W. Calorimeter calibration constants were redetermined with Joule heating using a 100 ohm resistor in a cell in place of electrodes. This served as a non-electrolyzing reference cell. Calibrations in reference cells were carried out in silicone oil and in 0.1 M LiOH. Heat-conduction calorimeters were also calibrated electrolytically with 0.2 cm diameter silver or 0.1 cm diameter palladium wire cathodes in 0.1 M LiOH. Input powers of 0.2-12 watts were used in all reference cell and electrolytic cell calibrations.

A typical calibration curve for a reference cell in the heat-conduction calorimeter is shown in Figure 7. Again, the results are linear over the power range used. Calorimetric cell constants were determined from the slope of the line of input power versus heat sensor voltage response. Typically, calibration constants for NRL's heat conduction calorimetric cells were approximately 9.30 W/V.

Data Acquisition/Reduction

Data collection equipment consisted of a Gateway 2000 - 33 MHz, 386 computer that was interfaced to Keithley electronics via a KM488DD IEEE-488 interface board. Keithley electronics included three model 195A digital multimeters, a model 706 100-channel scanner, and a model 228A voltage/current source. A Cole-Parmer thermistor thermometer and several Electrosynthesis Model #420X/415 power supply/potentiostatic controllers were also used. Constant current was supplied to a cell or a series of cells by manually setting the voltage across a calibrated $0.1 \pm 1\%$ ohm standard resistor on an Electrosynthsis potentiostatic controller.

Data acquisition software consisted of a GW BASIC program written at NRL by Dr. William Barger (Code 6170). The program, named FUSIONXX (XX=01-56), underwent continuous revision between the summer of 1992 and June 1995. The program collected, recorded and stored up to 100 channels of data every eight minutes (about 2 s/channel). Parameters measured include (1) voltage across a $0.01 \Omega \pm 1\%$ standard resistor (to calculate cell current), (2) cell voltage, (3) resistance of cathode, (4) cell temperature, (5) bath temperature, (6) room temperature, and (7) time. Sequential measurements on these parameters were generally made every eight minutes. Versions of FUSIONXX (XX=32-56) written in 1995 also contained a subroutine to give a real-time plot of excess power in a cell as a function of time.

Data reduction software included a series of GW BASIC programs written at NRL. The programs were named CLIPPERX, COMBINE, HALFERX, and CALC_X (X=1-5). After processing the data through these BASIC programs, the ASCII data were read into either Sigmaplot or Microcal Origin graphics software for plotting.
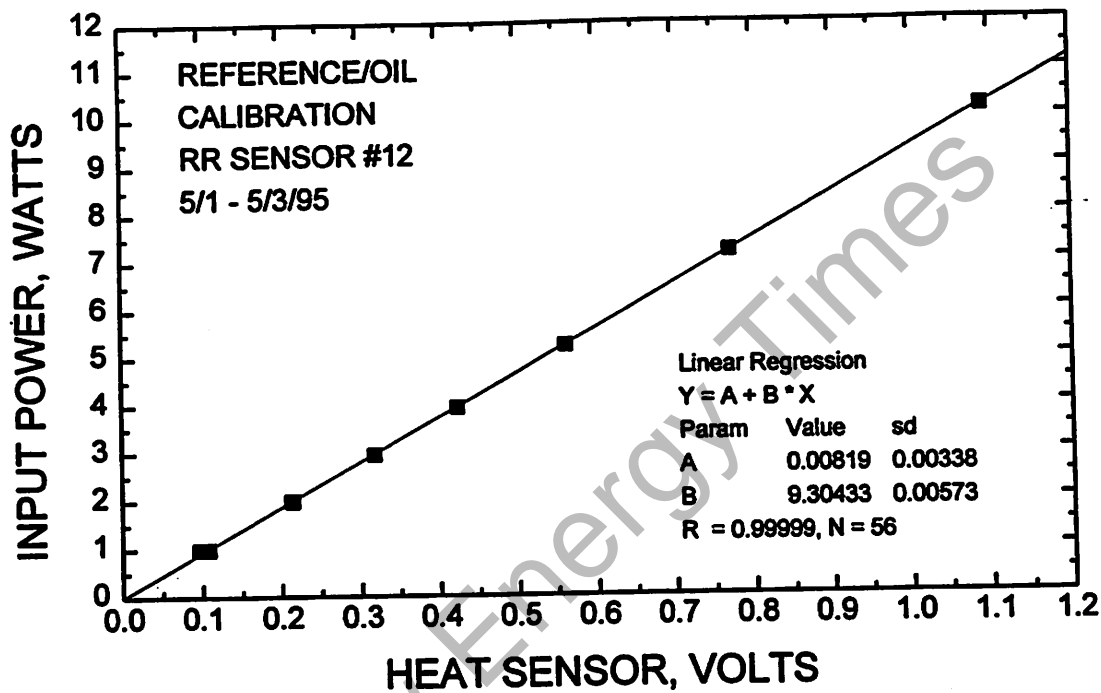
Fig. 7 - Calibration of a reference cell filled with silicone oil in the heat-conduction calorimeter filled with 0.1 M LiOH

The thermodynamic aspects of isoperibol calorimetry that must be considered when assessing excess enthalpy in cold fusion experiments were discussed in papers by Pons and Fleischmann [18] and by Miles [9]. The former gave the differential equation governing the behavior of isoperibol calorimeters and the latter gave the following calorimetric approximation

$$(E(t)-\gamma E_H)I + P_X = a + K\Delta T + P_{gas} + P_{calor} \tag{1}$$

where $E(t)$ is the measured cell potential at time t, γ is the Faradaic current efficiency for D_2O electrolysis, E_H is the thermoneutral potential, I is the cell current obtained by measuring the voltage supplied by the potentiostat across a 0.100 ohm resistor, P_X represents any excess power, a is a constant, K is the calorimetric cell constant, ΔT is the temperature increase in the cell above the bath temperature, P_{gas} is the rate of enthalpy transfer outside the cell from D_2, O_2 and D_2O exit gases and P_{calor} is the rate of enthalpy transfer from the cell due to evaporation. Equations for P_{gas} and P_{calor} were also given in the papers. Both terms depend on current, I. Neglecting these terms would underestimate the output power of the electrochemical cell. The calorimetric approximation, with the P_{gas} and P_{calor} terms neglected, also assumed that the bath and room temperature are constant and that any power effects due to deuterium loading or deloading are negligible.

Excess power in isoperibol calorimeters was calculated from the approximate equation

$$P_X = \text{POWER OUT} - \text{POWER IN} = (a + K(\Delta T)) - [(E(t)-\gamma E_H)I] \tag{2}$$

In NRL isoperibol calorimeters, excess power measurements were generally good to ±10% of the electrochemical input power. Thus, at two watts input power the excess power in the cell had to be greater than 200 mW for detection.

Excess power in heat-conduction calorimeters was calculated from the approximate equation

$$P_X = \text{POWER OUT} - \text{POWER IN} = (a + KV_{TED}) - [(E(t)-\gamma E_H)I] \tag{3}$$

where V_{TED} is the voltage response of the thermoelectric heat sensors and the other variables are the same as above.

Experimental Results/Discussion

Cathodes Processed at NRL

Palladium Cathodes

Metallurgy/Bulk Analyses. Several batches of palladium cathodes were produced and characterized at NRL between May 1992 and June 1994. All batches were made from the same initial batch of palladium sponge (Johnson Matthey, 99.999%). Table 2 shows 18 selected elements from the GDMS Analyses of the starting material and a few processed cathodes. The complete GDMS analytical report on these materials can be found in Appendix A. Concentrations are expressed as ppm by weight in both tables.

GDMS is a direct elemental analysis method for solids. It analyzes for 76 elements in one cycle and has detection limits in the ppb concentration range. The method is considered to give a pseudo-bulk analysis of the material because samples are analyzed end-on and several mm are consumed in an analysis. As

Table 2 - Glow-Discharge Mass Spectroscopic Analyses of NRL Palladium Cathodes
(concentration in ppm by weight)

Element	Pd sponge 9/16/92	Pd sponge 3/31/94	Pd rod 3/31/94	Pd rod 11/28/94	Pd plate 3/31/94	Pd/0.62%B 7/31/94
B	0.1	0.007	<0.005	<0.001	<0.005	6200
C	5	<10	<1	0.01	<0.1	<1
N	1	<0.1	<0.1	0.03	<0.1	<0.1
O	10	<20	<0.5	0.36	<1	<10
Mg	0.1	<0.01	1.2	—	1.7	3.5
Al	0.5	0.06	0.3	0.52	0.3	4.1
Si	0.6	0.15	1	0.32	9.6	15
Ca	0.5	<0.05	0.8	0.67	1.1	7.9
Cr	2.5	2.8	1.1	1.2	1.8	0.98
Mn	0.9	1.3	0.75	—	1.1	8.2
Fe	45	31	30	33	50	56
Ni	1.3	1.1	0.84	0.96	1.3	1.4
Cu	0.8	0.44	31	24	12	26
Zn	0.9	0.3	1	1.1	2	2.3
Rh	8	6.3	9.3	10.5	11	11
Ag	1.5	1.6	1.1	1.1	1.7	0.75
W	1	0.01	0.5	3.4	3	2.2
Pt	12	6.3	31	29	26	47
Total	92	82	111	106	124	197

seen from the Table, the as-received palladium sponge had several metallic impurities present at the ppm concentration level, namely - sodium, titanium, chromium, iron, nickel, rhodium, silver, tantalum, tungsten, platinum, and gold. As such, the purity of the palladium sponge was found to be only 99.99% and not 99.999% as expected.

GDMS analyses of NRL-processed palladium rod and plate cathodes showed an increased concentration of copper, tungsten and platinum over the starting material. These impurities were likely introduced into the samples during processing from the arc melter and the tools used to handle

the material. In spite of the higher concentrations of these few impurities, the analyses showed that the purity of the processed materials remained essentially 99.99%.

Loading Experiments. NRL electrochemical experiments were begun knowing that SRI International (Menlo Park, CA) researchers had identified [19] at least three criteria that were necessary for excess power production in deuterium-loaded palladium cathodes. These criteria were that (1) a palladium cathode have an average deuterium loading approaching or exceeding unity (D/Pd $\geq$ 0.9), (2) the high level of deuterium loading be maintained for considerable periods of time (300 hours for 0.3 cm diameter cathodes), and (3) the deuterium-loaded palladium cathode be subjected to a high interfacial current density (200 mA cm^{-2} for 0.3 cm diameter cathodes). The criteria were generally accepted by the research community. Thus, one immediate goal of the anomalous effects program was to achieve high levels of deuterium loading in palladium cathodes.

Electrochemical loading experiments at NRL were undertaken using the collective wisdom of NAWC and SRI researchers who had already been working in the area for 2-1/2 years. Although SRI was not formally a part of The Navy Program, NRL recognized that SRI's experimental program was a high quality research effort and a serious attempt to understand the observations of anomalous effects in the D/Pd system. SRI had run over 200 loading experiments by the time the NRL experiments began and they had identified [19] several critical factors for achieving high loadings. These included electrode pre-treatment, electrolyte composition, low temperature/high D$_2$ pressure, high (stable) current density, hydrogen recombination poisons, and the *in situ* formation of ionically conductive films (Si, Al). Thus, some of SRI's experimental procedures were adopted by NRL. These included the *in situ* resistance measurement of the cathode to monitor loading, annealing the cathode to relieve stress, an acid etch of the cathode in either "heavy" or "light" aqua regia, as appropriate, to pretreat the surface, and an addition of aluminum [17] to form a surface film. The use of 1 M electrolyte in quartz cells was tried in some NRL experiments, but it was not routinely adopted. A recent publication by Green et al. [20] showed that "the crucial feature of the electrode pre-treatment used by McKubre and co-workers is evidently the vacuum-annealing step".

SRI had also carried out numerous calorimetric experiments by the time the NRL work began although their experiments differed from those being carried out at NAWC in a couple of ways. For example, at that time, SRI was performing all of their experiments in thermodynamically closed electrochemical cells with D$_2$ partial pressures between ambient and 10,000 psi. The use of closed cells simplified the calorimetric analysis, but introduced problems of pressure build-up and possible cell explosions. SRI was also using two different types of calorimeters (a differential mass flow calorimeter and an isothermal flow calorimeter) in their experiments. For reasons of simplicity and safety, NRL chose to pursue the type of open-cell calorimetry done at NAWC.

In all, 36 NRL palladium cathodes were run in NRL loading experiments. Some of these (28) were also run in NRL isoperibol calorimeters to verify the anomalous power reported by NAWC, SRI and others. The experimental details of the NRL electrochemical loading/calorimetric experiments are summarized in the Table found in Appendix B. Experimental details and results of experiments on NRL palladium cathodes can also be found in NRL laboratory notebooks # N-7725, N-7726 and N-7817 assigned to Dr. Dawn Dominguez. The notebooks cover the time from 1-15-93 to 10-7-94.

During all of the NRL experiments, cathode loading was monitored *in situ* by measuring the change in the axial resistance of the palladium with deuterium or hydrogen content as described by McKubre [14]. Drs. Gillespie and Ehrlich of the Materials Science Division (Code 6341) at NRL aided NRL researchers in making four-point probe electrical resistance measurements of the cathode. These investigators had already published [21] results from an experiment on the palladium-deuterium

system where cathode loading was inferred from resistance measurements. The average specific resistance, R_0, and resistivity of NRL palladium rod cathodes was 81 ± 2 $\mu\Omega$ cm^{-1} and 10 $\mu\Omega$-cm, respectively. The latter agrees reasonably well with the literature value of 11 $\mu\Omega$-cm for palladium metal at 20°C [22].

Plots of the resistance ratio-loading variations in the H/Pd and D/Pd systems at room temperature are shown in Figure 8 [23]. These curves were determined from the results of several resistance-loading studies [24-28], and also from volumetric measurements of gas displacement during loading in closed systems at constant temperature and pressure [19]. Loading atomic ratios, H/Pd and D/Pd, are often inferred from these plots, but care is taken in assuming a precise level of loading based on resistance measurements alone since other factors (temperature, electrode cracking, loading inhomogeneities, electrode impurities) can affect the resistance of the palladium [14].

With these considerations in mind, deuterium and hydrogen loadings in palladium cathodes were estimated in NRL experiments from the curves shown in Figure 8 and measurements of resistance changes in palladium electrodes. During many experiments, the degree of deuterium loading attained on palladium cathodes was not sufficiently high to satisfy SRI's first criterion for excess power production. For example, in early 1993, deuterium loading in NRL palladium rod (0.4 cm diameter x 3.5 cm length) cathodes consistently (4 times in 4 experiments) reached a level where the D/Pd loading atomic ratio was only 0.7-0.75. The Pd-H(D) binary phase diagram [29] indicates that at 298K this level of loading corresponds to the α,β mixed-phase region; loading beyond this level would occur in the pure β-phase. Hydrogen loading reached levels where the H/Pd loading atomic ratios were as high as 0.9-0.95 (2 experiments). Representative resistance ratio-time plots for two of these cathodes (#93011501 and #93011502) are shown in Figure 9. In contrast, a resistance ratio-time plot for an Engelhard (purity 99.9%) palladium rod cathode (0.3 cm diameter x 3.0 cm length) run in a SRI deuterium loading experiment is shown in Figure 10. The average specific resistance and resistivity of the Engelhard material was 169 ± 10 $\mu\Omega$ cm^{-1} and 12 $\mu\Omega$-cm, respectively.

On comparing the resistance ratio-time plots from the LiOD/D$_2$O experiments (Figures 9 and 10) both can be seen to reach a maximum resistance change of 2.0 that is expected for deuterium-loaded palladium. However, important differences between the plots can also be noted. For example, the resistance ratio for the NRL palladium cathode remained at the maximum value in spite of increases in current while the resistance ratio for the Engelhard cathode decreased gradually at a given current and decreased in a step when the current was increased. The dynamic current response of the Engelhard cathode was that which typically led to high deuterium loading (D/Pd ~ 0.9 inferred from the resistance ratio minimum of 1.7 in the example shown) while a response like that of the NRL cathode did not result in a loading beyond the 0.7-0.75 level. The Engelhard cathode was, therefore, a possible candidate for excess power production whereas the NRL cathode was not a candidate because it could not be loaded to a high D/Pd level.

Another observation from the plots was that the NRL palladium cathode loaded faster than the Engelhard cathode in spite of its larger diameter. However, the grain size of the two cathode materials was different. NRL palladium cathodes had an average grain size of 60 μm (based on the abstract of a Johnson Matthey patent application) [30] while the average grain size of the Engelhard cathode was 100s of μm. The smaller grain size (more grain boundaries) in the NRL cathodes could explain the faster diffusion, if loading occurred by a grain boundary diffusion mechanism. This observation led NRL researchers to postulate that faster loading was somehow detrimental for achieving a high degree of loading. Thus, attempts were made to decrease the rate of loading in NRL palladium cathodes in two ways. In one, the current density used to charge (load) the cathodes was decreased (from ~ 22 mA cm^{-2}), and, in another, the grain size of the palladium was increased.
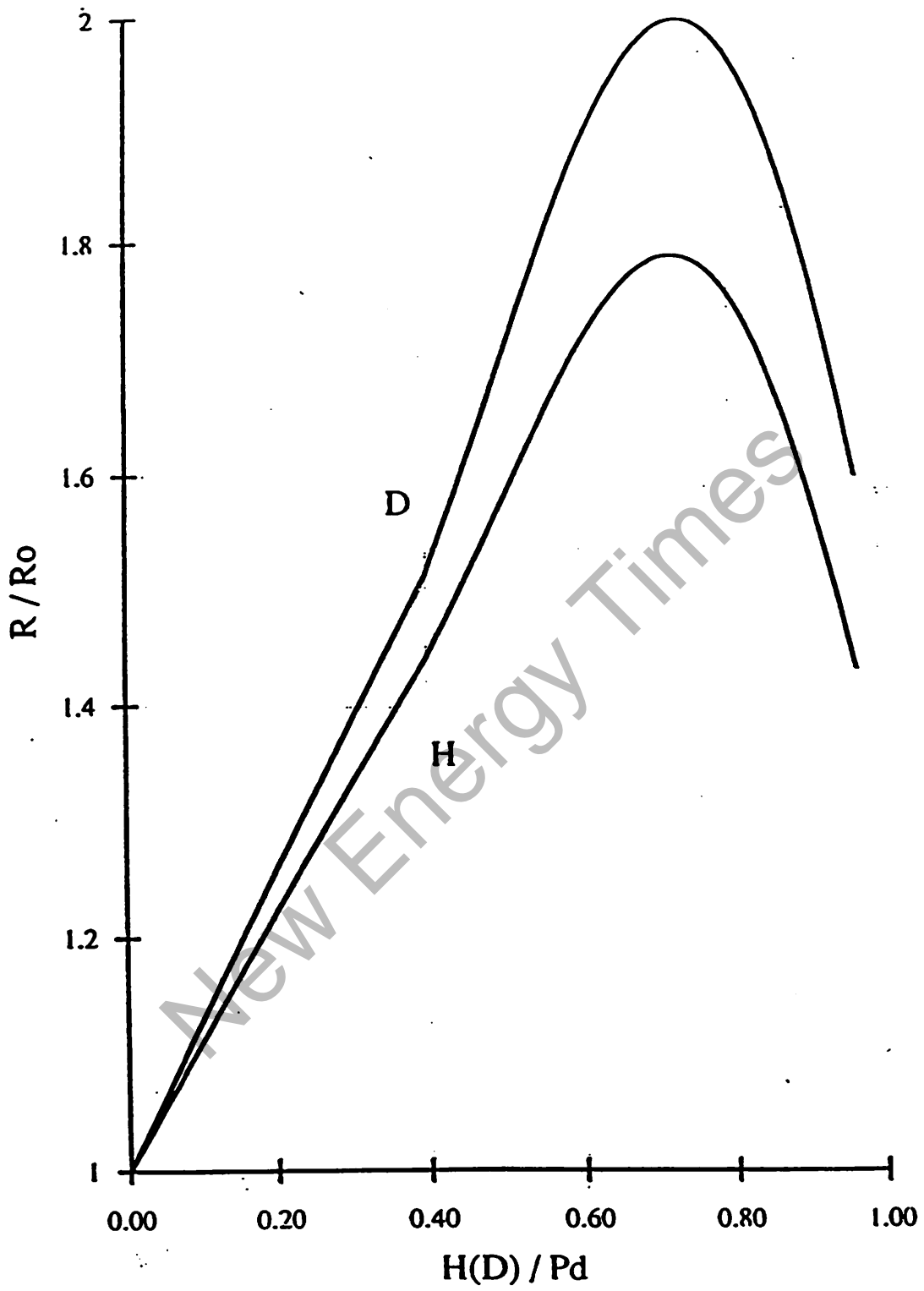
Fig. 8 - Resistance ratio-loading variations in the H/Pd and D/Pd systems at room temperature (from reference 19)
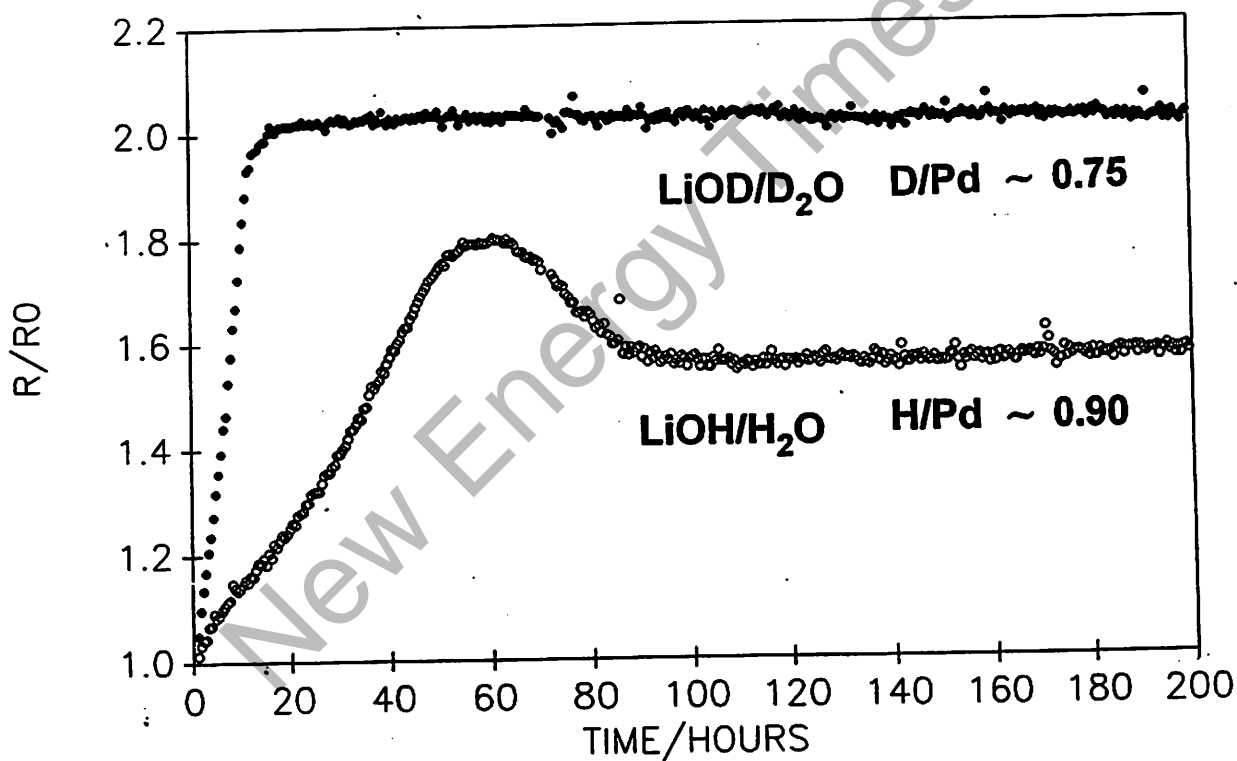
Fig. 9 - Resistance ratio (R/R_0) vs. time for NRL palladium rod cathodes annealed in vacuum ($< 10^{-5}$ torr) at 650°C for 1 hour. The average specific resistance of NRL palladium rod cathodes was 81 ± 2 $\mu\Omega$ cm^{-1}. Closed circles - deuterium (cathode #93011501), open circles - hydrogen (cathode # 93011502)
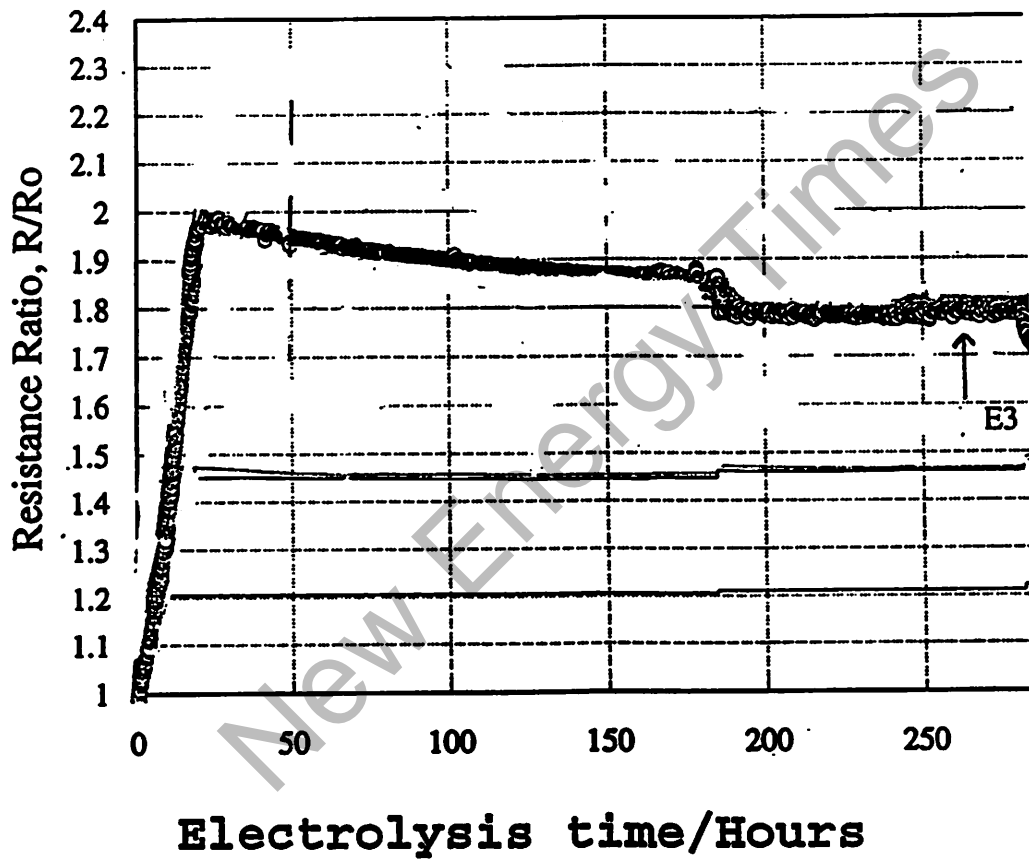
Fig. 10 - Resistance ratio (R/R_0) vs. time for deuterium loading of an Engelhard (batch #3) palladium rod cathode run at SRI. The cathode was annealed in vacuum ($< 10^{-5}$ torr) at 850°C for 4 hours. The average specific resistance of Engelhard palladium rod cathodes was 169 ± 10 $\mu\Omega$ cm^{-1}

Experiments to Slow the Rate of H(D)/Pd Loading

The current density on NRL palladium cathodes, with an average grain size of 60 μm, was decreased in three deuterium loading experiments. In one experiment, the current density on the cathode (#93020902) was 10 mA cm^{-2} and in two experiments it was 2 mA cm^{-2} (cathode #93021702 and #93020901). No improvement in deuterium loading was evident in these experiments.

Loading experiments were carried out on three pairs of NRL palladium rod (0.4 cm diameter x 3.5 cm length, A=4.5 cm^2) electrodes with different microstructures (i.e., grain sizes). Different microstructures were obtained by varying the time and temperature of the anneal at the end of the material processing. One pair of electrodes was not annealed at all, the second pair was annealed at 650°C for 1 hour, and the third pair was annealed at 1100°C for 20 hours. This processing resulted in electrodes with elongated grains resulting from cold working the material and those with equiaxed grains. Electrodes annealed at 650°C and 1100°C had average grain sizes of 44 and 600 μm, respectively. Optical metallographs of three of the palladium rod electrodes are shown in Figure 11. The unannealed electrodes likely had more defects and more strain than the annealed electrodes. Thus, the effects of defects and strain on loading were also investigated.

Loading experiments were also carried out on three pairs of NRL palladium plate (0.07 cm x 0.7 cm x 3.5 cm, A=4.9 cm^2) cathodes that were annealed simultaneously with the rod electrodes. Plate electrodes were examined because the microstructure of plates is easier to control than that of rods. As such, the plate electrodes were expected to have a more uniform cross-section than the rod electrodes. The uniform cross-section was expected to (1) remove diffusion barriers due to stresses that might have been present in the rods, (2) lead to more uniform loading and (3) lead to faster loading. Optical metallographs of three of the palladium plate electrodes are shown in Figure 12. A comparison of the micrographs for the corresponding rod and plate cathodes shows little or no difference in microstructure.

The dimensions of the plate electrodes were chosen so that their surface areas would be nearly identical to the rod electrodes. Thus, the current densities on the rod and plate electrodes were the same at a given applied current. Electrode charging in these experiments began with a current density of 22 mA cm^{-2}. The average specific resistance and resistivity of NRL palladium plate cathodes were 187±11 $\mu\Omega$ cm^{-1} and 9 $\mu\Omega$-cm, respectively.

Relative resistance-time plots for the three pairs of palladium rod and plate electrodes are shown in Figures 13 and 14, respectively. Several observations regarding cathode loading can be noted from these plots. First, deuterium loading in palladium rod cathodes (#93060301, #93060303 and #93060305) did not exceed a D/Pd atomic ratio of 0.7-0.75, despite the extent of electrode processing. Second, deuterium loading in palladium plate cathodes (#93080601, #93060803 and #93060805) appeared to increase slightly with the first current increase, but, thereafter, only decreased or remained unaffected by further current increases. As such, deuterium loading levels remained essentially 0.7-0.75 in the plate cathodes, despite the extent of electrode processing. Third, hydrogen loading into the β-phase, where the H/Pd atomic ratio was 0.8-0.85, occurred in a large grain sized palladium rod cathode (#93060306). Hydrogen loading did not exceed a H/Pd atomic ratio of 0.7-0.75 in palladium rod cathodes with less processing (#93060302 and #93060304). Fourth, hydrogen loading in palladium plate cathodes increased with electrode processing. Hydrogen loading reached a level where the H/Pd atomic ratio was 0.8-0.85 in an electrode with no processing (#93080604), but it was increased to where the H/Pd atomic ratio was approximately 0.95 with
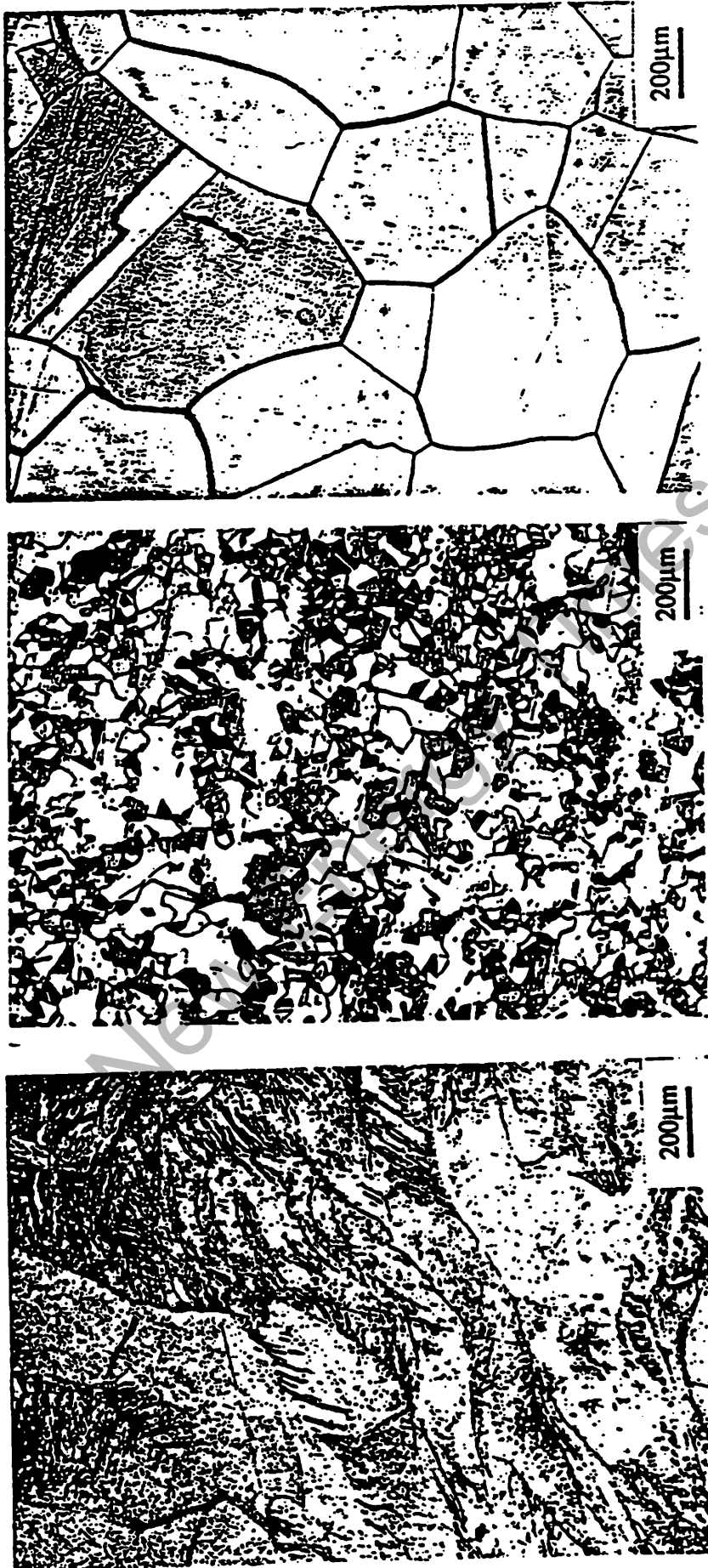
Fig. 11 - Optical micrographs of pure palladium rod cathodes processed at NRL showing micrstructure at three different conditions (a) as processed, (b) annealed at 650°C for 2 hours, and (c) annealed at 1100°C for 20 hours
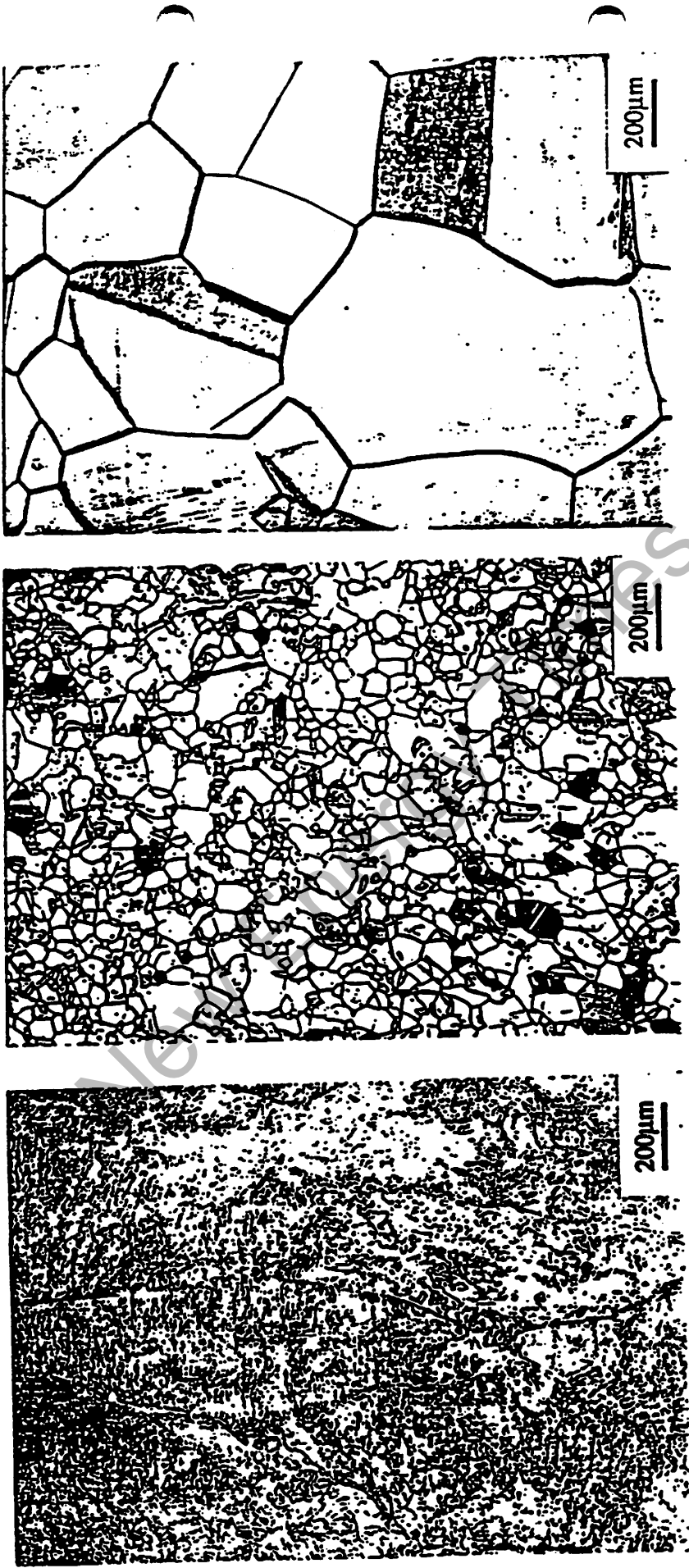
Fig. 12 - Optical micrographs of pure palladium plate cathodes processed at NRL showing micrstructure at the same conditions as in Figure 11

32
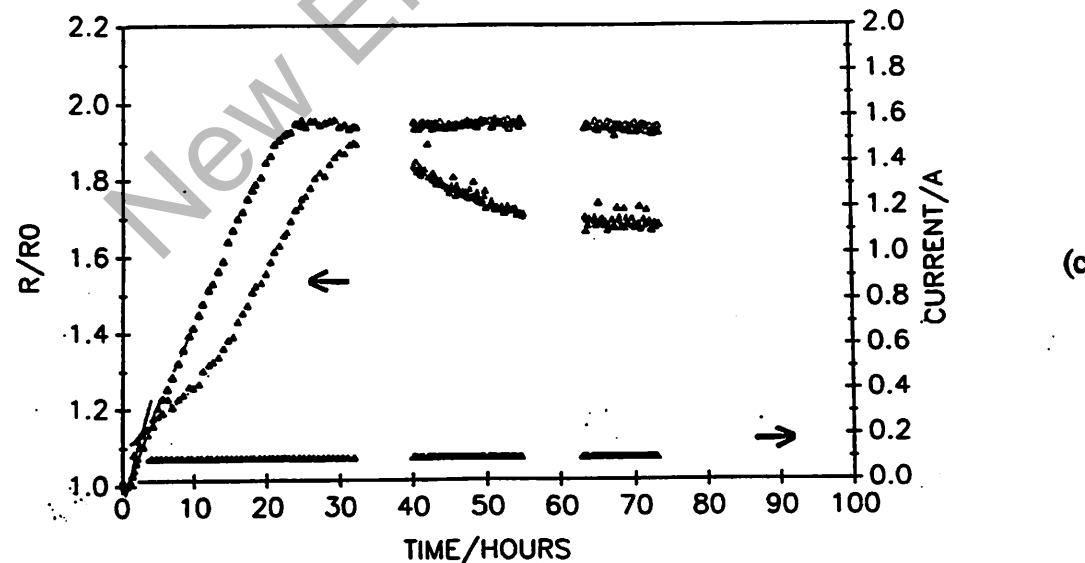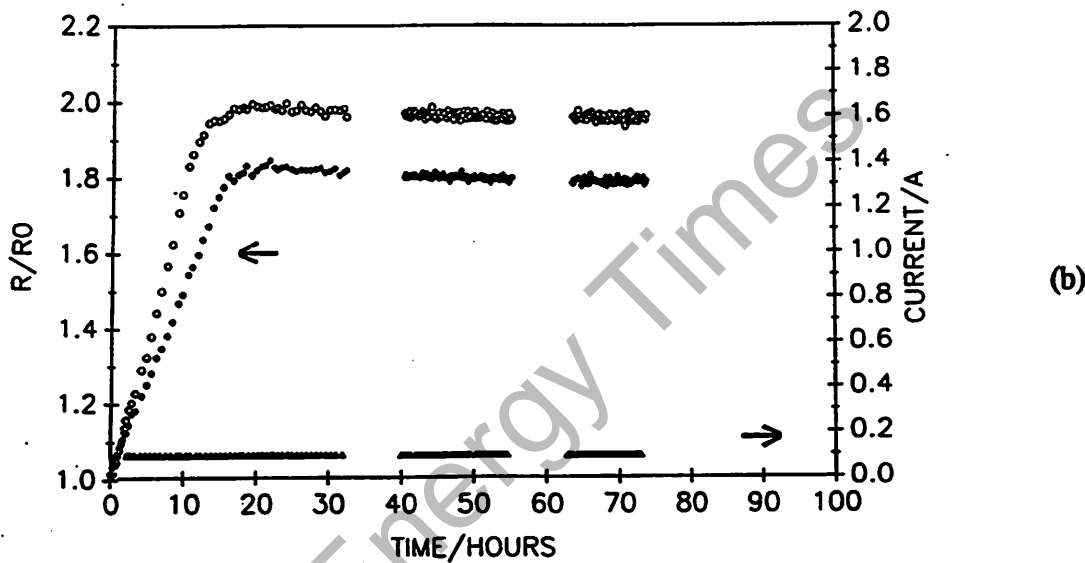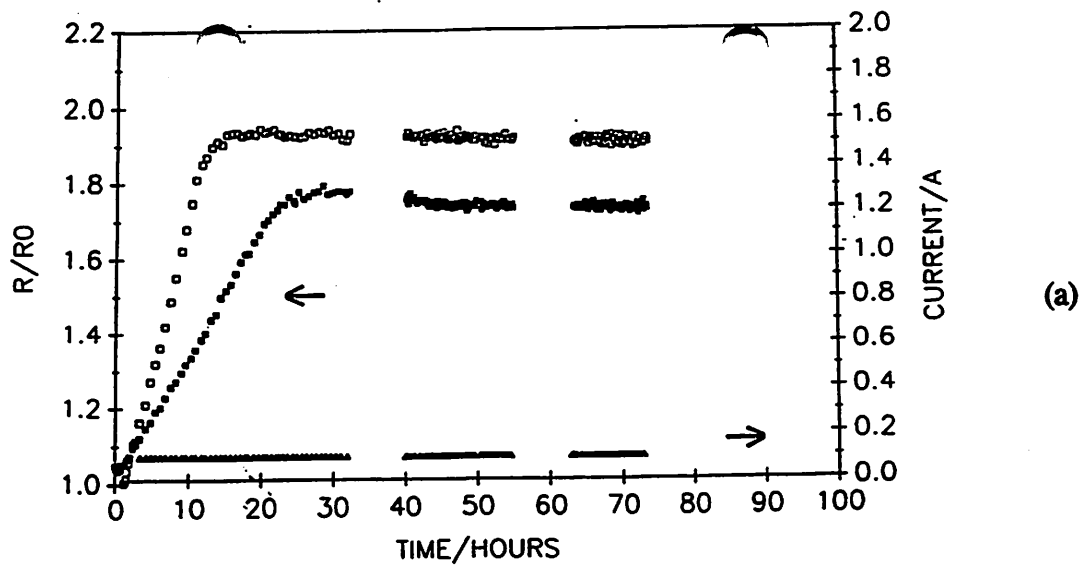
Fig. 13 - Resistance ratio (R/R₀) vs. time for NRL palladium rod cathodes (a) unannealed electrodes with elongated grains, (b) annealed electrodes with an average grain size of 44 μm, (c) annealed electrodes with an average grain size of 600 μm. Open symbols - deuterium, closed symbols - hydrogen

33
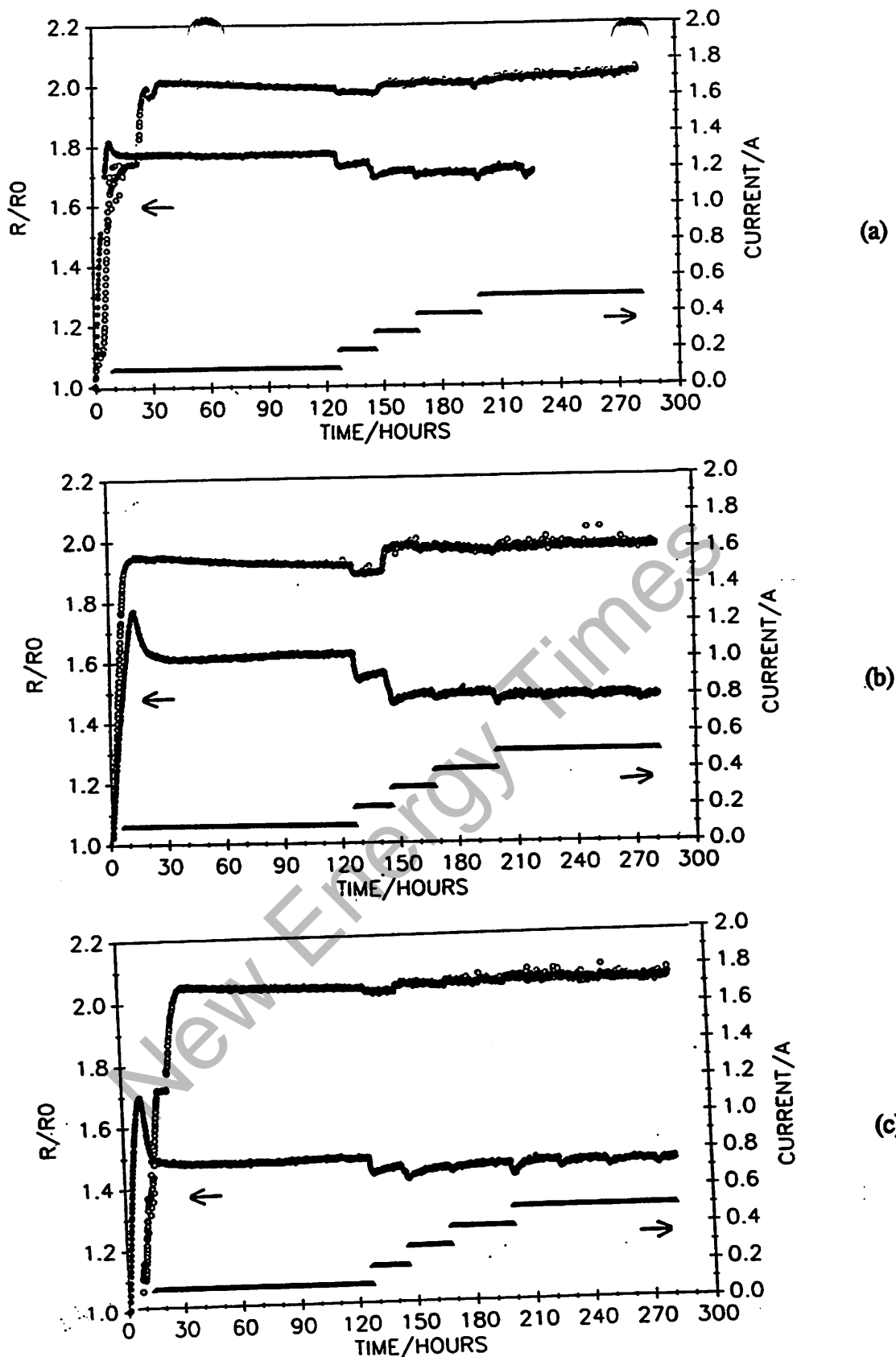
Fig. 14 - Resistance ratio (R/R_0) vs. time for NRL palladium plate cathodes (a) unannealed electrodes with elongated grains, (b) annealed electrodes with an average grain size of 44 μm, (c) annealed electrodes with an average grain size of 600 μm. Open symbols - deuterium, closed symbols - hydrogen

34

electrode processing (#93080602 and #93080606). Moreover, the resistance of the palladium plate cathodes showed the appropriate dynamic response to current necessary to attain high loading.

As predicted, deuterium loaded more slowly in both rod and plate cathodes with a large grain morphology. Also, thin palladium plate electrodes loaded more rapidly to D(H)/Pd ~ 0.7 than 0.4 cm diameter palladium rod electrodes with comparable grain sizes. The latter can likely be attributed to the more uniform cross-section of the plate electrodes and to their higher surface area to volume (A/V) ratio. The influence of the A/V ratio on loading palladium with hydrogen to the β-phase had been observed by Hoare [31] who compared loading ratios in foils, wires and beads in an acid solution.

As a result of the studies on palladium rod and plate electrodes with different microstructures, NRL concluded that increasing the average size of grains in palladium cathodes to around 600 μm generally slowed the rate of loading, and that this was probably useful for increasing the degree of loading. In addition, hydrogen loading experiments in both rod and plate electrodes provided evidence that reducing the strain in the palladium led to higher loading. However, high deuterium loading, where D/Pd $\geq$ 0.9, was still not achieved. The difficulty, in loading palladium rod cathodes with deuterium to high D/Pd atomic ratios, was not anticipated when the NRL electrochemical experiments began since results from NAWC implied that loading was under control. However, results subsequently published by Riley et al. [32] and reported by SRI (and eventually published [33]) supported NRL's experimental evidence that attaining high D/Pd loading ratios in palladium cathodes was difficult.

To understand what was affecting the cathodes' inability to load, electrodes and electrolyte from the aforementioned loading experiments were examined by x-ray photoelectron spectroscopic (XPS) analysis and inductively-coupled plasma (ICP) atomic emission spectroscopic analysis, respectively. XPS analyses were carried out to learn what had deposited on the palladium during an electrolysis experiments. As-received electrodes had only palladium, oxygen and carbon on their surfaces. Used electrodes had silicon, oxygen, carbon, copper, zinc, calcium and sulfur on their surfaces. Often, surface films on the palladium were so thick (100s of Å) that no palladium could be detected in the near surface region. A more detailed discussion of the XPS results can be found later in this report. Similar types of surface films on palladium cathodes run in D_2O electrolysis experiments had been described in the literature [34-36]. Some species observed on the cathode were likely leached out of the borosilicate-glass cells by contact with the warm, highly alkaline electrolyte over the prolonged period of the experiments (~620 hours and ~450 hours for the rod and plate experiments, respectively).

It was generally recognized that electrolyte impurities, as well as those in the bulk palladium, could affect the level of deuterium and hydrogen loading. As a result, ICP analyses were carried out on the electrolyte solutions to determine what impurities were introduced during the electrolysis. An analysis looked for fourteen elements that were copper, zinc, iron, niobium, silicon, calcium, boron, magnesium, nickel, sodium, potassium, tantalum, platinum and aluminum. Six of these elements were found at a concentration level of 1 ppm or higher - these were silicon, boron, sodium, potassium, niobium and aluminum (the latter was deliberately added to increase loading). Of these, only silicon was detected (10-30 ppm) in freshly prepared electrolyte. At first, it appeared that silicon was added to the deuterium oxide as an impurity in the lithium foil since an analysis (Table 3) of the foil (lot #G21C01) indicated that silicon was an impurity present at the 100 ppm by weight concentration level. Later, a calculation showed that 100 ppm silicon impurity in the lithium foil yields 0.07 ppm silicon in a 0.1 M LiOH solution. Thus, the silicon detected by ICP must have come from the deuterium oxide glass bottle and from the cell.

Table 3 - Analyses of NRL Cell Components Provided by Suppliers
(concentration in ppm by weight)

Element	Pt 99.9% wire, gauze typical	Nb mesh typical	Li 99.9% foil lot # G21C01	lot # J20D07	lot # H08E7	lot # L27D09
Ag	3					
Al	<1	<10	14	9	2	8
Au	30					
B	2	5				
Ca	<1	<10	84	78	102	65
Cl			30	20	20	30
Cu	6	20	20	20	20	20
Fe	20	<10	3	4	1	9
Ir	30					
K	<1		3	2	1	2
Mg	<1	<10	8	5	3	6
N		25	43	15	100	136
Na	<1		74	90	128	57
Ni	5	<10				
Os	10					
Pd	50					
Rh	70					
Ru	3					
Sb	10					
Si	<1	<10	100	8	8	8
Sn	20	<10				
Ta		135				
W		<100				
Total	259	185	379	257	385	341

ICP analyses also showed that silicon, boron and aluminum were consistently found at higher levels in LiOH than in LiOD indicating a greater solubility of the glass in LiOH. This was consistent with film thicknesses inferred from XPS data (i.e., apparent thicker films on electrodes run in LiOD). Of

particular interest was the finding that no copper, zinc, iron nor platinum were detected above 0.1 ppm in any of the solutions although these elements were easily seen on the palladium with XPS.

Elemental analyses of some individual components in an NRL electrochemical cell were provided by the manufacturers. Data from the analyses are summarized in Table 3. Concentrations are expressed as ppm by weight in the table. The table shows that some elements detected by XPS and ICP were found in individual cell components at the ppm concentration level. Some of these elements were calcium, copper, sodium and silicon. It was also interesting to note the variation in the elemental composition of the four batches of 99.9% lithium foil purchased from the same manufacturer. The first batch had an exceptionally high silicon content (100 ppm by weight) while batches 3 and 4 had high nitrogen contents (100 and 136 ppm, respectively). Batch #3 also had high sodium (128 ppm) and calcium (102 ppm) concentrations.

Experiments to Achieve High H(D)/Pd Loading

SRI had reported [19] that it was possible to load palladium with either deuterium or hydrogen to an atomic ratio H(D)/Pd $\geq$ 1 and to sustain this loading by careful control of the electrode pretreatment, the electrolyte composition, and the current density. As such, the cathode surface preparation was improved and the electrolyte purity was increased in the next series of NRL experiments to increase the loading in palladium cathodes to the H(D)/Pd ~ 0.9 level. Changes were made to decrease the thickness of surface films on the palladium that could prevent the cathode from loading. NRL palladium rod and plate cathodes used in this series were processed so that the grain size of the palladium was 600 μm based on the earlier NRL results.

The surface preparation of the cathode was altered to produce a cleaner surface at the start of each new loading experiment. This was done by carrying out the aqua regia etch of the cathode in a plastic (Nalgene, polymethylpentene) beaker instead of a borosilicate-glass beaker. The change was made because XPS analyses of cathode surfaces before and after the aqua regia etch in borosilicate-glass showed that a large (probably several atomic percent) amount of silicon was deposited on the palladium surface during the etch. Silicon deposition during the etch was eliminated by using a plastic beaker.

Electrolyte purity was increased in several important ways in this series of experiments. First, LiOD electrolyte solution was prepared with higher purity Ontario Hydro Virgin Reactor Grade Heavy Water (99.93% D) rather than Cambridge Isotope Laboratory (99.9%) D_2O. The substitution was made because the Ontario Hydro D_2O had a lower impurity content than the Cambridge Isotope D_2O. A generic analyses of the Ontario Hydro D_2O showed that it has ⟨0.05 ppm total organic carbon compared to 0.12-0.14 ppm total organic carbon in the Cambridge D_2O. Elemental analyses by ICP at Ontario Hydro also showed lower levels of metallic impurities in the Ontario Hydro D_2O, and anion analyses showed lower levels of chloride, sulfate and phosphate anions. Ontario Hydro was also the source of the deuterium oxide used by the SRI group in recent successful loading experiments.

Secondly, electrolyte purity was improved by decreasing its storage time in the brown glass bottles that originally contained deuterium oxide. This was accomplished by preparing the electrolyte immediately prior (within 24 hours) to a loading experiment and discarding any that was not used. Thirdly, either previously-used borosilicate-glass or quartz test tubes were used as electrolysis cells. This was done to reduce the amount of impurities that might be leached from new borosilicate-glass cells by the alkaline electrolyte. Finally, the anode material was changed from platinum-clad niobium mesh to platinum wire or platinum gauze in some experiments. This change was made to eliminate the thin film of platinum and niobium metal from dissolving in the electrolyte and depositing on the cathodes. ICP

analyses of electrolyte from a new series of cells that incorporated the changes mentioned showed lower concentrations of Si, B, Na, K, Nb and Pt. XPS analyses of cathode surfaces from cells with pure platinum anodes also showed that no niobium was present.

In all, ten electrochemical loading experiments were carried out in this series - six with hydrogen and four with deuterium. All ten of these cathodes were successfully loaded into the β-phase of palladium. Hydrogen and deuterium loading generally reached H/Pd and D/Pd levels of 0.85-1.00 and 0.85-0.90, respectively. Moreover, the resistance of three out of four of the cathodes loaded with deuterium exhibited the dynamic response to current necessary for high loading, and indictative of a promising material for generation of anomalous effects.

Thus, by the end of 1993 NRL researchers had acquired the ability to successfully load NRL palladium cathodes with either hydrogen or deuterium. The apparent keys to the achieving high levels of loading were (1) using large grain size palladium cathodes and (2) doing clean electrochemical experiments. The latter was one of the initial goals of NRL researchers.

During 1994, eleven more deuterium loading experiments were carried out on NRL palladium cathodes in alkaline electrolyte. Five out of seven (71%) of these cathodes, run under the usual conditions, loaded into the β-phase (cathodes #93101906, 94061005, 94061006, 94021005, 94021006) while the other two cathodes (#94021001 and 94021002) failed to load beyond a D/Pd ~ 0.7. The other four cathodes that didn't load into the β-phase were run in experiments where there was variation in the usual conditions. The experimental variations included (1) substituting less pure Cambridge Isotope Laboratory deuterium oxide in one experiment for the high purity Ontario Hydro deuterium oxide, (2) reusing a platinum-clad niobium and a platinum anode without acid cleaning to see whether the anodized surface layer formed in a previous experiment would slow further metal dissolution and (3) using a cathode annealed at SRI under their usual conditions (in vacuum $< 10^{-5}$ torr at 850°C for 4 hours). The four cathodes used in the unsuccessful loading experiments were coded #93101904, #94061001, #94061004, and #94021004, respectively.

Figure 15 shows the progress made in loading NRL palladium cathodes with deuterium into the β-phase (D/Pd $\geq$ 0.75). In comparison, SRI recently reported [33] that in experiments representing their "best efforts" to attain high deuterium loading, 57% of the cathodes achieved a D/Pd loading of 0.9 or better, and 83% loaded into the β-phase. Thus, when applying SRI's experimental protocols, NRL could reproducibly attain high deuterium loading in NRL palladium cathodes. The degree of reproducibility was nearly comparable to that achieved by SRI.

Calorimetric/Radiation Measurements. Calorimetric measurements on NRL palladium rod cathodes were made in isoperibol calorimeters. Calculations of excess power were made once the current applied to the cell was increased to 500 mA or more. For cathodes with a surface area 4.5 cm^2, this corresponded to current densities of at least 100 mA cm^{-2} on the cathode and electrochemical input powers to the cell of 1-2 watts. The excess power calculated for both the hydrogen and deuterium-loaded cathodes ranged from 0.80-1.24.

Eight NRL palladium cathodes were found to produce power in excess of the input power at levels of 10% or more. These cathodes are identified in Table 4 and the level of "excess power" produced is shown. As shown in the Table, four of the cathodes were run in D$_2$O electrolysis experiments and four were run in H$_2$O electrolysis experiments. Resistance measurements indicated that only three of the cathodes loaded into the β-phase. Only one of the "highly-loaded" cathodes was run in D$_2$O.
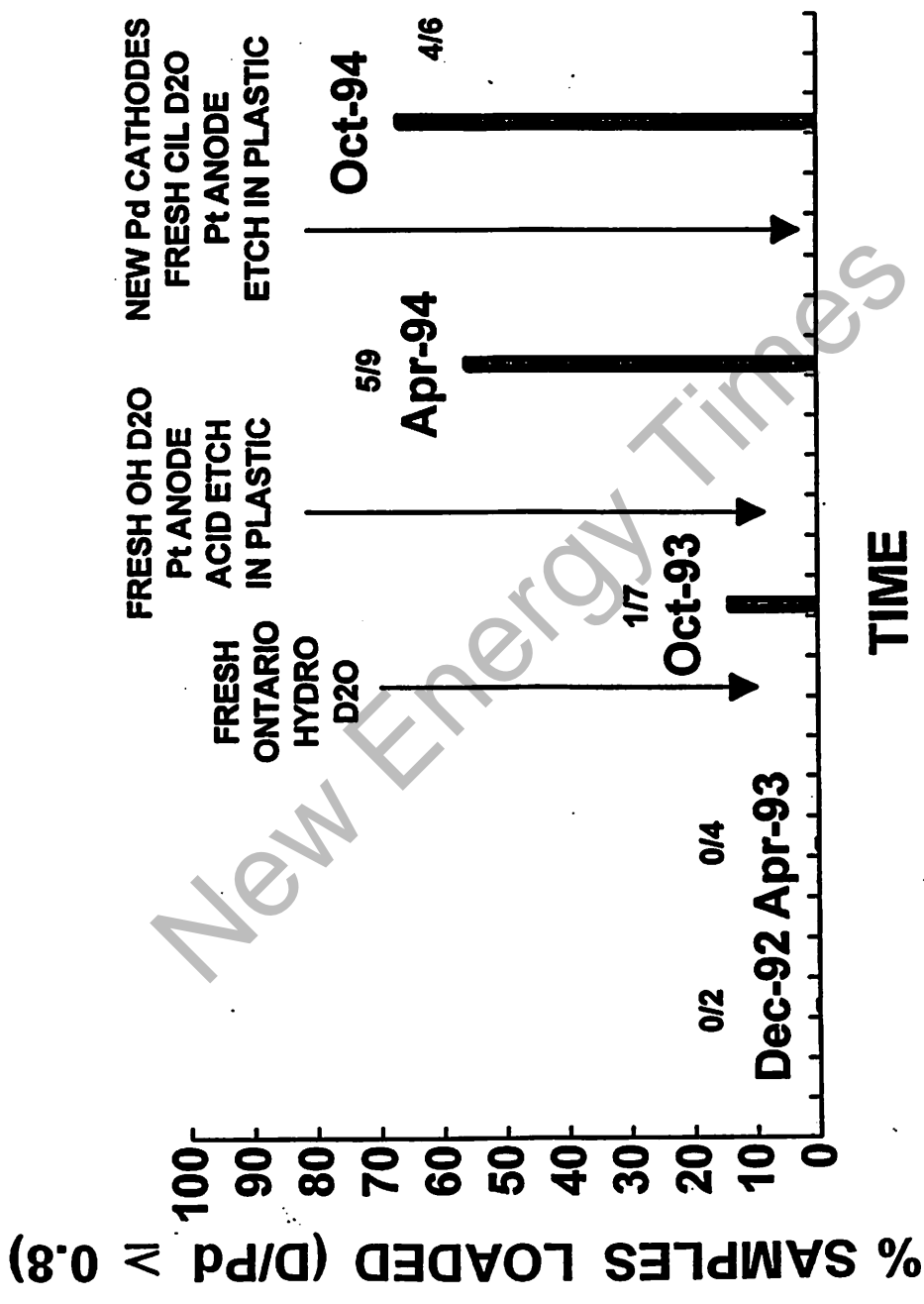
Fig. 15 - Progress in loading NRL palladium cathodes with deuterium

Table 4 - Excess Power Determinations on NRL Palladium Rod Cathodes

Experiment	Cathode	Code	Electrolyte	Input Power (W)	Excess Power (mW)/%	D(H)/Pd
4_1	Pd_G	93020901	0.1M LiOD/D_2O	1.7	200/12	.7
4_2	Pd_H	93020902	0.1M LiOD/D_2O	1.6	380/24	.7
	Pd_H	93020902	0.1M LiOD/D_2O	4.1	615/15	.7
5_1	Pd_E	93021701	0.1M LiOH/H_2O	1.7	200/12	.7
5_2	Pd_C	93021702	0.1M LiOD/D_2O	1.7	290/17	.7
6_4	Pd_L	93060304	0.1M LiOH/H_2O	1.3	225/18	.7
8_1	Pd_U	93090301	0.1M LiOD/D_2O	4.0	400/10	.8
8_2	Pd_V	93090302	0.1M LiOH/H_2O	1.3	140/11	1.0
	Pd_V	93090302	0.1M LiOH/H_2O	6.5	780/12	1.0
8_5	Pd-Y	93090303	0.1M LiOH/H_2O	1.3	140/11	.9

A statistical analysis of the calorimetric data showed that temperature fluctuations caused a 5% uncertainty in the measurements at an input power of 1.6-1.7 W. At input powers of 4 W and 6.5 W the uncertainties increased to 7 and 10%, respectively. Assuming a normal distribution of errors in measurement, the percentages translate into the following uncertainties at the 99% confidence level (three sigma) - ± 255 mW, ± 870 mW and ± 1950 mW for input powers of 1.7 W, 4.0 W and 6.5 W, respectively. Thus, the "excess powers" calculated for all but two of the cathodes were not found to be statistically significant. The "excess powers" calculated for the two remaining deuterium-loaded cathodes (#93020902 and #93021702) were marginally significant. However, the fact that these cathodes didn't appear to be highly-loaded renders the calorimetric results improbable. Temperature fluctuations were likely greater than usual during these experiments or another unidentified source of error increased the uncertainty level of the calorimetric measurements.

Radiation measurements were made during these electrochemical experiments using the germanium gamma-ray detector. No radiation above the background level was measured and no new peaks were noted in the gamma-ray spectra.

Palladium/10% Silver Cathodes

The palladium/10% silver alloy was examined at NRL because Fleischmann and Pons were supposedly [37] carrying out successful experiments with this material. (Two samples of "palladium/silver" alloy from Fleischmann and Pons were supplied to NAWC and SRI. Both of these samples turned out to be palladium/cerium when analyzed.) Silver forms a substitutional alloy with palladium; alloying with silver expands the palladium lattice [29]. Alloys are also used to prevent cracking of the palladium lattice during loading due to the increased lattice expansion in the material. In addition, alloying increases the hardness of the material and, thereby, slows the rate of loading [38].

Metallurgy. Palladium/10% silver cathodes were produced and characterized at NRL during the summer of 1992. Only a single batch of material was made. ICP optical emmision spectroscopic analysis (Shiva Technologies, Inc., Syracuse, NY) showed that the composition of the material was 10.4% silver by weight. The as-prepared material was not analyzed further. Palladium sponge (Johnson Matthey, "99.999%") was used to prepare the material which was made into rod-shaped electrodes 0.4 cm in diameter. Cathodes 3.5 cm in length were used at NRL and cathodes 1.5-2.0 cm in length were used at NAWC. The electrodes were machined to have rounded ends and grooves as shown in Figure 4. All palladium/10% silver cathodes were annealed at 650°C in vacuum for two hours. These annealing conditions produced cathodes with an average grain size of 40 μm.

A separate metallurgical study was undertaken to compare the grain growth behavior of palladium/10% silver alloy and pure palladium. Grain growth characteristics at a deformation level of 80% cold-rolled are shown in Figure 16 for two temperatures, 650°C and 950°C. Corresponding microhardness plots are shown in Figure 17. From Figure 17 it is clear that as grains grow, hardness decreases. The rate of grain growth in palladium/10% silver alloy is much slower than pure palladium. Typical examples of optical micrographs of palladium/10% silver alloy annealed at 1100°C are shown in Figure 18 whereas micrographs of pure palladium annealed at 650°C are shown in Figure 19.

Loading Experiments. Four palladium/10% silver cathodes processed at NRL were used in two separate loading experiments carried out in 1992. In each experiment, one electrode was used in a heavy water cell and the second electrode was used in a light water cell. The two cells, containing different electrolytes, were connected electrically in series. Experimental details and results of experiments on NRL palladium/10% silver cathodes can be found in NRL laboratory notebooks # N-7661 and N-7662 assigned to Dr. Dawn Dominguez. The notebooks cover the time from 2-10-92 to 1-14-93.

As usual, loading was monitored *in situ* by measuring the change in the axial resistance of the cathode with deuterium or hydrogen content. The average specific resistance and resistivity of the palladium/10% silver rod cathodes were 168±9 $\mu\Omega$ cm^{-1} and 21 $\mu\Omega$-cm, respectively. The latter was a little low compared with the literature value of 25 $\mu\Omega$-cm at 300 K [39,40].

After charging the cathodes with an initial current density of 23 mA cm^{-2}, the resistance ratios reached their maximum values of 1.7 and 1.5 for electrodes loaded with deuterium and hydrogen, respectively. The maximum resistance ratio of 1.5 observed for a hydrogen-loaded cathode agreed with the value reported by Szafranski and Baranowski [25]. No literature data were found for a deuterium-loaded palladium/10% silver cathode.

Increases in the applied current did nothing to lower the resistance of any of the cathodes. Assuming that palladium/10% silver would have a resistance ratio-deuterium/hydrogen loading response similar to palladium, NRL researchers concluded that the palladium/10% silver failed to load into the β-phase with either deuterium or hydrogen. As such, it was decided that further experiments on palladium/10% silver cathodes would be curtailed until high loadings were achieved in palladium cathodes.

Calorimetric/Radiation Measurements. Calorimetric measurements on palladium/10% silver cathodes at NRL were made in isoperibol calorimeters. Calculations of excess power in the four cells were done once the applied current was increased to 500 mA or more. This corresponded to current densities of at least 100 mA cm^{-2} on the cathode and electrochemical input powers to the cells of 1-2 watts. The excess power calculated for both the hydrogen and deuterium-loaded cathodes ranged from 0.80-1.15 over a two month period. An explanation for "excess power" levels less than 1.00 was that the calorimeters leaked and the vermiculite insulation deteriorated from absorbed water. As such, the
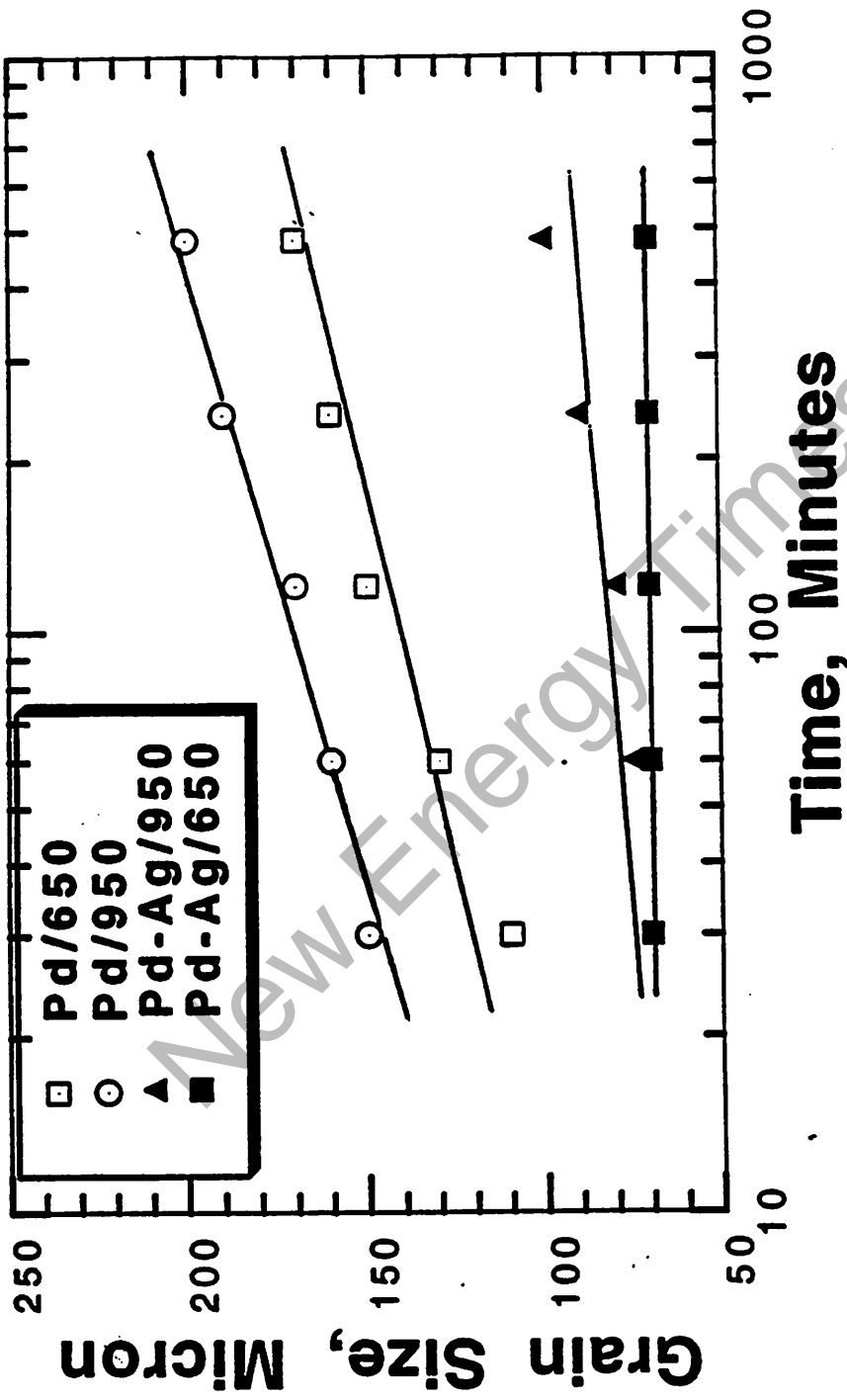
Fig. 16 - Grain growth vs. time plots for pure palladium cathode materials process at NRL. The starting materials were deformed to 80% by cold rolling and annealed at 650°C and at 950°C. Open symbols for palladium and closed symbols for palladium/10% silver

42
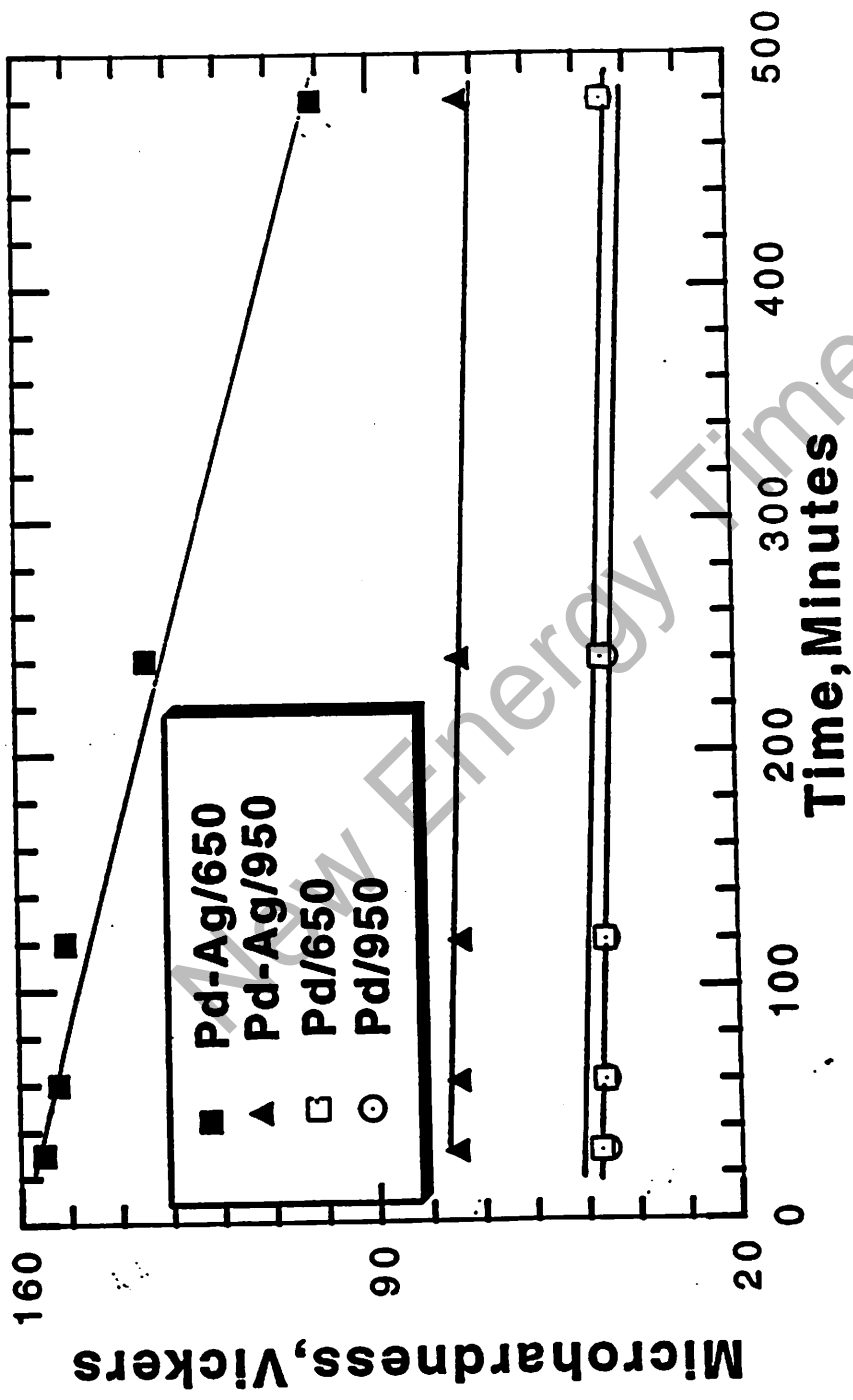
Fig. 17 - Microhardness vs. time plots for the same materials under similar conditions as shown in Figure 16

43

As-Rolled   **15 min**   **30 min**

100 µm

1 hr   **2 hrs**   **4 hrs**

Fig. 18 - Optical micrographs of palladium/10% silver alloy plate processed at NRL showing grain growth after annealing at 1100°C for different times
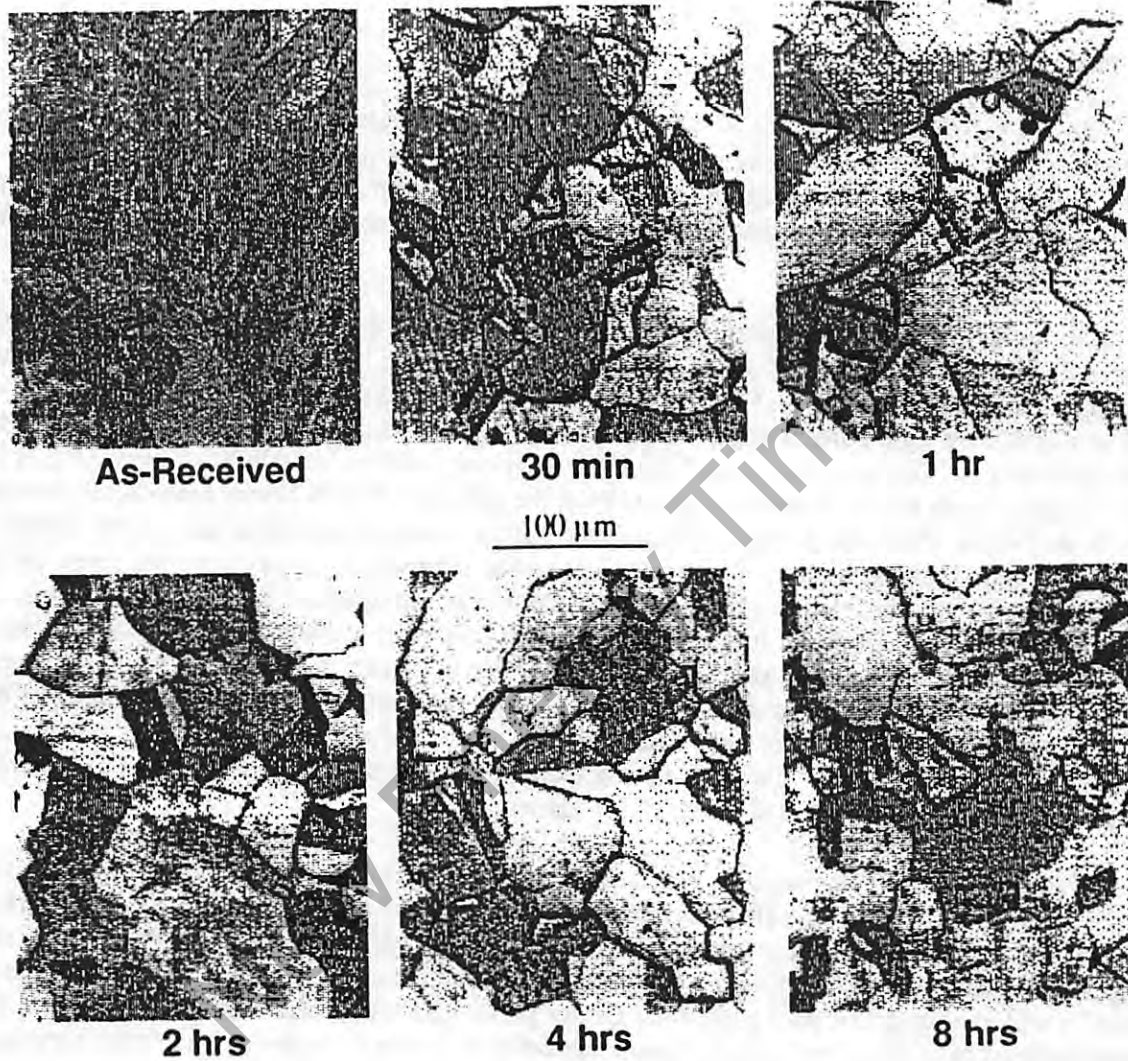
Fig. 19 - Optical micrographs of palladium rod processed at NRL showing grain growth after annealing at 650°C for different times

calorimetric measurements varied by ±20% of the input power. No excess power was measured for any of the cells containing NRL palladium/10% silver cathodes beyond the ±200 mW level of accuracy.

Radiation measurements were made during these electrochemical experiments using the germanium gamma-ray detector. No radiation above the background level was measured and no new peaks were noted in the gamma-ray spectra.

Palladium/Boron Cathodes

Alloying palladium with boron was done based on positive results with boron (B_2O_3) additions to the electrolyte at SRI. Also the literature [41 and references therein] indicated that alloying with boron expands the palladium lattice by forming an interstitial alloy with palladium; other metals form substitutional alloys. Preparations of the palladium alloy with low boron contents were attempted to keep within the miscibility regime.

Metallurgy. Three compositions of palladium/boron alloy were prepared at NRL and characterized during the summer of 1994. Individual samples were identified by a code name and distributed as shown in Appendix C. The three alloy compositions had nominal boron concentrations of 0.75, 0.50 and 0.25 weight percent boron. GDMS analyses of the three as-prepared materials can be found in Appendix A. The analyses showed the three alloy compositions actually contained 0.62, 0.38 and 0.18 weight percent boron. Selected elements from the palladium/0.62% boron analysis can be seen in Table 2. As before, electrode processing introduced copper, tungsten and platinum into the material. Additionally, magnesium, aluminum, silicon and calcium had relatively high concentration levels in the alloys. The material was made into rod-shaped electrodes 0.4 cm in diameter and 3.5 cm in length for NRL experiments. It was also made into 0.6 cm and 0.2 cm diameter rod electrodes for distribution to other laboratories (NAWC, SRI, Utah State and University of Utah). None of the electrodes were machined to have rounded ends or grooves because of the material's hardness. Annealing samples of the palladium/boron alloys at 650°C for two hours resulted in an average grain size of 90 μm for the material. At NRL, platinum wires for resistance measurements were then spot-welded to the electrodes directly or to short posts attached at the ends of the electrode.

X-ray diffraction studies were also carried out at NRL to characterize the three compositions of palladium/boron alloy. A Phillips diffractometer system was used for the x-ray studies with a generator setting of 50 kV, 30 mA and a copper target. Two distinct phases of the same cubic structure were found in all three compositions of the alloy. The diffraction patterns for the three alloy compositions are shown in Figure 20 with the pattern of pure palladium. Lattice parameters for the samples were measured. The two distinct phases have the same crystal structure but different lattice parameters. The lattice parameter in one phase remains constant with changes in the boron content of the alloy whereas the lattice parameter of the other phase increases with an increase in the boron content. As the boron content increases, the fraction of one phase decreases at the expense of the other phase, as expected. The change in lattice parameter with boron content happens in the phase where the starting lattice parameter is the same as pure palladium.

Samples of the three palladium/boron alloy compositions were also heated to 650°C for one hour and then quenched to freeze the structure into the single phase present at 650°C. The cooling rate during quenching (~ 10 s) of the alloy samples with 0.38 and 0.18% boron contents was not fast enough to freeze the structure, but the structure of the 0.62% boron sample was frozen into a single phase.
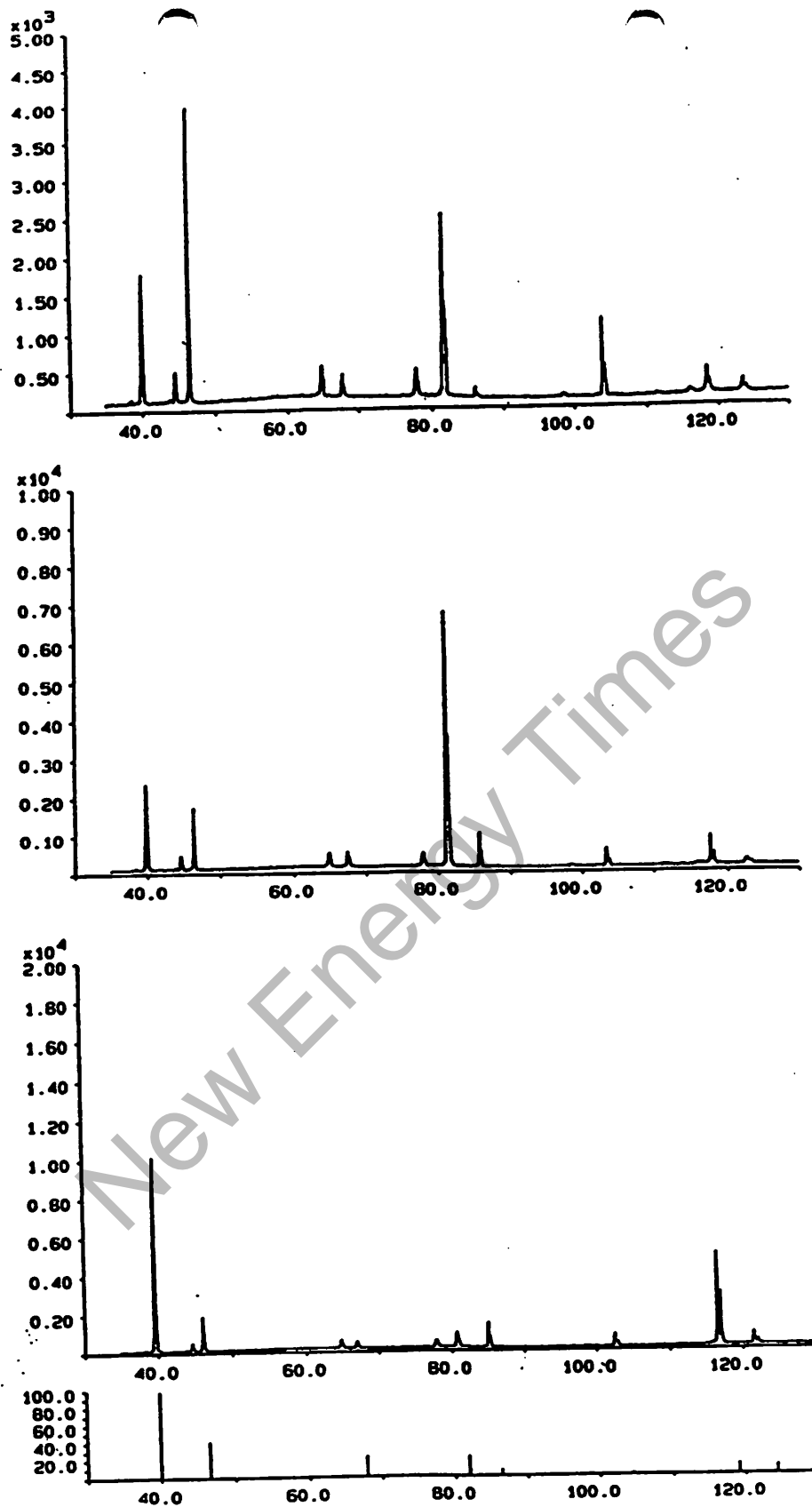
Fig. 20 - X-ray diffraction patterns of (a) palladium/0.18% boron, (b) palladium/0.38% boron, (c) palladium/0.62% boron, and (d) pure palladium. Diffraction patterns were obtained on a Phillips diffractometer with generator settings of 50 kV, 30 mA and a copper target

Only the palladium/0.62% boron alloy was studied under a transmission electron microscope. The sample was prepared by sectioning, grinding, electropolishing and ion milling processes. The final sample was 0.3 cm in diameter and approximately 150 Å thick. A transmission electron micrograph is shown in Figure 21 whereas Figure 22 shows the selected area diffraction (SAD) pattern. Figure 21 supports the x-ray diffraction data where two phases, one major and one minor, are observed. The minor phase is roughly 10 to 100 Å in diameter and has a lattice parameter larger than the major phase. The SAD pattern, Figure 22, shows rings slong with the main pattern. The rings refer to the minor phase whereas the main pattern refers to the major phase. Lattice parameters of the two phases measured from x-ray diffraction and SAD are consistent.

Loading Experiments. Two palladium/0.62% boron cathodes were used in loading experiments at NRL. Neither of the other two compositions of alloy was examined. The two palladium/0.62% boron cathodes were run individually in heavy water electrolyte. As usual, loading was monitored *in situ* by measuring the change in the axial resistance of the cathode with deuterium content. The average specific resistance and resistivity of the palladium/0.62% boron cathodes were 98 ± 2 $\mu\Omega$ cm and 12 $\mu\Omega$-cm, respectively. No literature value of resistivity for the palladium/0.62% boron alloy (or for the other two alloy compositions) was found. Its resistivity was not expected to differ much from palladium's, however. Experimental details and results of experiments on NRL palladium/boron cathodes can be found in NRL laboratory notebook # N-7818 assigned to Dr. Dawn Dominguez. The notebook covers the time from 10-24-94 to 6-30-95.

Palladium/0.62% boron cathodes loaded much more slowly (i.e., weeks) than pure palladium cathodes even with a slightly higher current density on the cathode (34 mA cm^{-2} vs. 23 mA cm^{-2} for palladium). This was anticipated due to the increased hardness of the alloy material. The cathodes loaded to a maximum resistance change of 1.9 that is close to the value 2.0 expected for deuterium-loaded palladium. The cathodes failed to load any further though the current density was increased to 500 mA cm^{-2}. Thus, assuming the resistance ratio-deuterium loading curve is similar to that of palladium, the palladium/0.62% boron alloy didn't load into the β-phase.

Two additional palladium/0.62% boron cathodes were used in NRL experiments setup by Dr. Melvin Miles of NAWC. These experiments were undertaken for the purpose of replicating excess power production from deuterium-loaded palladium/0.62% boron cathodes in the NRL heat-conduction calorimeters. The cathodes were assembled in NAWC-type cells using the procedures that led to excess power generation at NAWC. Since no resistance meaasurements were made on these cathodes, no loading information was acquired. No radiation measurements were made during these experiments either.

Calorimetric Measurements. Calorimetric measurements on palladium/0.62% boron cathodes were unsuccessful due to calorimeter problems (*vide infra*) that were not yet understood. However, the high sensitivity (± 1 mW) of the heat-conduction calorimeters permitted the observation of deuterium absorption into the cathodes. This was accomplished by measuring the difference between the output and input powers for the cells. With 30 mA applied current and cell voltages of about 3 volts, the initial input power to the cells was 45 mW (for about 40 hours). About one hour after the current was turned on, the output power for each cell stabilized at around 52 mW (heat sensor voltage for each cell ~5.5 mV x calibration constant 9.3 W/V). Thus, deuterium absorption in both cathodes appeared to be exothermic by about 7 ± 1 mW for 20 hours. This translated into a heat of absorption of approximately -6 kJ mole^{-1}. The value for the heat of absorption that was measured is about six times lower than that reported [42] in the literature for pure palladium (-35 kJ mole^{-1}). Although, this value could be different for palladium/boron, the data showed that the calorimeters were sensitive to ± 2 mW and that the heat of absorption could be measured.

0.2 μm
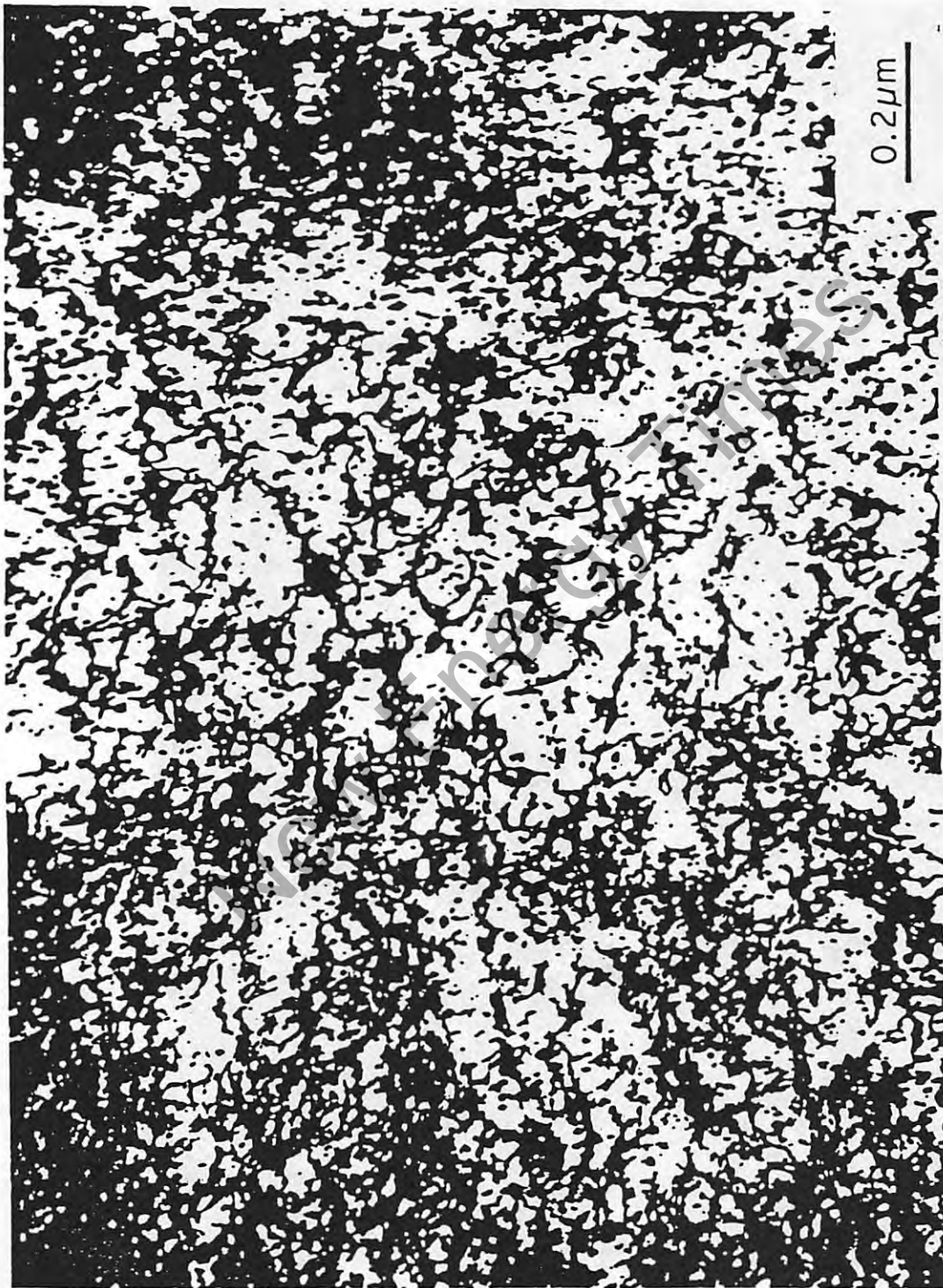
Fig. 21 - Transmission electron micrograph of palladium/0.62% boron showing two phases. The minor phase is roughly 10 to 100 Å in diameter
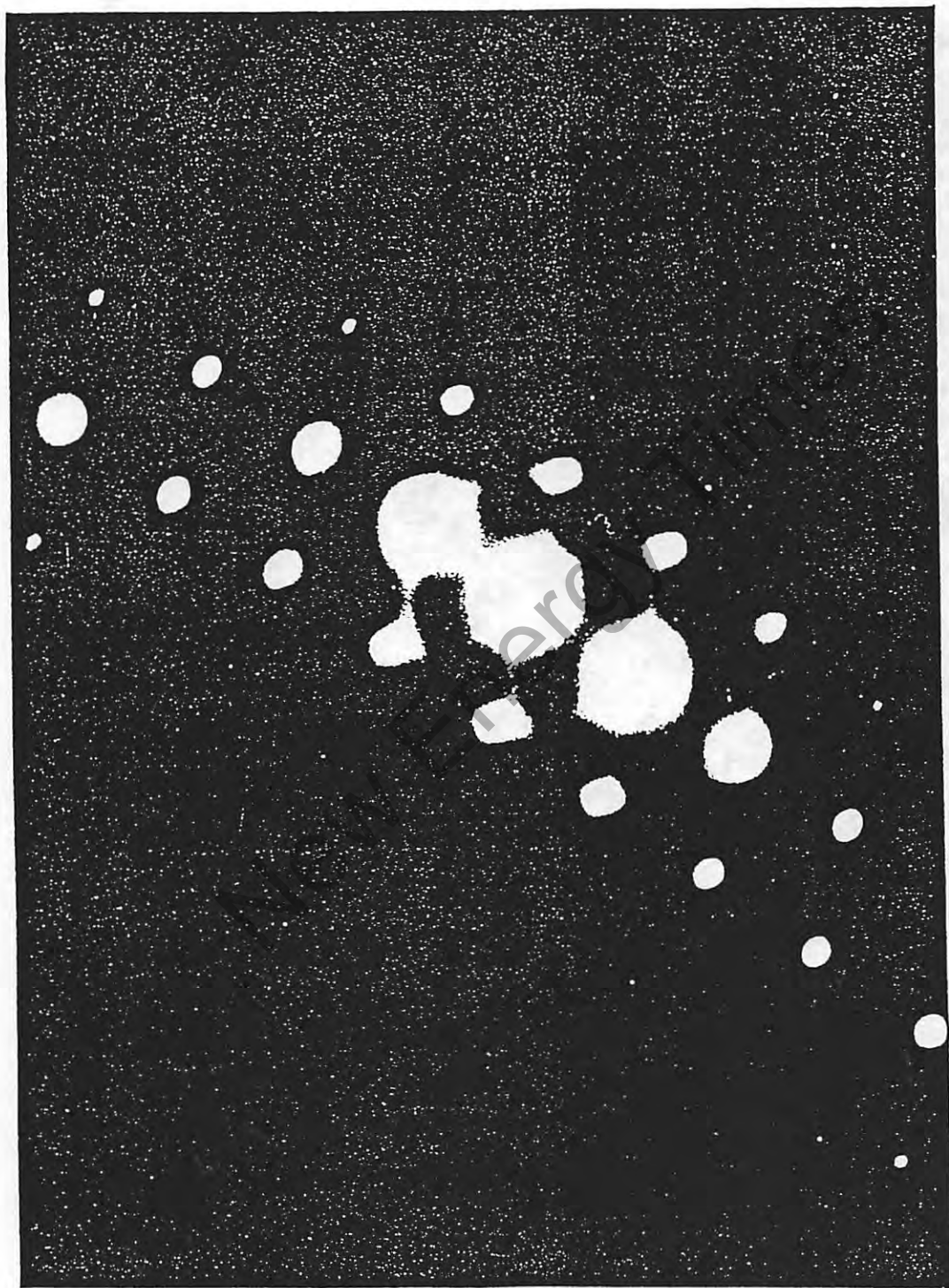
Fig. 22 - Selected area diffraction (SAD) pattern of the same area as Figure 21 showing rings along with the main diffraction spots. The rings represent the minor phase shown in figure 21

50

Metallurgy/Bulk Analyses. GDMS analyses of as-received palladium rod and wire can be found in Appendix A. Selected elements from the analyses can also be seen in Tables 5 and 6, respectively. Concentrations are again expressed as ppm by weight in the tables. As seen from the tables, the Johnson Matthey 0.1 cm diameter palladium wire (stock #10960, lot W12954) provided to NRL by NAWC was the highest purity material examined (including the NRL materials). The analysis indicated that the wire

Table 5 - Glow-Discharge Mass Spectroscopic Analyses of Commercial Palladium Rod Cathodes
(concentration in ppm by weight)

Element	Engelhard #3 99.9%	Johnson Matthey "Special batch"	Johnson Matthey 99.9%
B	140	23	4.1
C	<1.8	<1	<0.1
N	<0.23	<0.1	<0.05
O	<290	<20	<6
Mg	0.59	0.09	0.09
Al	12	1.1	7.6
Si	280	1.8	16
Ca	66	7.5	5.1
Cr	15	1.3	1.6
Mn	0.51	0.22	0.84
Fe	69	14	37
Ni	1.7	0.58	1.4
Cu	13	2.6	6.5
Zn	<0.021	0.55	3.6
Rh	<9.3	24	71
Ag	<.76	1.6	0.7
W	1.1	0.06	0.91
Pt	22	28	960
Total	930	128	1123

Table 6 - Glow-Discharge Mass Spectroscopic Analyses of Commercial Palladium Wire Cathodes
(concentration in ppm by weight)

Element	Johnson Matthey 99.9%	Johnson Matthey 99.997%	Johnson Matthey Miles (NAWC)	Good fellow 99.95%
B	17	0.01	0.007	2.5
C	<5	<1	<1	<1
N	<0.1	<5	<3	<0.1
O	<10	<20	<10	<10
Mg	0.29	0.008	0.009	0.04
Al	59	0.34	0.63	2.3
Si	67	43	3.5	6.6
Ca	7.3	0.11	0.29	<0.05
Cr	5.3	0.25	0.21	0.68
Mn	1.6	0.01	0.004	0.17
Fe	95	1.1	2.9	30
Ni	54	0.05	0.03	1.4
Cu	24	0.11	0.76	22
Zn	5.2	0.10	0.02	2.5
Rh	110	0.56	4.2	6
Ag	29	<0.1	0.45	13
W	1.4	0.15	0.10	0.2
Pt	1100	1.9	2.2	80
Total	1591	74	29	179

is 99.997% palladium. The next highest purity material is another batch of the same palladium wire (stock #10960, lot W7403) also from Johnson Matthey. Both had exceptionally low iron and platinum concentrations - even lower than the "99.999%" palladium sponge used as the starting material in the NRL preparations. The lot W7403 material had an elevated silicon content, however, which lowered its purity from the nominal 99.997% level to 99.99%.

The Johnson Matthey "special batch" was nominally a 99.99% pure, 0.4 cm diameter palladium rod material that was special-ordered by Fleischmann and McKubre (SRI). The material was designated "Type A" which meant it was supposed to be similar to the 1989 palladium that Pons

and Fleishmann used to obtain the excess power reported in their first manuscript. It was designed to have a low light element content (particularly, carbon) and a low platinum content. The GDMS analysis validated the design requirements.

Also noted in the tables is that the "99.9%" Johnson Matthey 0.1 cm diameter wire (stock #10280, lot K11C06) and 0.4 cm diameter rod (stock #98529, lot F13E05) were only marginally 99.9% materials. Both had extremely high platinum contents. The 0.3 cm diameter Engelhard 99.9% rod (designated batch #3 at SRI) and the 0.1 cm diameter Goodfellow 99.95% wire (#005150/11) had the purities advertised, however. The platinum concentration in the Engelhard palladium was comparable to that in the NRL palladium. The Engelhard palladium had higher boron, oxygen, aluminum, silicon and calcium contents than the NRL material, however. The Goodfellow 0.4 cm diameter, 99.95% pure palladium rod (#007940/5) was not analyzed by GDMS.

Optical micrographs of palladium samples from commercial sources are shown in Figures 23 to 33. These samples had gone through different thermomechanical treatments. For example, optical micrographs of Figures 23 and 24 show different grain morphology for two batches of palladium (rod and wire, respectively) obtained from Johnson Matthey. In one, the grains are relatively equiaxed whereas in the other they are elongated. In spite of the differences in grain morphology, these two samples were both heat-producers at NAWC. A micrograph of the Johnson Matthey "special batch" palladium rod in Figure 25 shows a grain morphology which is different from micrographs shown in Figures 23 and 24. The fine, equiaxed grains seen in Figure 25 developed as the result of annealing at 1100°C for 20 hours. The morphology of the grain depends on how much residual stress was in the sample before annealing, and on the annealing conditions. This is evident by comparing Figures 25-31. Annealing the 99.9% palladium samples at 1100°C for 20 hours produced large grains as shown in Figures 26-29 whereas annealing the 99.99+% palladium samples under the same conditions resulted in small or elongated grains as shown in Figures 30 and 31, respectively. Grain morphologies, illustrated by the micrographs of Figures 25-31, in different samples responded differently to annealing conditions based on the sample's processing history.

Optical micrographs were also obtained on different batches of Engelhard palladium from SRI. As seen in Figure 32, grain morphologies in the batch #1 and batch #3 materials are very similar although the batch #1 material generally loaded better [33] and produced excess power more frequently than did the batch #3 material. A micrograph of an actual heat-producing sample (designated P15 at SRI) of Engelhard batch #1 palladium also showed nothing unusual about its morphology.

As a result of the NRL metallurgical studies, a possible correlation was found between sample purity and the grain morphology produced on annealing at 1100°C for 20 hours. For example, in the high purity (99.99% or better) materials examined, hardly any grain growth occurred on annealing whereas the lower purity (99.9%) materials readily grew large grains. Very pure samples are expected to have very rapid rates of grain growth. Other factors such as the amount of deformation encountered during cold working and the grain size before cold working can have an adverse effect on grain growth. Examination of heat-producing palladium from NAWC (Figures 23 and 24) and SRI (Figures 32 and 33) showed nothing unusual about the grain morphologies of the materials.

Loading Experiments. Almost all of the commercial palladium cathode materials (except the Goodfellow 99.99+% palladium wire #005155/11 shown in Figure 31) were used in deuterium loading experiments. Experimental details and results of experiments on commercial palladium
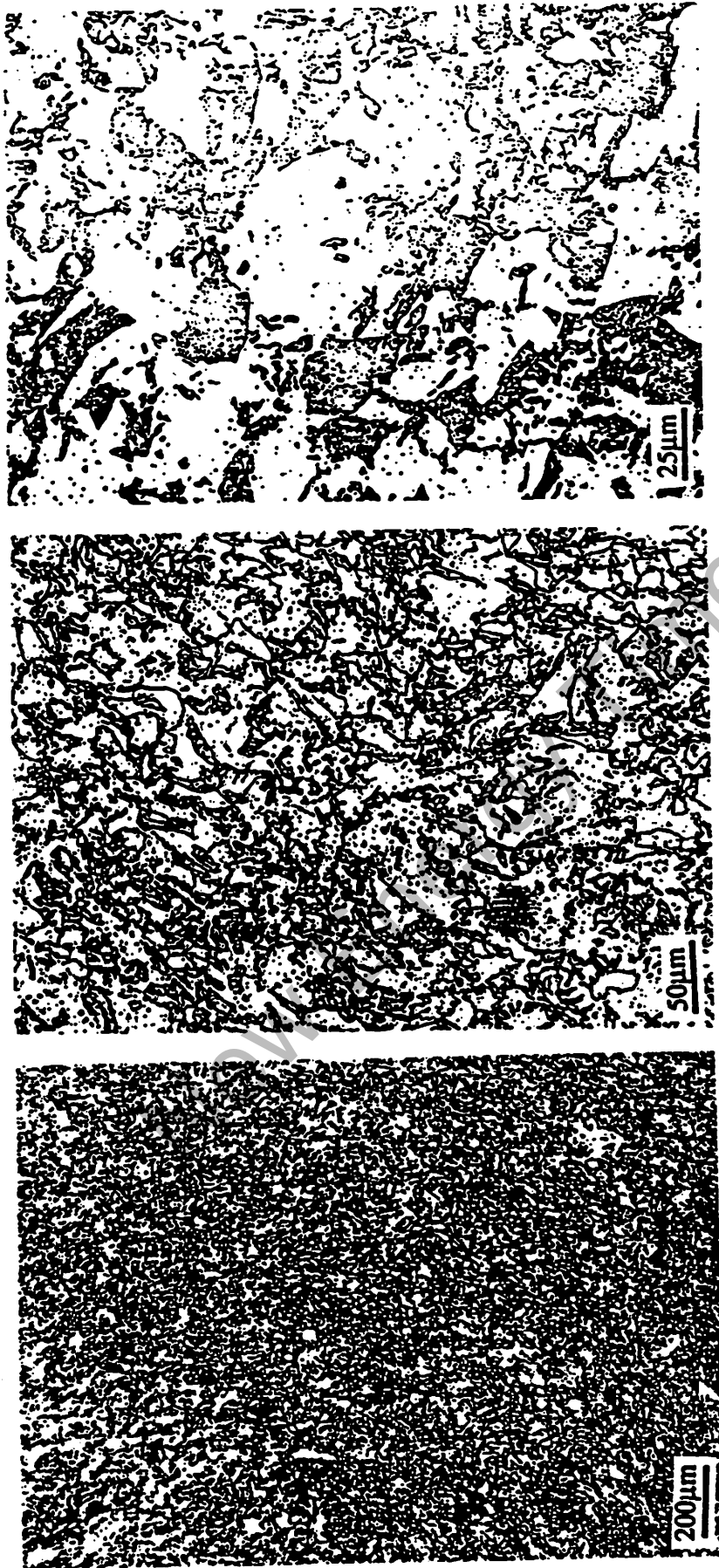
Fig. 23 - Optical micrographs of Johnson Matthey 0.6 cm diameter palladium rod (#12557B, lot 19638) obtained from Dr. Melvin Miles (NAWC) at different magnifications showing fine, relatively equiaxed grains. This sample was a heat-producer at NAWC
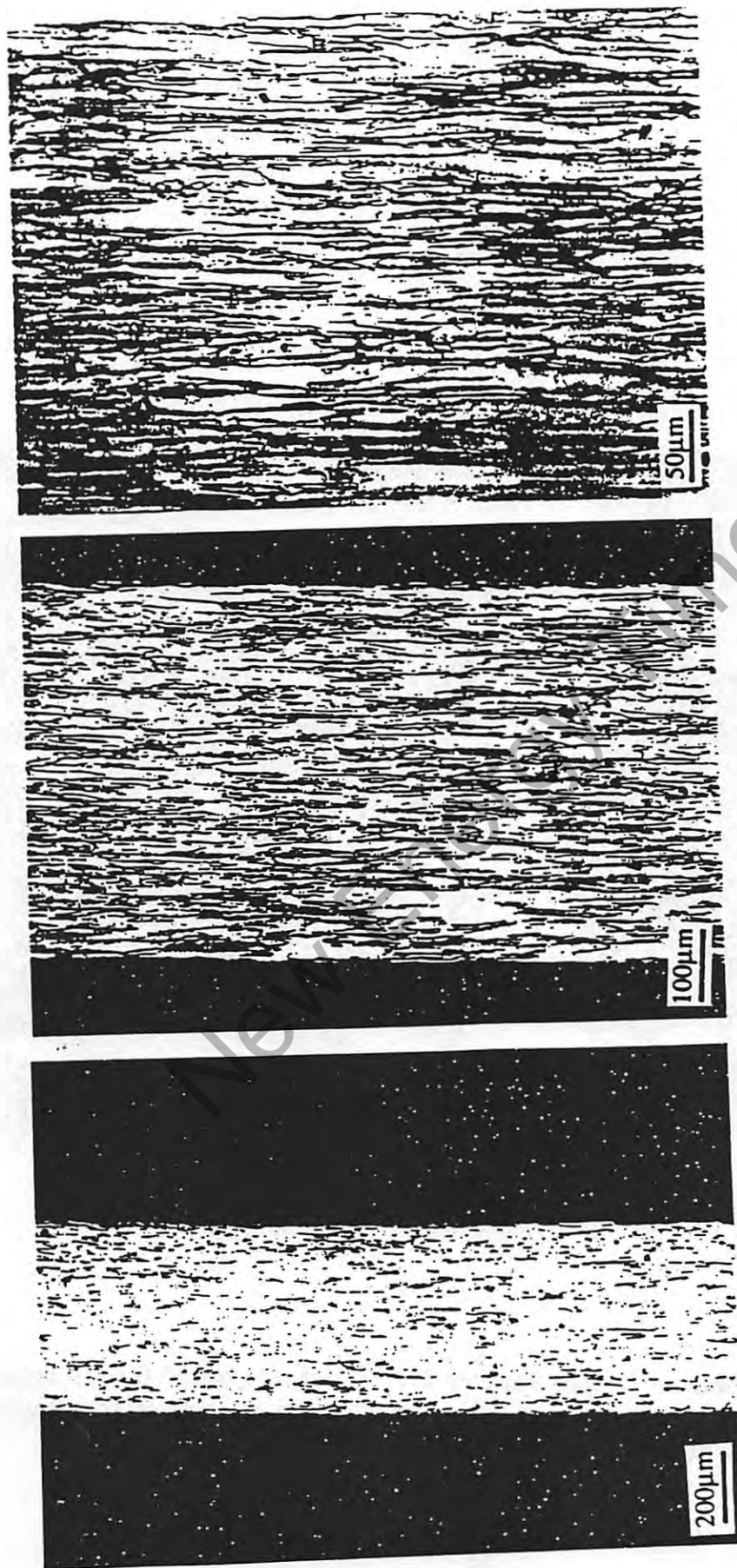
Fig. 24 - Optical micrographs of Johnson Matthey 99.997% 0.1 cm diameter palladium wire (#10960, lot W12954) in the as-received condition at different magnifications showing elongated grains. The material was supplied to NRL by Dr. Melvin Miles (NAWC). This material was a heat-producer at NAWC
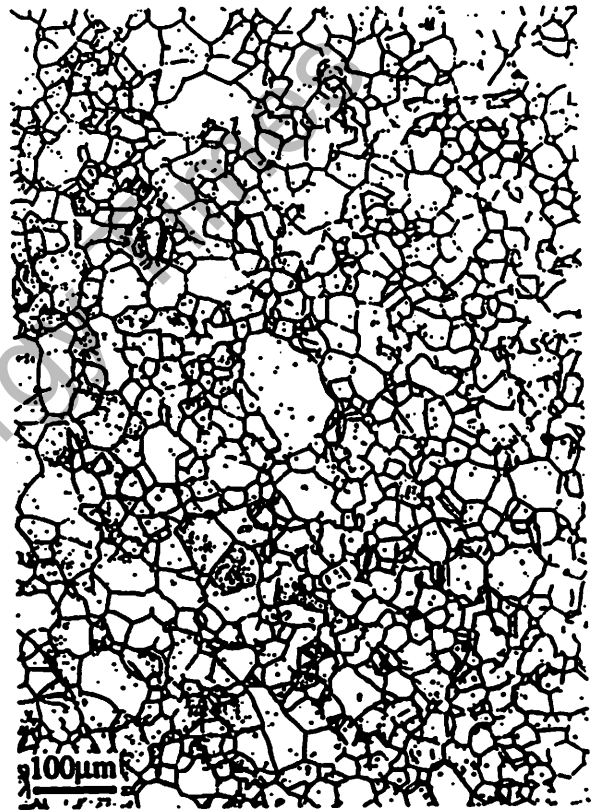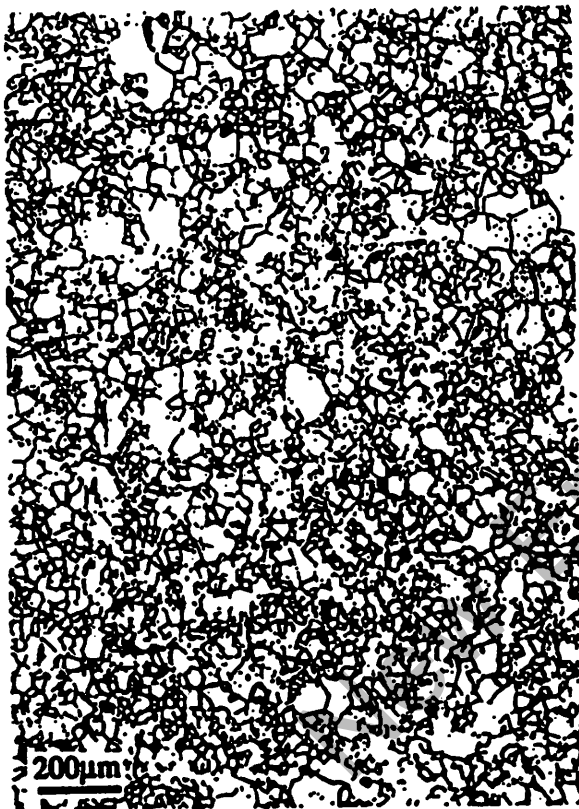
Fig. 25 - Optical micrographs of Johnson Matthey 99.99% "special batch" 0.4 cm diameter palladium rod in the as-received condition at different magnifications showing fine, equiaxed grains. The material was supplied to NRL from SRI
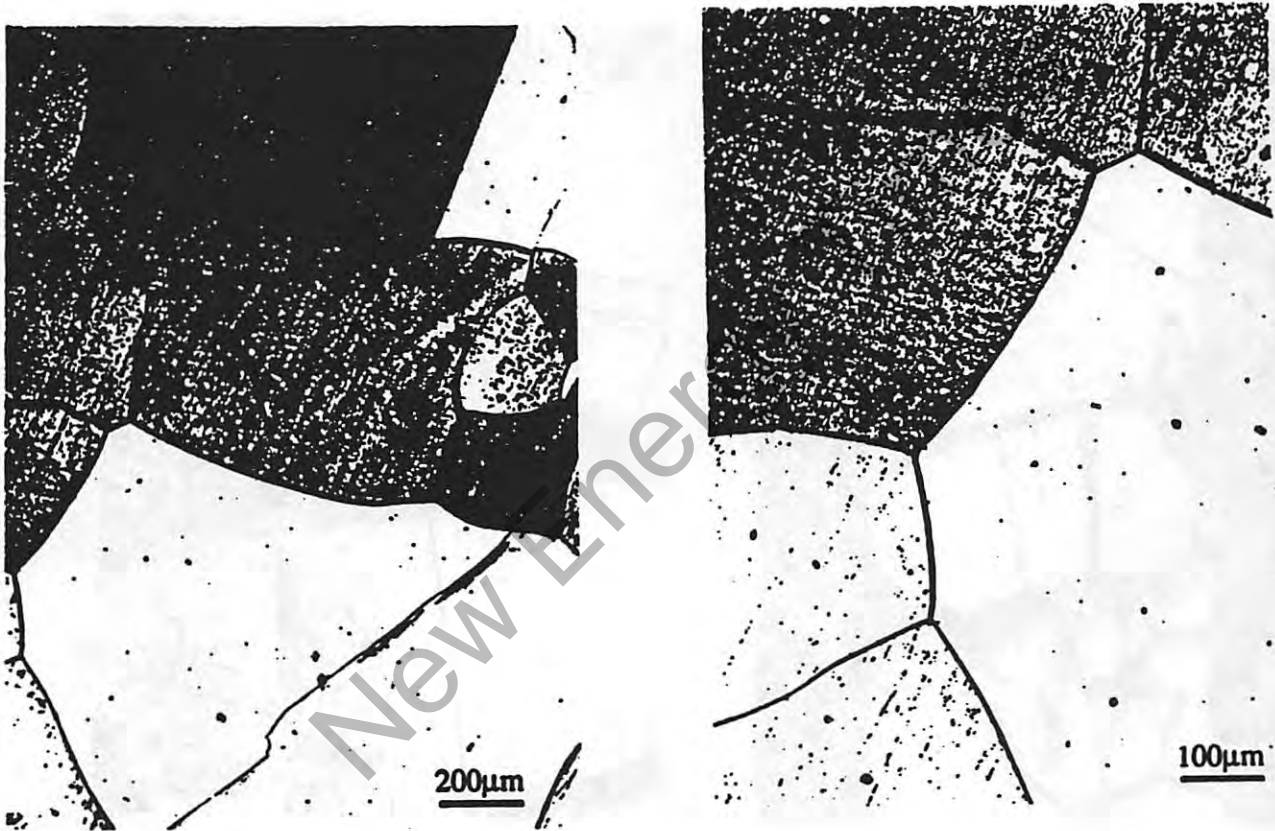
Fig. 26 - Optical micrographs of Johnson Matthey 99.9% 0.4 cm diameter palladium rod (#98529, lot F13E05) after annealing in vacuum ($< 10^{-5}$ torr) at 1100°C for 20 hours at different magnifications showing large grains

Fig. 27 - Optical micrographs of Johnson Matthey 99.9% palladium wire (#10280, lot K11C06) after annealing in vacuum ($<10^{-5}$ torr) at 1100°C for 20 hours at different magnifications showing large grains
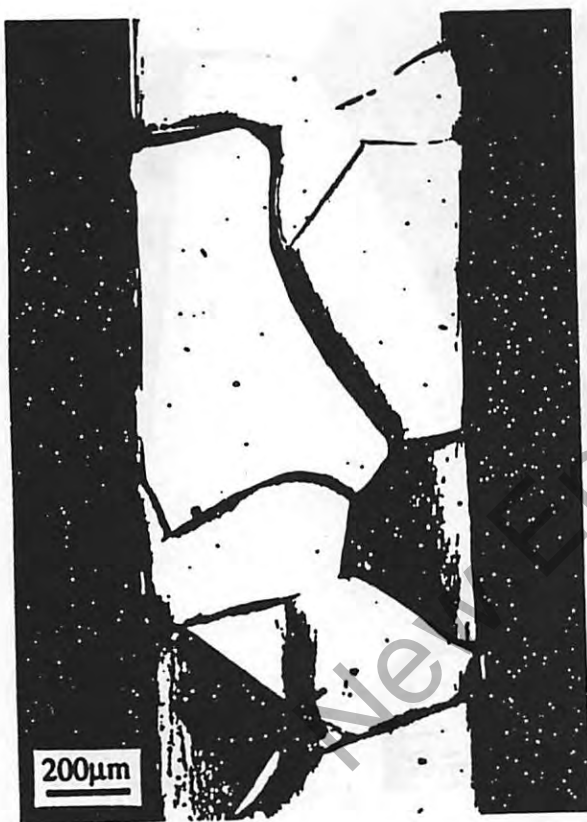
Fig. 28 - Optical micrographs of Goodfellow 99.95% palladium wire (#005150/11) after annealing in vacuum ($< 10^{-5}$ torr) at 1100°C for 20 hours at different magnifications showing large grains

Fig. 29 - Optical micrographs of Goodfellow 99.95% palladium rod (#007940/5) after annealing in vacuum ($< 10^{-5}$ torr) at 1100°C for 20 hours at different magnifications showing large grains
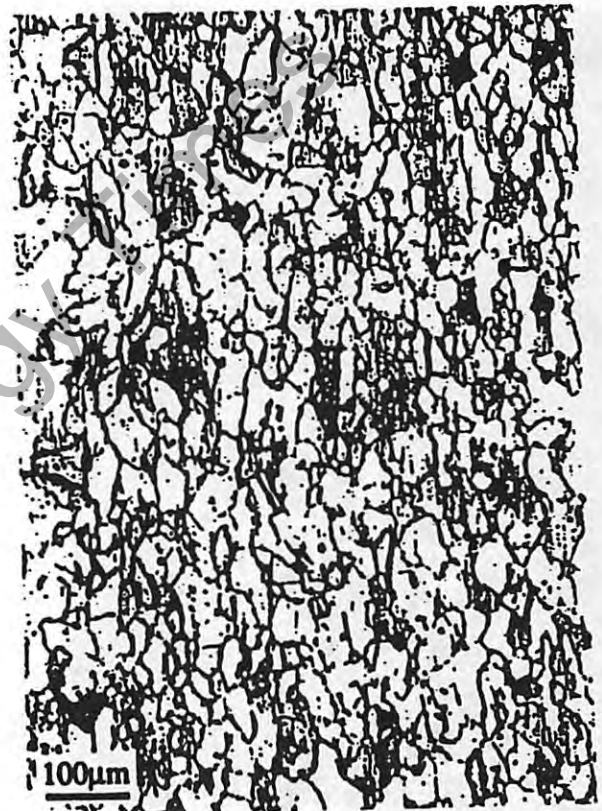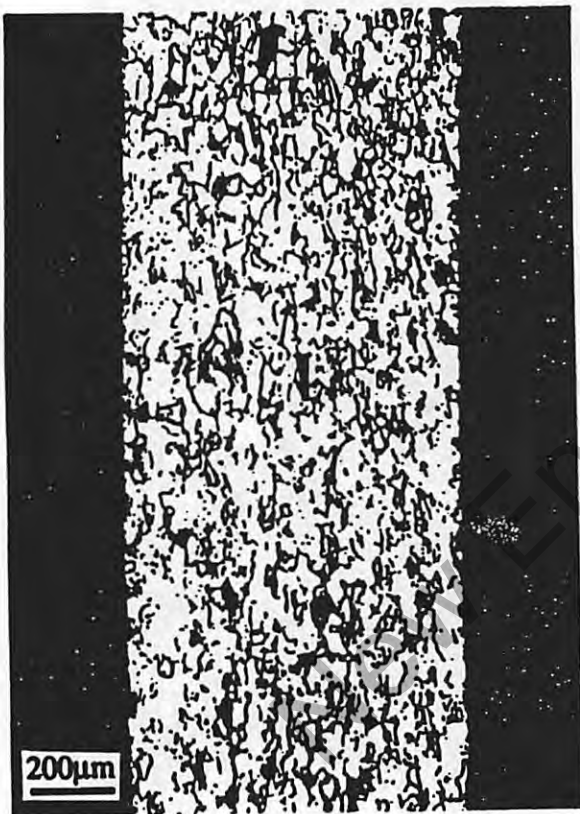
Fig. 30 - Optical micrographs of Johnson Matthey 99.997% palladium wire (#10960, lot 7403) after annealing in vacuum ($<10^{-5}$ torr) at 1100°C for 20 hours at different magnifications showing hardly any grain growth
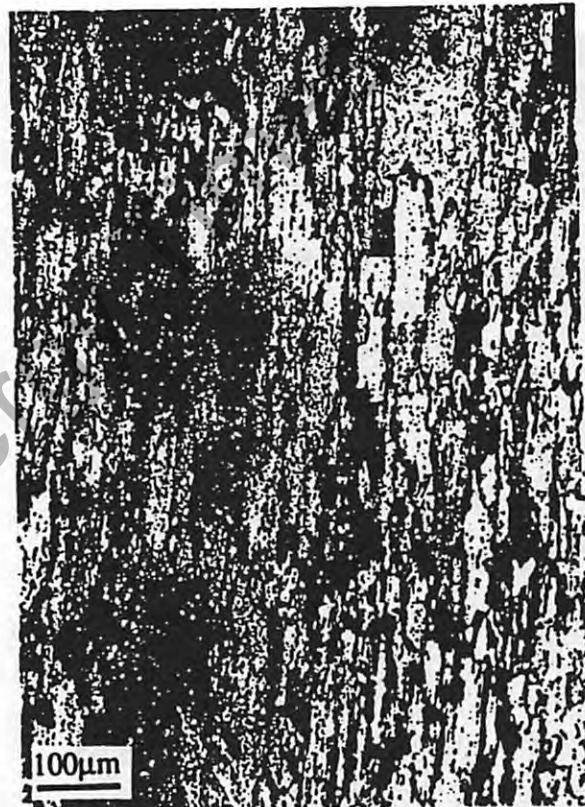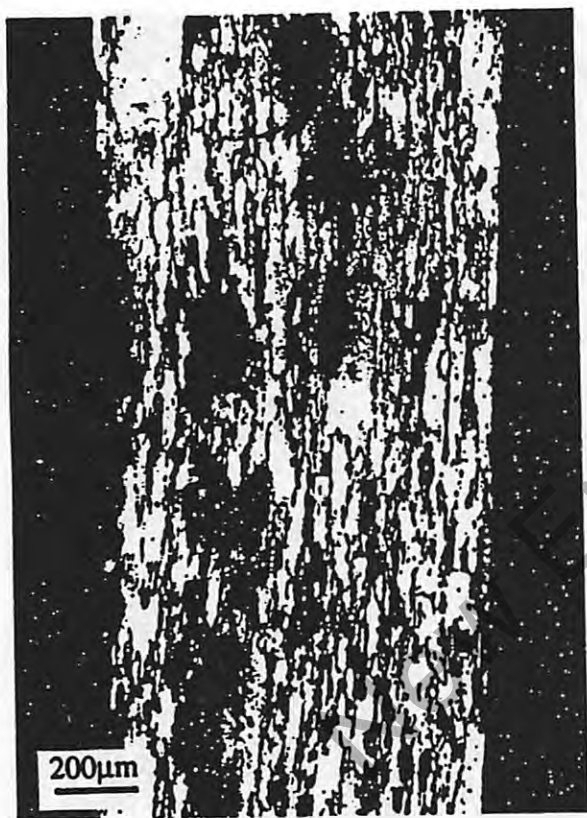
Fig. 31 - Optical micrographs of Goodfellow 99.99+% palladium wire (#005155/11) after annealing in vacuum ($<10^{-5}$ torr) at 1100°C for 20 hours at different magnifications showing hardly any grain growth
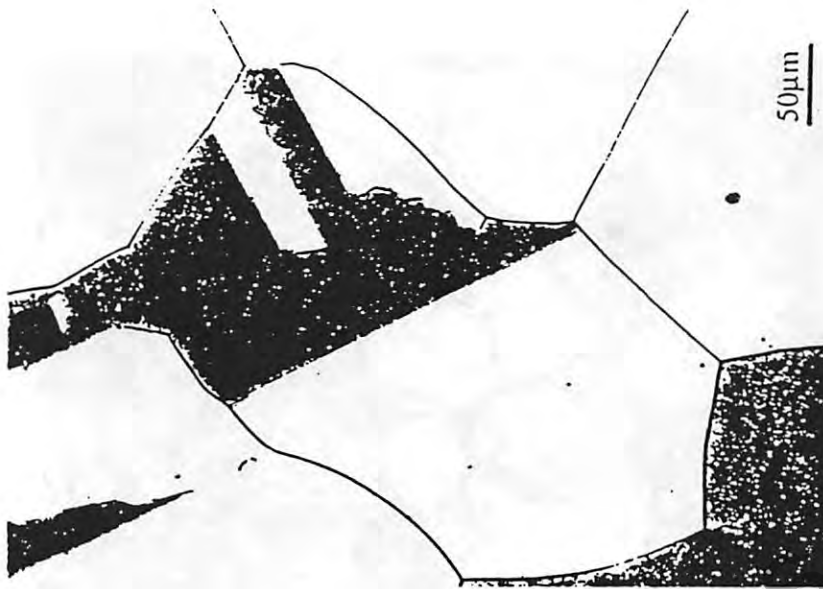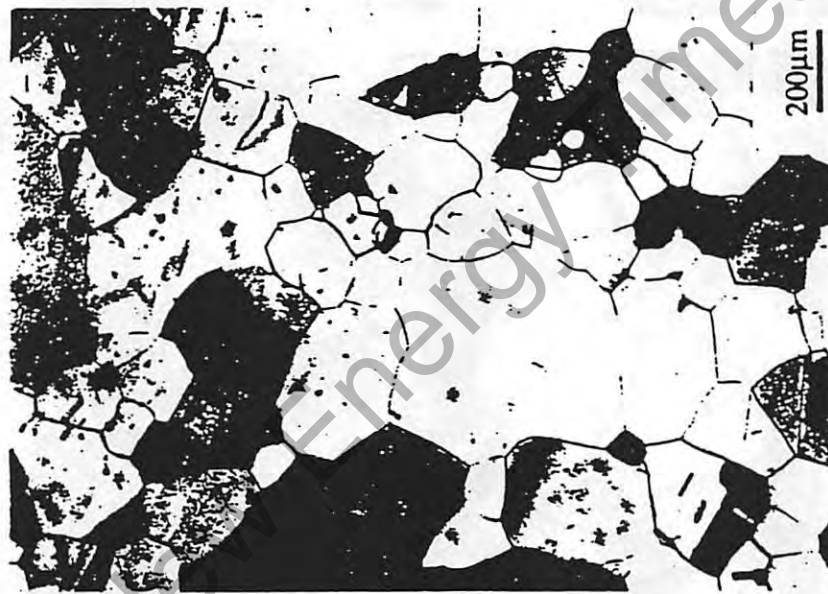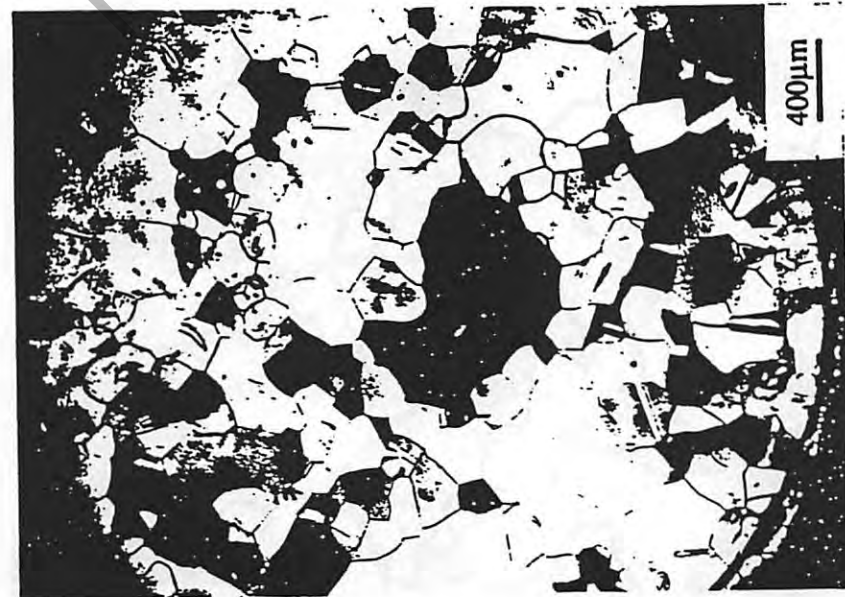
Fig. 32 - Optical micrographs of Engelhard batch #3 0.3 cm diameter palladium rod from SRI after annealing in vacuum ($<10^{-5}$ torr) at 850°C for 4 hours. The micrographs are seen at different magnifications showing large grains close to the center and finer grains near the surface because of the gradient of residual stress before annealing

63

200μm
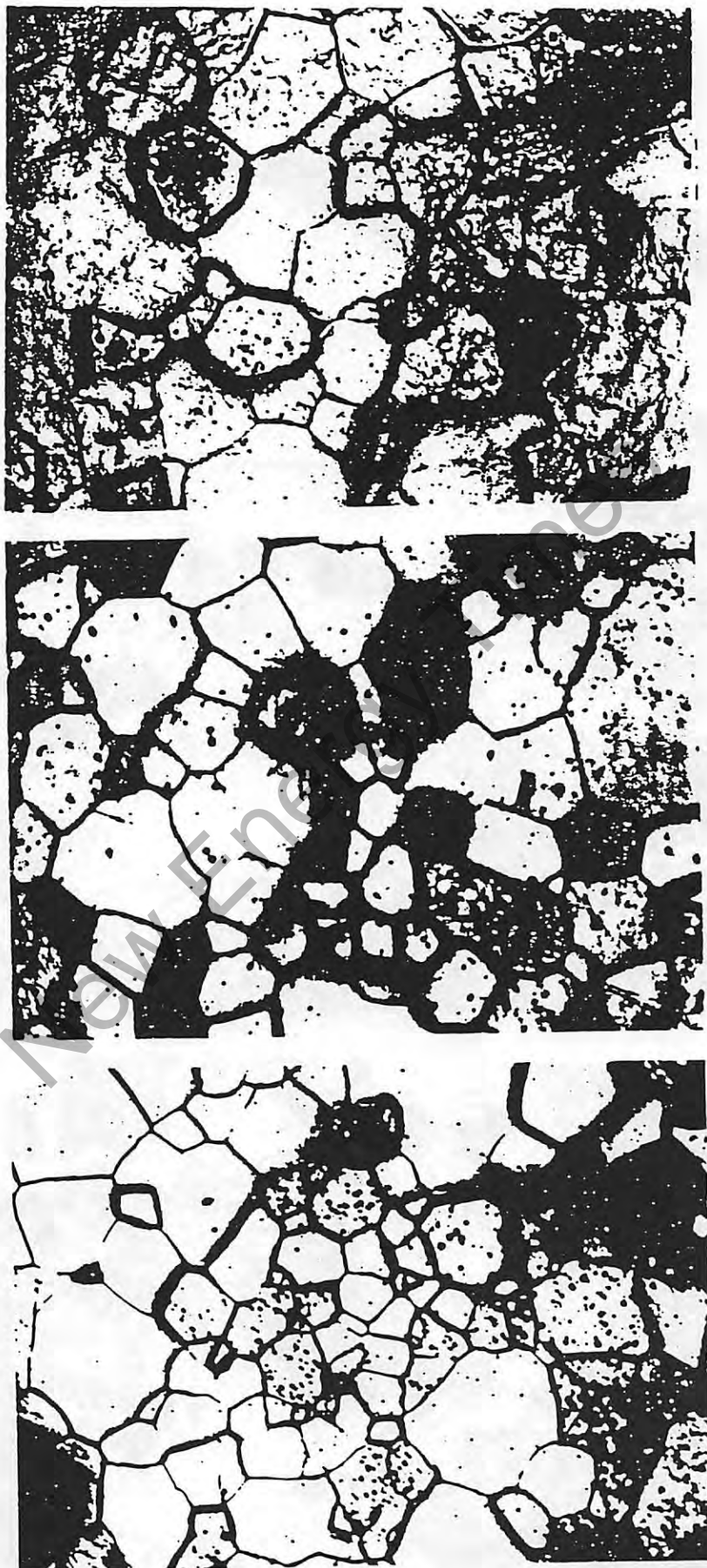
Fig. 33 - Optical micrographs of Engelhard palladium rods from SRI (a) batch #3, (b) batch #1, and (c) batch #1 - "heat producer" showing hardly any difference in grain morphology

cathodes can be found in NRL laboratory notebooks # N-7817 and N-7818 assigned to Dr. Dawn Dominguez. The notebooks cover the time from 5-25-94 to 6-30-95.

Three of the commercial palladium materials didn't load beyond the D/Pd=0.7-0.75 level in NRL experiments. These were the two Johnson Matthey high purity (99.997%) wires - stock #10960, lots W12954 and W7403 (3 experiments) and the Goodfellow 99.95% rod - #007940/5 (1 experiment). The Johnson Matthey "special batch" material only loaded beyond the D/Pd=0.7-0.75 level in one of two experiments. The highest D/Pd atomic ratio attained for this material was 0.82.

Three of the four materials (the Johnson Matthey high purity wires and the Goodfellow 99.95% rod) that failed to load very well were not annealed. The anneal step was omitted because NAWC had apparently been successful at generating anomalous excess power from cathode materials used in the as-received condition. Only the Johnson Matthey "special batch" rods were annealed for the NRL experiments. The anneal was carried out at 1100°C for 20 hours. Micrographs of the Johnson Matthey lot W12954 wire (Figure 24) and the "special batch" material in the as-received condition (Figure 25) showed an elongated or small grain morphology, respectively. The morphology of the "special batch" material was not examined after annealing and the morphologies of the other high purity wire (lot 7403) and the Goodfellow rod (#007940/5) were not examined in the as-received condition. It is likely that all these samples had similar elongated or small grain morphologies, however.

Four of the other commercial palladium cathode materials loaded into the β-phase. A loading atomic ratio of D/Pd=0.90 was achieved in the Johnson Matthey 99.9% rod - stock #98529, lot F13E05 (1 experiment) and in the Goodfellow 99.95% wire - #005150/11 (1 experiment). The former was not annealed for the loading experiment, but the latter was annealed at NRL under the conditions used to produce the large grains shown in Figure 28.

Engelhard (batch #3) 99.9% rods loaded to D/Pd levels of 0.90 and 0.82 in two experiments. These samples were annealed at SRI under their usual conditons (850°C for four hours) that produced the morphology shown in Figure 32. Similarly, the Johnson Matthey 99.9% wire (stock 10280, lot K11C06) loaded to D/Pd levels of 0.88 and 0.82. The wire was not annealed in the first experiment, but, in the second, it was annealed at 1100°C for 20 hours to produce the large grains shown in Figure 27.

As a result of the deuterium loading studies done at NRL, a possible correlation was found between sample morphology and the extent of loading. For example, many samples with elongated grains or small, equiaxed grains didn't load beyond the D/Pd=0.7-0.75 level whereas samples with a large grain morphology loaded into the β-phase.

Calorimetric/Radiation Measurements. No calorimetric measurements were made during any of the experiments using commercial palladium cathodes. Radiation measurements were made with a sodium iodide detector during these electrochemical experiments. No radiation above the background level was measured.

Electrode Surface Analyses

Impurities on the cathode surface are expected to exert an influence on the ability of cathodes to attain H/Pd ratios near unity and to retain this high loading for the time required to obtain excess heat. For example, Pd (and Pt) are the most efficient electrocatalysts for promoting reduction of D_2O and H_2O

to form D_2 and H_2. The presence of other impurities would reduce the rate of this reaction (depending on the impurity, this could amount to many orders of magnitude). In addition, the ability to promote the dissociation of D_2 to form adsorbed D and, subsequently absorbed D, could be reduced by the presence of surface and bulk impurities. As mentioned, Pt, a common contaminant found in Pd, is an excellent electrocatalyst for reduction of D_2O. However, its presence could also be deleterious to obtaining high loadings since Pt is an excellent recombination catalyst for the reaction: $D_{ads} + D_{ads} = D_2$. Since absorbed D is known to occupy interstitial positions within the Pd lattice, impurities, especially those of the lighter elements, can block these positions. For example, C atoms can penetrate into the Pd lattice if exposed to C-containing gases at moderate temperatures [43] (as might occur during processing). Interstitial solid solutions up to $PdC_{0.15}$ can form which can totally block the formation of ß-PdH which develops at H/Pd = 0.65 and is a precursor phase to the attainment of high loading. B, which also enters the Pd lattice interstitially, is known to totally block ß-Pd-H formation at a concentration of 16 atomic percent [44]. Blockage of H atom ingress by the presence of high concentrations of C and B in the Pd lattice could also be caused by the formation of carbides and borides of Pd. B, at concentrations less than 10 at.% where borides do not form as indicated by the Pd-B binary phase diagram, will promote H absorption due to the expansion of the Pd lattice caused by the presence of B [41]. Thus, smaller amounts of interstitial impurities could actually exert a positive influence on the attainment of high loadings.

This section will be devoted to surface analyses of cathodes before and after electrolysis using XPS. XPS generally analyses the top ~50 Å of a sample. XPS data will include composition as a function of depth employing argon ion sputtering to gradually erode away the surface film. Although most of the emphasis will be on NRL Pd (i.e., Johnson Matthey Pd sponge processed into rod at NRL) tested at NRL, data from other cathode materials and heat-producing cathodes from two other laboratories, NAWC and SRI, will also be presented. XPS results can be compared with bulk sample analyses such as that shown in Tables 2, 5 and 6 obtained by GDMS.

XPS of Unused Cathodes

A survey spectrum of a Johnson Matthey 99.9% purity wire as received is shown in Figure 34A. Although the Pd 3d doublet is clearly visible, the surface is composed mostly of carbon and oxygen due to the large difference in peak area sensitivity factors (Pd3d=4.64, C1s=0.296, O1s=0.711). Si, Cl and Mg are also present but to a much lesser extent than C and O. This is a representative spectrum for all cathode materials examined which included NRL Pd and Pd-B rod, Engelhard #3 and Johnson Matthey "special batch" rods from SRI, Goodfellow 99.95% and 99.99+% wire, and Johnson Matthey 99.9% and 99.997% wire. The principal contaminants were always C and O and the Pd 3d doublet was always visible. The C1s peak was always anywhere from approximately half to double the height of the Pd 3d doublet. This puts the contamination level of all surfaces easily over 50 at.%. Other minor contaminants found included S and Na. On the surface most of the elements as determined from their binding energy were in the oxidized state except C which will be discussed below. Sample preparation such as vacuum annealing and acid etching in aqua regia did not appear to significantly alter the surface composition. These data illustrate the ability of the Pd surface to become significantly contaminated upon exposure to air and water.

Most of the contamination observed in Figure 34A is found to reside in approximately the top 10Å as illustrated in the survey shown in Figure 34B obtained after a 10s argon ion sputter (sputter rate ≈ 1Å/s for SiO_2). Most of the original C and O have been removed and the Pd peaks now dominate the spectrum. An additional 20s sputter produces a further reduction in contaminant levels (see Figure 34C) although the effect is not as dramatic as that observed with the initial 10s sputter. Figures 34B and C also indicate the presence of Pt in this sample. This agrees with the GDMS results for this material which
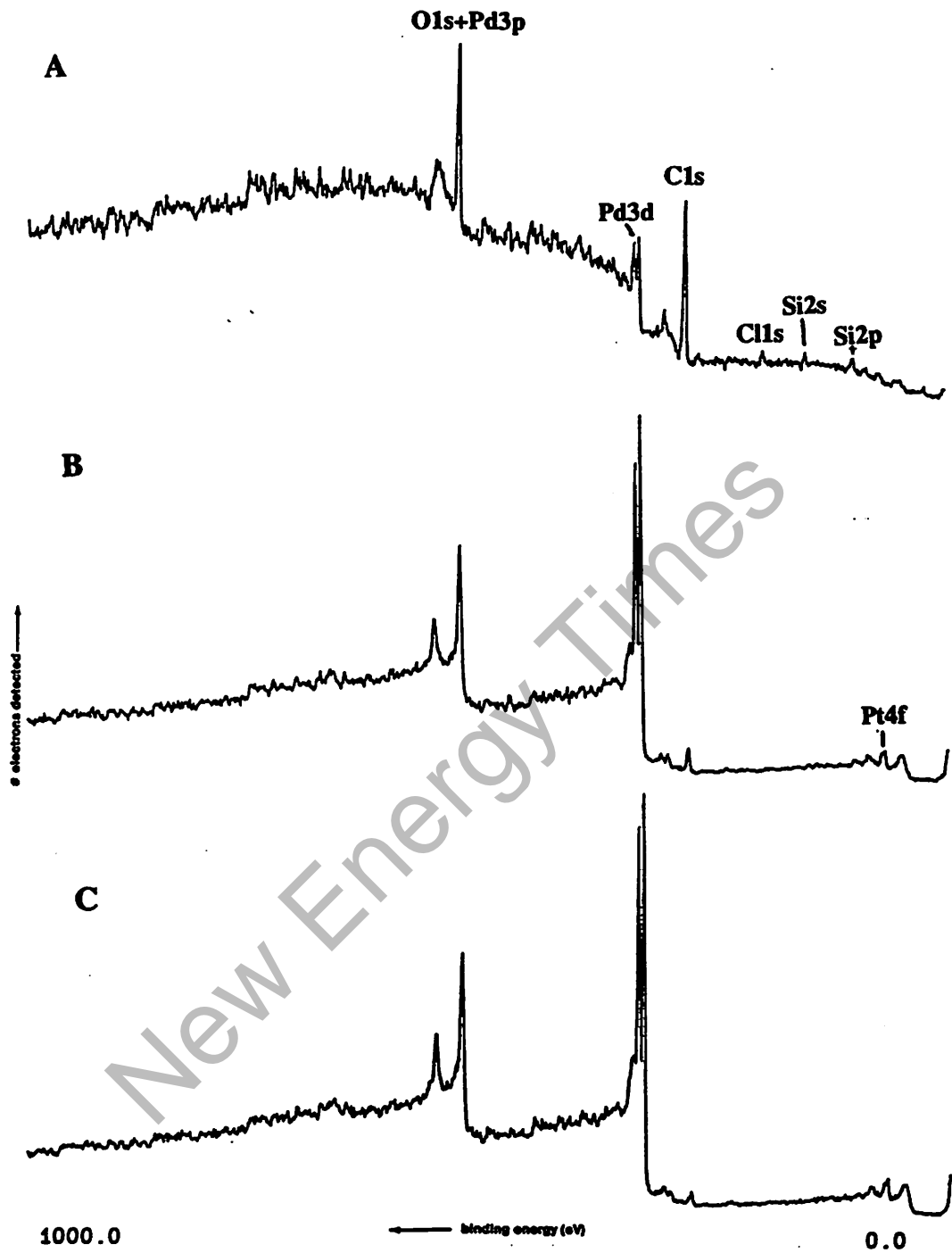
Fig. 34 - XPS survey spectra obtained from a 1mm diameter Johnson Matthey 99.9% purity Pd wire (#10280, Lot K11C06). A: Surface, B: After 10s sputter, C: After 30s sputter. Scans from 0 eV (right) to 1000 eV (left) binding energy

showed the presence of 1100 ppm Pt impurities. In the samples sputtered for longer than 30s, all the impurities were removed except C (and Pt for 99.9% purity Pd). C would persist to the deepest levels indicating either that it was a bulk contaminant or that it diffused from the surface to the bulk during processing. Shown in Figure 35 is the C1s region obtained after a 1200s sputter from a Pd-0.62 wt.%B rod which had been annealed for 2 hours at 600°C. Two types of C are clearly present. The low binding energy peak at 284.0 eV is attributed to graphitic C while that at 285.5 eV is normal 'hydrocarbon-like' C. The graphitic C is likely to be the carbon occupying the interstitial sites while the other C is contamination in the form of bulk C deposits. The presence of C in the interstitial sites could strongly influence the loading characteristics of the cathode materials as described above.

XPS of Non-Heat Producing Cathodes

Appendix B will be used to reference all NRL-processed cathodes investigated here at NRL. Only selected cathodes from Sets 8 through 12 were examined with XPS. The data are divided into two groups based on the XPS results. The first group comprises the thickest overlayers containing large concentrations of both Cu and Pt relative to Pd. The Cu and Pt can either be near the surface or buried under a silicate-containing overlayer. All these samples were obtained from Sets 8 and 9 and all were electrolyzed for approximately 1000 hours. The second set of samples all contained thinner overlayers than the first and contained very little Cu. A high Pt concentration, however, was found on all these samples. Samples in Sets 10 and 11 are part of this group. These samples were all electrolyzed for 500 hours or less and they received, as the cathodes in Set 10, a large number (6) cathodic-anodic current reversals.

Figures 36 and 37 are survey spectra taken from the surface and various depths of selected samples from an NRL Pd plate cathode, experiment 8_3, and an NRL Pd rod cathode, experiment 9_6, respectively. Figure 36 will be discussed first. The following elements are found at the surface: Si, O, C, Cu, Nb, Pt, Zn, Na, Mg and Ca. The Zn and Na were ubiquitous in small quantities in nearly all the samples examined by XPS. Ca and Mg are similar to Zn and Na but several examples of much higher Ca concentrations have been found (for example electrode 9_4). These contaminants are often those that are found in water. Nb is found on all samples in which a Pt-clad Nb mesh was used as the anode. Nb is exposed to the electrolyte at all points where the material has been cut and at spot-welds where damage to the Pt film can occur. The Cu (its potential source will be discussed later) is found to be in the +2 oxidation state as is indicated by the two sets of 3p doublets occurring between 930 and 970 eV. Due to their small area sensitivity factors, the major components of this surface are O, Si and C. Besides Cu (which has a sensitivity factor similar to that of Pd and Pt), the oxygen is also associated with both C, as evidenced by the small shoulder on the high binding energy side of the C1s peak, and Si. The binding energy of the Si peaks suggests the presence of a silicate-type species. The bulk of the C detected on the surface is merely the so-called 'adventitious' carbon contamination found on all surfaces. No Pd is evident on the surface. In fact, Pd is not detected until after approximately 150s of sputtering and even then the Pd $3p_{3/2}$ peak is only a small shoulder on the Pt $3d_{3/2}$ peak. The Pd peak does not become easily discernible until somewhere between 360 and 600 seconds of sputter time. As sputtering proceeds both Cu and Pt, which was just observable on the surface, increase as the quantity of silicate species slowly decreases. The Cu and Pt reach a maximum after about 600s of sputter time and then decrease as the amount of Pd increases. After 1500s both Cu and Pt are still present which indicates that a relatively thick overlayer has grown on this electrode. Similar results were obtained with electrodes 9_3, NRL rod and 8_6, NRL plate which were electrolyzed in LiOH/H_2O.

The data shown in Figure 37 contain similar characteristics as that in Figure 36 except that a silicate overlayer is not observed on the surface (as evidenced by the presence of low O and very little

295.0

UPPER BINDING ENERGY (eV)

binding energy (eV) →

275.0

LOWER BINDING ENERGY (eV)

← # electrons detected
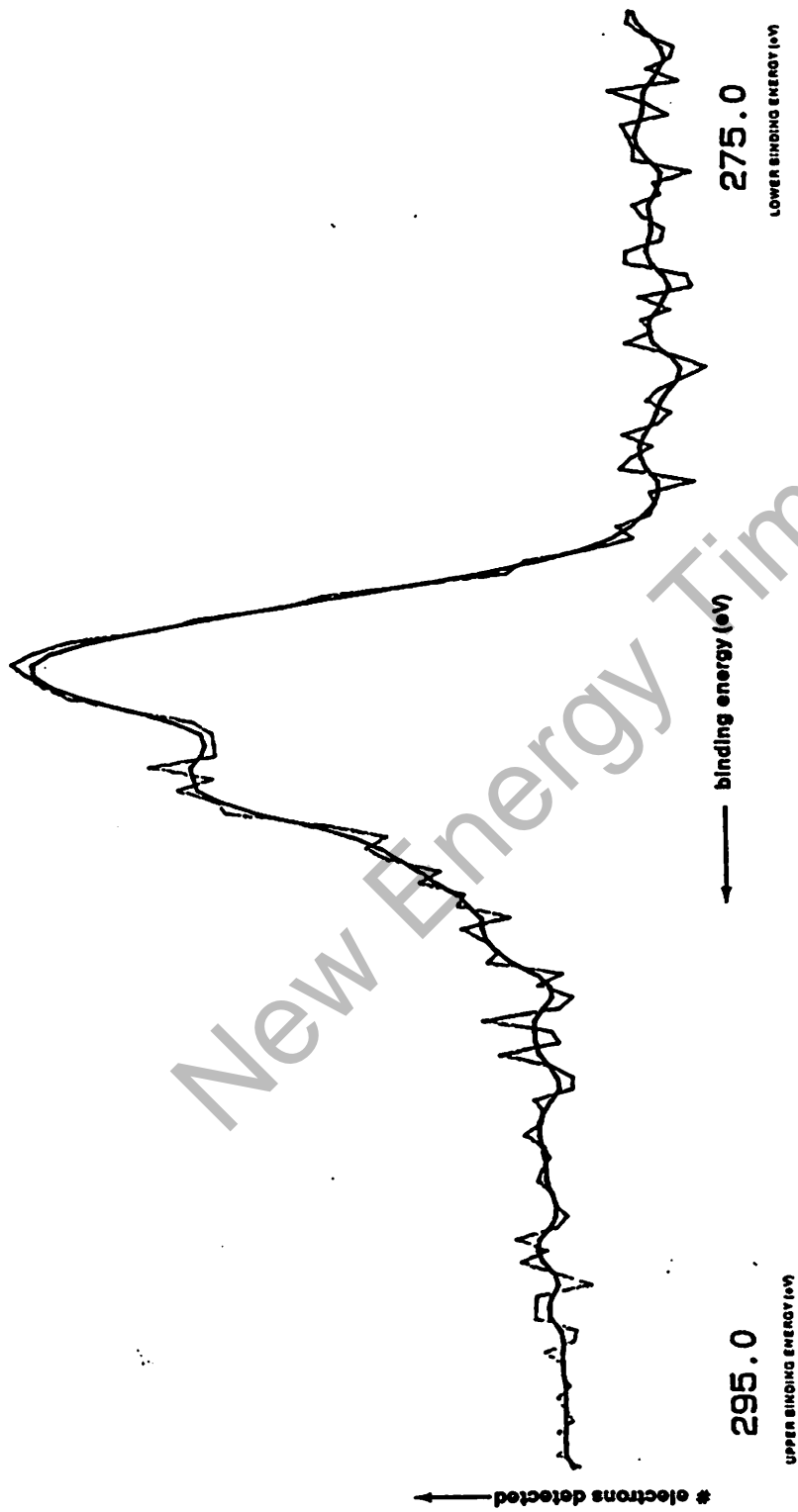
Fig. 35 - XPS C1s regional scan after a 1200s sputter taken from a Pd-0.62B NRL Pd rod annealed for 2 hours at 600°C

69
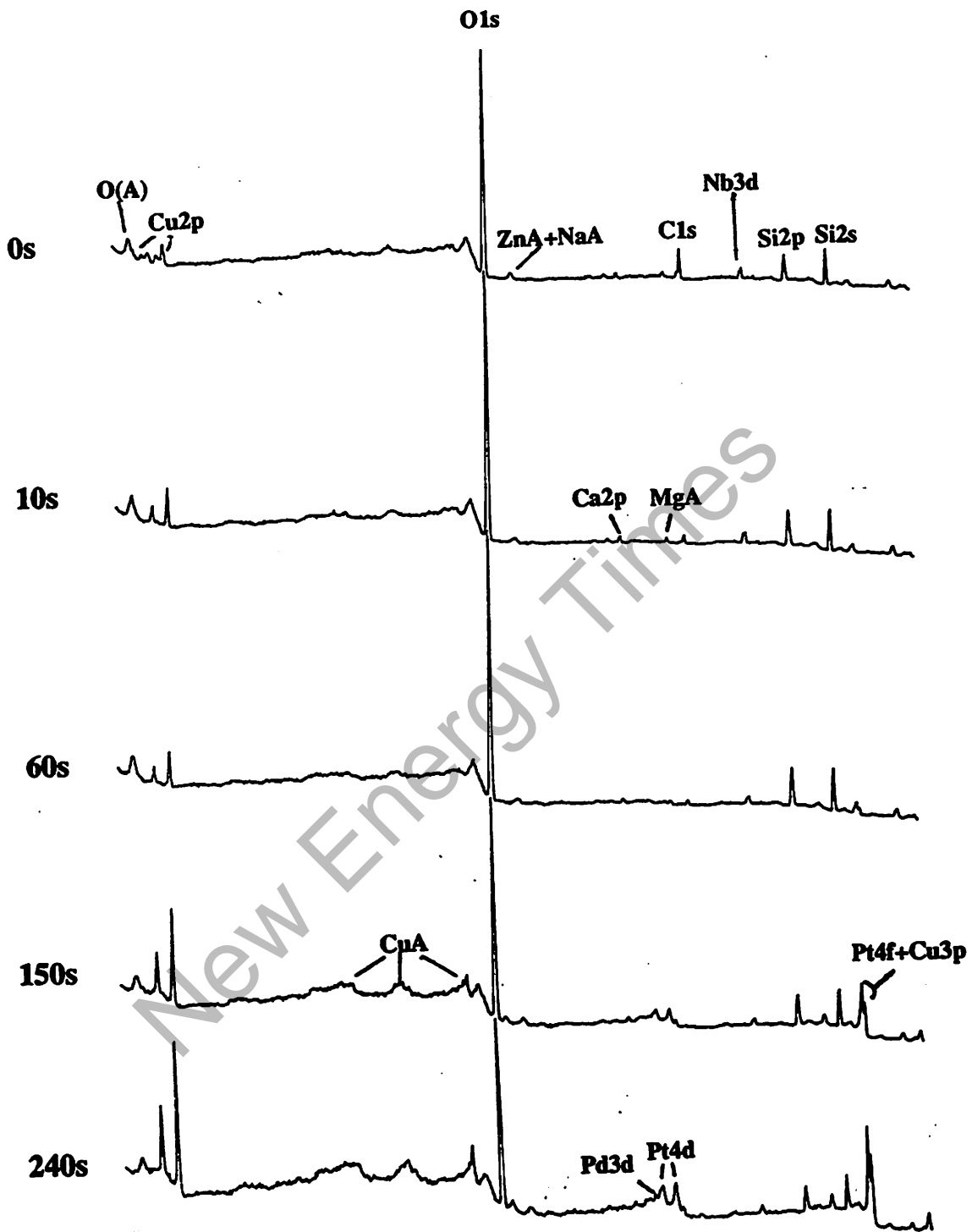
Fig. 36 - Series of XPS survey spectra obtained at various total sputter times from NRL Pd plate electrode 8_3. Scans from 0 eV (right) to 1000 eV (left) binding energy

360s

600s

Pd3d

900s

1200s ÷2.5

1500s ÷2.5

1000.0 ← binding energy (eV) 0.0
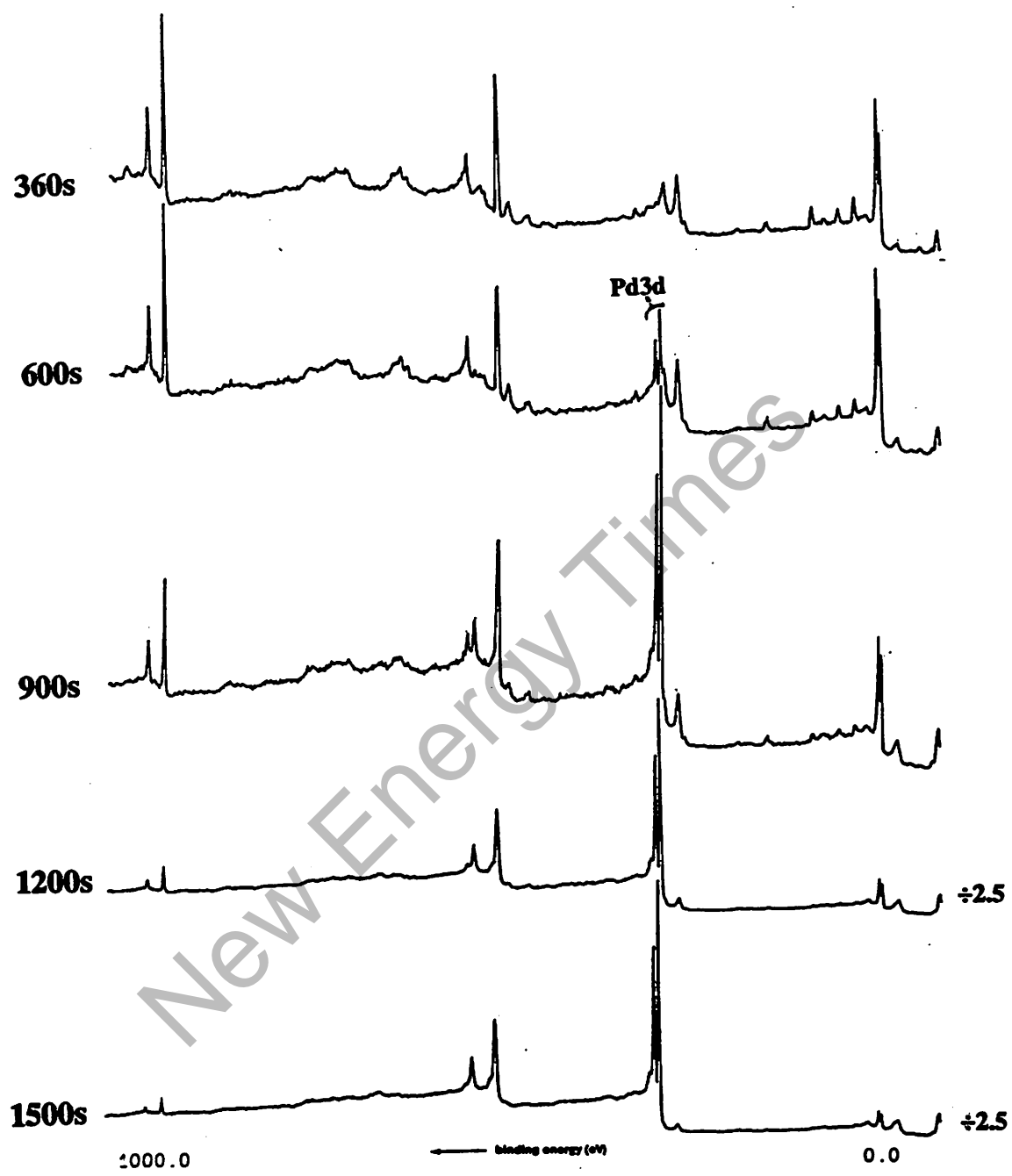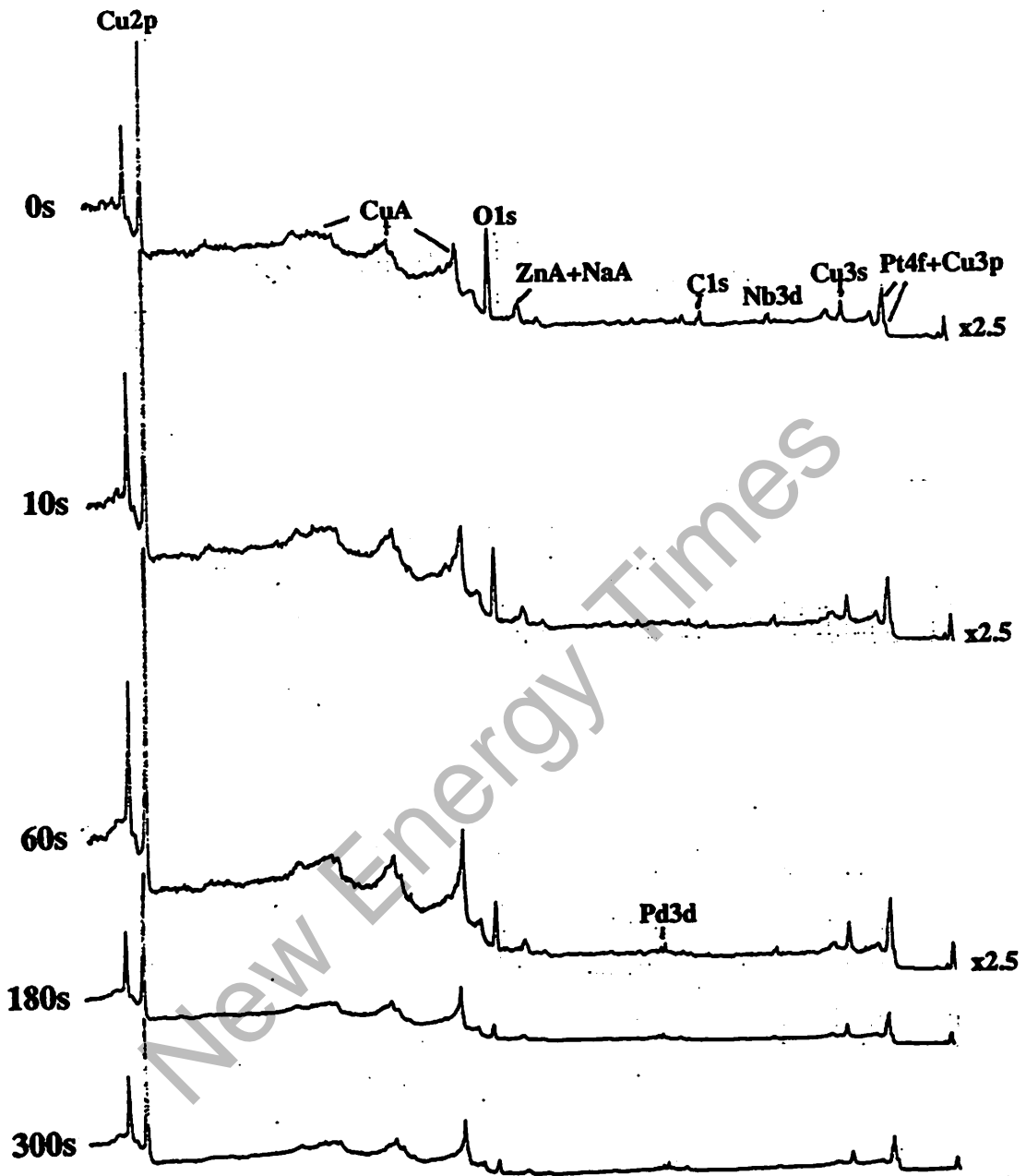
Fig. 36 - continued

Fig. 37 - Series of XPS survey spectra obtained at various total sputter times from NRL Pd rod electrode 9_6. Scans from 0 eV (right) to 1000 eV (left) binding energy

600s

900s

1200s

1800s

Pd3d
Pt4d

Fig. 37 - continued

73
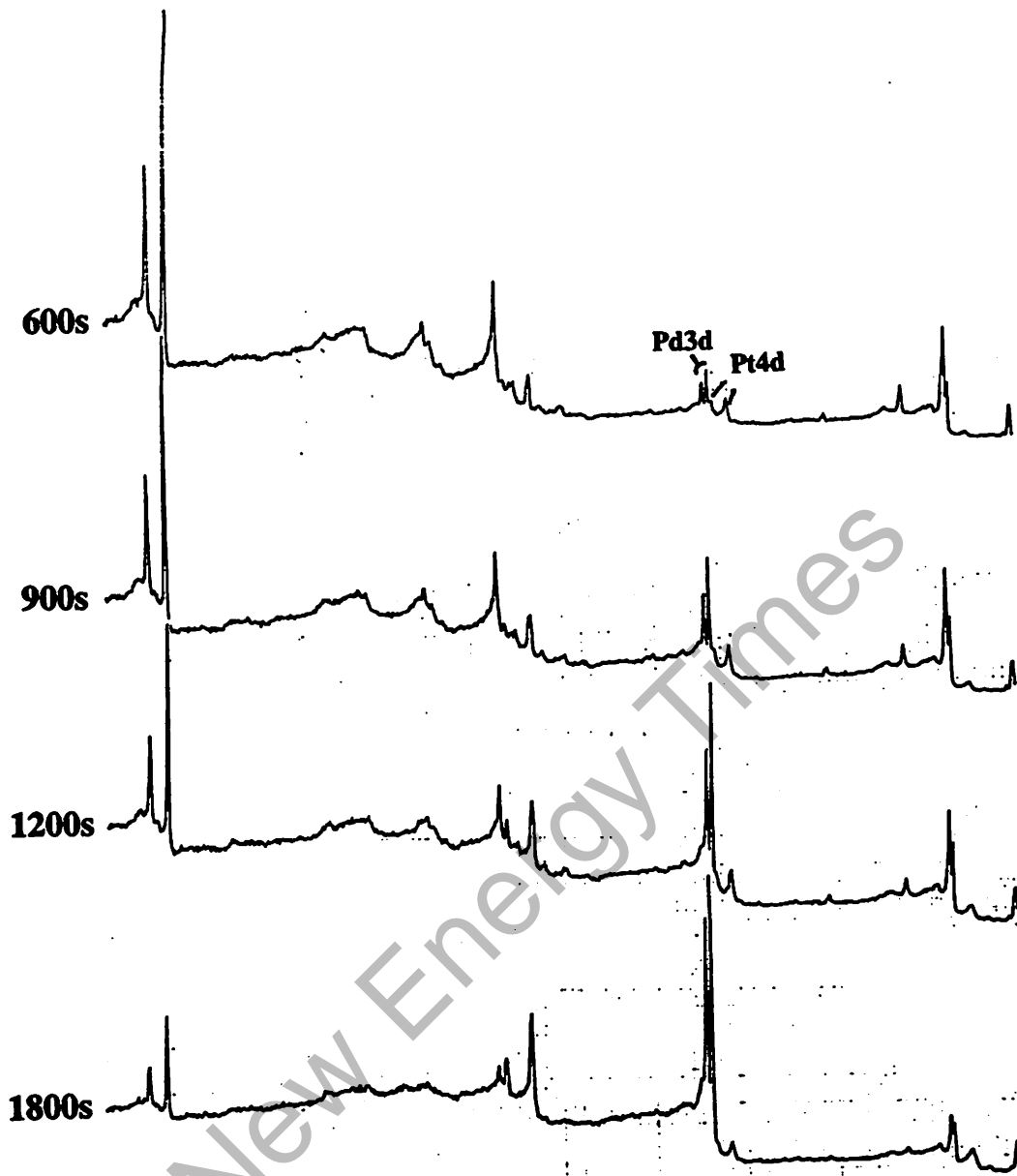
Si). Again, no Pd is detected on the surface. The lack of Si most likely reflects the use of quartz as the cell container rather than Pyrex. Quartz is expected to be more stable in the highly basic electrolyte. The near surface region is highly enriched in Cu in the early stages of sputter etching. Pt, just detectable as a small shoulder on the low binding energy side of the Cu3p peak at 77 eV on the surface, increases slowly with sputter time. After 1800s total sputter time only Cu, Pt and Pd are observed in the survey which is similar to that recorded for the sample depicted in Figure 36.

An example of the thinner type overlayer is shown in Figure 38 for an NRL palladium rod cathode from experiment 10_1. The surface contains silicate along with C and Pt. No Cu or Pd is observable in the first survey spectrum. After removal of much of the surface C contamination with a 10s sputter etch Pd is observed along with a significant increase in Si, O and Pt. Further sputtering causes removal of the silicate with a concomitant increase in Pd. After 180s the Si has all been removed but Pt is still present. This decreases until after 600s it is just barely discernible above the noise. Compared to the final spectra shown in Figures 35 and 36 obtained at 2.5 and 3 times the total sputter time for this sample, it is easy to observe that the film on this electrode is much thinner. In addition, Cu never becomes a significant component of this film.

As described previously, there was a correlation of film thickness with total electrolysis time. In addition, composition with respect to Cu is very different between the two different types of electrodes. Interestingly, there also was a correlation with the maximum D/Pd obtainable. The thinner, non-Cu-containing overlayers reached loadings of D/Pd = 0.7 while the thicker, Cu-containing overlayers were found on samples with D/Pd = 0.9. This indicates that the development of these Cu-rich layers at long electrolysis times may have been beneficial to obtaining high loadings by acting as a blocking agent to D egress from the Pd lattice. The quest for low levels of excess heat with more sensitive calorimeters might have proven very interesting with these samples.

Alluded to in the above discussion are the sources of some impurities. Si most certainly comes from the etching of the Pyrex or quartz container by the concentrated LiOD or LiOH. ICP analysis of the used solutions from Sets 7, 8 and 9 indicated that Si was present anywhere from approximately 30 to 80 ppm in the experiments where Pyrex containers were used while around 10-20 ppm were found for experiments conducted in quartz holders. The source of Pt, found on every electrode examined with XPS, was likely from oxidation of the Pt anode at high current density. ICP analysis, however, showed less than 0.1 ppm Pt in all solutions from Sets 7-9. Another possible source was the Pd itself since most Pd used contained above 30 ppm Pt. Only one very high purity Pd cathode containing a very small Pt level (Pt by GDMS = 1.9 ppm) was examined. This cathode was a Johnson Matthey 0.1 cm diameter wire, 99.997% purity, from experiment 12_8. XPS indicated that very little Pt was present on this electrode.

A similar argument applies to the Cu except that, unlike Pt, there is no pure source of Cu exposed in the cell. Sources of Cu include: D_2O, Li used to make LiOD from the D_2O, spot-welds where Cu-containing tips are used, the Pt anode, the Pd cathode, Pyrex or quartz and the Teflon used for the cell top and to shield the electrical connections. The Pyrex, quartz and Teflon seem unlikely candidates to supply such large amounts of a metallic impurity. The spot-welds are unlikely as Cu was found on several cathodes where the tips were made of Pd and Pd-Ag alloy. Also, the cathodes were always acid etched after spot welding was completed. Only one case was recorded where Ag was found on an electrode but this was an electrode which was not acid etched before it was put into the cell. The Li was reported to have 20 ppm of Cu but so little is used to make up the 0.1M concentration that there is not enough present to supply such large amounts of Cu assuming the cathode surfaces are uniformly covered. ICP analyses of used and unused solutions indicated that the copper concentration was never above 0.03 ppm. The Li was also reported to contain 90 ppm of Na and 78 ppm of Ca; these could have been the source of those impurities often found in small quantities on the cathode surface. The source of the D_2O
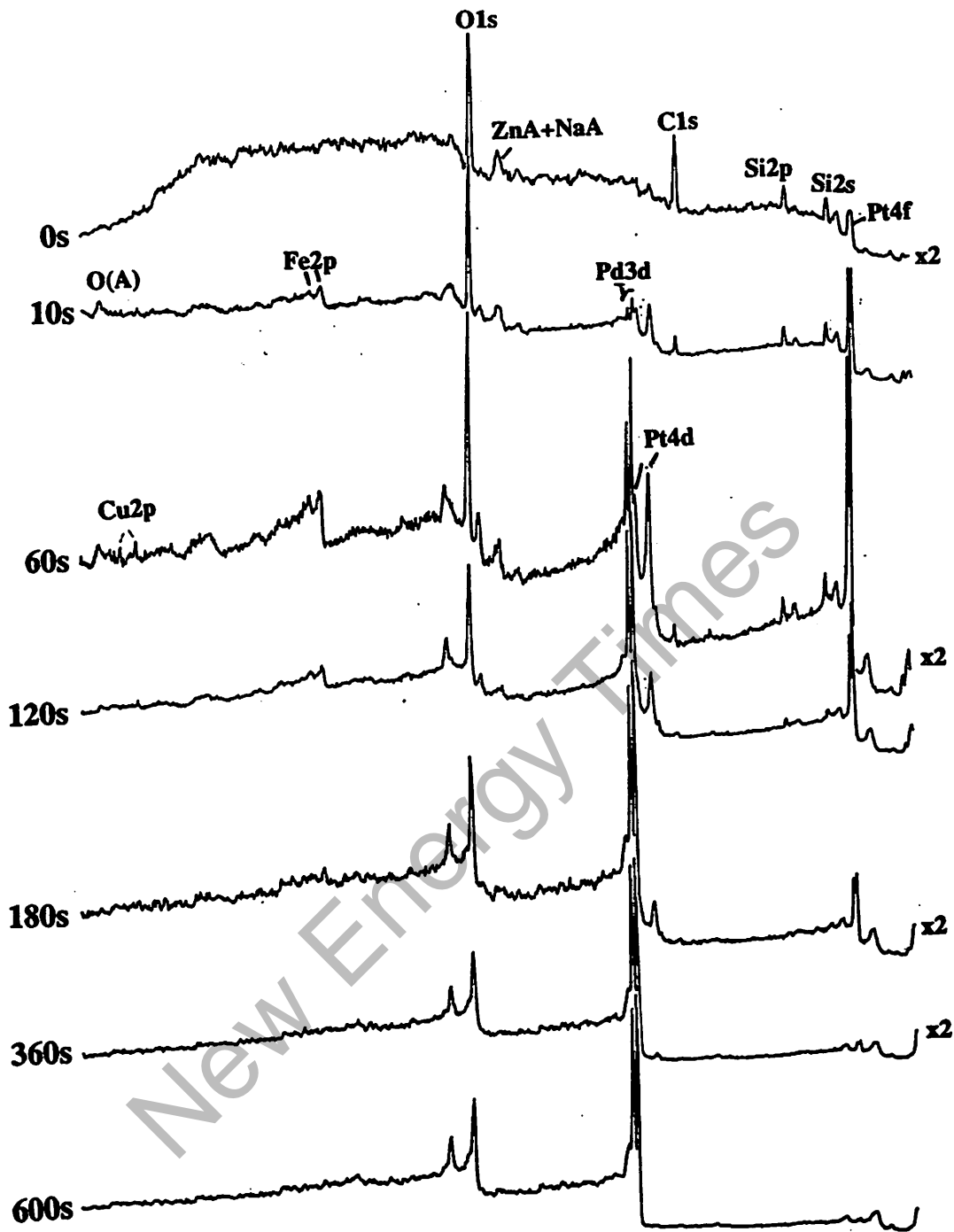
Fig. 38 - Series of XPS survey spectra obtained at various total sputter times from NRL Pd rod electrode 10_1. Scans from 0 eV (right) to 1000 eV (left) binding energy

75

appeared not to be the cause as believed in an earlier study [35]. Extremely pure D_2O was provided by Ontario Hydro in which the Cu concentration was less than 0.005 ppm. The Pt anode could be the source as no Pt was analyzed by GDMS (analysis of 99.9% platinum gauze (see Table 3) indicated that this material contained 6 ppm copper). A Pt anode was examined by XPS after an experiment but no Cu was observed on its surface. The final source is the Pd cathode itself. The NRL Pd material was found to contain 24 to 27 ppm Cu which was likely obtained from the arc melting of the sponge which was conducted on a Cu hearth. Calculations indicate that this is enough Cu assuming uniform distribution in the bulk (verified by depth measurement made with GDMS) to provide concentrations found in the surface films observed on used cathodes. Two cathodes, 9_4 and 9_6, which produced high Cu were reground and polished on a lathe and retested as electrodes 12_3 and 12_4, respectively. High Cu was found again on both cathodes. In addition, a higher than usual Ca level found on cathode 9_4 was repeated on 12_3. Cathode 12_4 was examined by GDMS as a function of depth. Cu was found at a concentration of nearly 80 ppm throughout the sample suggesting that initially this sample had a large Cu content. Cu was also found on an NRL Pd rod electrode tested at SRI in a degree of loading experiment (electrode P126). Cu was found on a 99.9% purity 0.1 cm diameter Johnson Matthey wire which contained 24 ppm Cu by GDMS. Little Cu was found on two NRL samples run at NAWC. Several different chemicals, however, were added to the electrolyte in an attempt to increase D uptake. These may have had an influence on Cu mobility. One anomaly, however, does exist and this is the large Cu concentration found on cathode 12_8, a 99.997% purity Johnson Matthey wire. GDMS indicated that this material contained only 0.11 ppm Cu. Electrical connections to this cathode were made, however, with Cu spot welding tips. Even though these cathodes were acid etched after spot welding, perhaps some Cu remained behind.

The room temperature mobility of species has been observed in the hydride battery material $LaNi_5$ [45]. Running the electrode through charge-discharge cycles causes the La to diffuse to the surface where it is oxidized by the KOH electrolyte. The $La(OH)_3$ blocks H ingress and reduces the efficiency of the battery. Normally La mobility in the $LaNi_5$ lattice is practically zero at room temperature. The authors believe that the enhanced La mobility is caused by the severe distortion at the boundaries of the hydrogen-rich and hydrogen-poor regions which arise during charging and discharging. The severe lattice defects occurring over relatively large areas cause short circuit diffusion paths for the La atoms. The same type of mechanism could account for the enriched Cu and Pt surface layers found on used Pd cathodes.

XPS of Heat Producing Cathodes

Two sources of heat-producing cathodes, NAWC and SRI, provided samples for XPS analysis. One SRI Pd cathode was examined: sample number P15, a Pd rod made from Engelhard #1 material which was SRI's most successful heat-producing material. This sample was annealed and electrolyzed in 1991. Details of the P15 experiment have been published [23]. From ICPMS data provided by SRI, the Engelhard #1 Pd is of 99.9% purity containing 140 ppm Pt plus significant levels of many other impurities. Heat producing electrodes from NAWC examined by XPS include: Johnson Matthey high purity wires from two different calorimeters, NRL Pd rod and NRL Pd-B alloy rods.

Shown in Figure 39 is a series of survey spectra taken of the surface of the SRI P15 cathode and after various sputter times. The surface is a mixture composed of carbon and oxygen containing species of which silicate is the most prevalent. Small amounts of Pt, S, Zn, Na and N are also seen. No Pd is present on the surface. After a 10s sputter some silicate is removed which results in a small increase in the C1s signal and a large increase in the Pt4f doublet. After 30s the Si is nearly all removed, the C begins to decrease and the Pt and Pd continue to increase. Cu is also visible now. After 60s the metallic
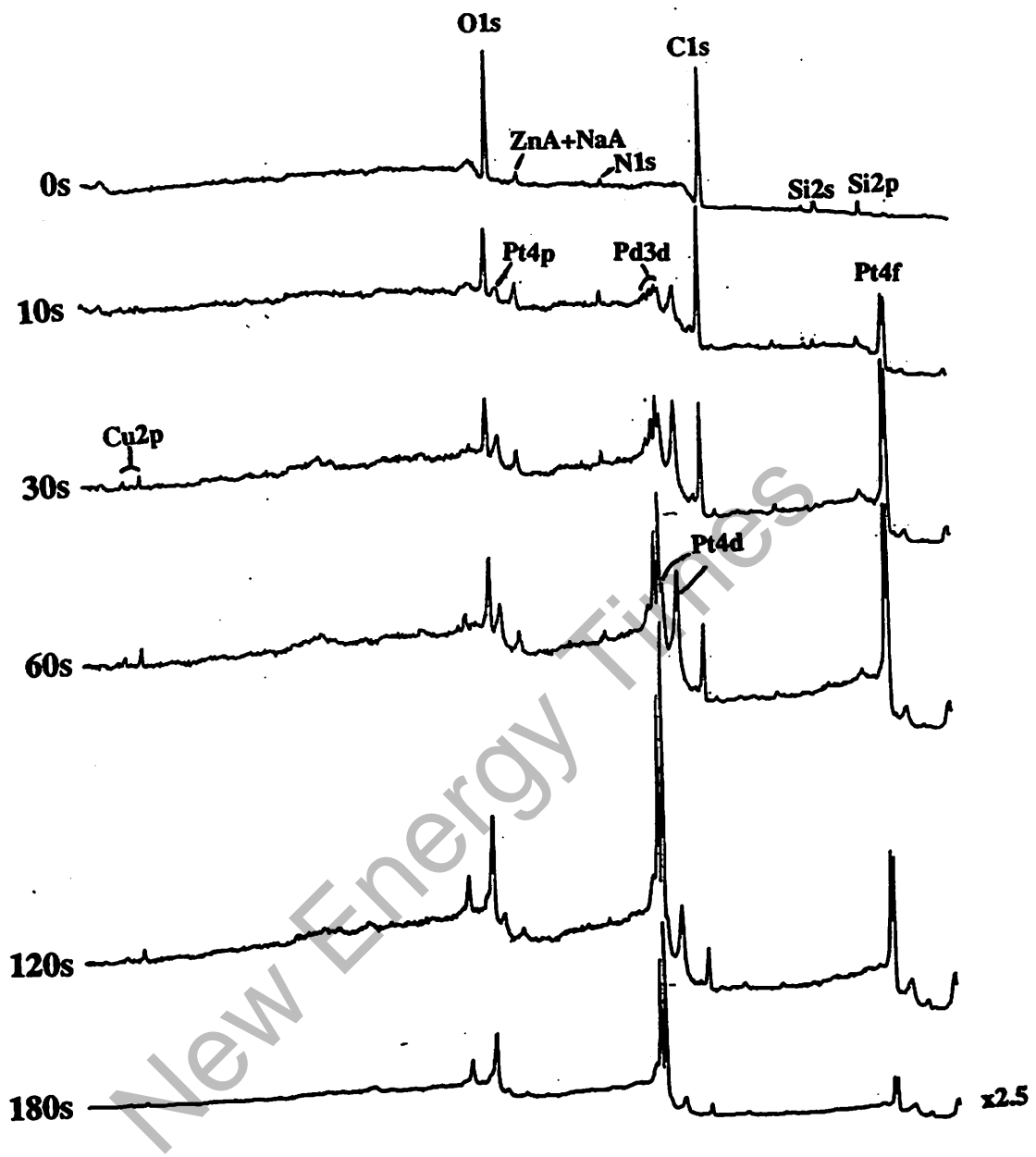
Fig. 39 - Series of XPS survey spectra obtained at various total sputter times from SRI excess heat producing electrode P15 made from Engelhardt #1 Pd. Scans from 0 eV (right) to 1000 eV (left) binding energy

240s

x2.5

300s

420s

600s

C1s

900s

Fig. 39 - continued

impurities, Cu and Pt, reach their maximum while C continues to decrease slowly and Pd increases. Further sputtering continues to uncover the Pd while the other impurities decrease. After 900s total sputter time, only Pt and C are still visible. These are contaminants which are likely part of the bulk. As evidenced by the peak binding energies, the carbon always was mostly in the graphitic state while the Pt, even on the surface, was in the metallic state. The profile does not look all that different from that obtained for relatively thin overlayer samples tested at NRL and depicted in Figure 38. The P15 electrode was loaded to a maximum D/Pd of 0.99 and it produced anywhere from 5 to 10% excess power over the total input power. These amounts were just below the sensitivity of the NRL isoperibol calorimeters. This fact makes trying to draw conclusions based on the XPS results as to what impurities are necessary on the surface to obtain high loadings and excess power very difficult. Also, at the end of SRI's experiments, they normally switch the potential on the cathode so that an anodic current is flowing in order to deload the sample before removal from the cell. This could oxidatively remove certain species from the overlayer that normally would have been present.

Analyses of early excess heat producing samples received from NAWC were plagued by the formation of thick layers due to the addition of thiourea and salts containing Al, Si, B, Li, Mg and Mn. Usually the purpose of these salts was to attempt to sustain heat production. Unfortunately, deposition of oxides of these elements likely covered or altered the layers present when excess heat production began. Examples of these electrodes are shown in Figures 40 and 41 for an NRL Pd rod and a Johnson Matthey high purity wire, respectively. The NRL electrode did not produce excess heat in its original test but after allowing it to sit in the electrolyte over a weekend with the potential off, approximately 11% excess heat was observed upon restarting the electrolysis. As observed in Figure 40 the sample was found to contain oxides of Ca, Mg, C, Si and Al. Multiple oxidation states were observed for oxygen and carbon as evidenced by the split peaks. Pd was not observed until the sample had been sputtered for a total time of 1800s. At this point the analysis was ended as most of the oxides were still very much present. The Johnson Matthey wire analysis (Figure 41) was somewhat different in that Pd was observed on the surface but changed very little through 2100s of sputtering. This may very well have been due to the presence of a scratch or nick in the analysis area which damaged the film. Evident in this profile are Mn, Mg, S and N (from thiourea) along with C, Si, Na, Zn and Ca. The Pt was still increasing after 35 minutes of sputtering and Cu was just beginning to be observed. Although a continuation of these profiles might have proved fruitful, the time available on the XPS was not infinite. Since these profiles took approximately eight hours to complete, a decision had to made as when to end a run and continue with another sample.

Cathodes received from NAWC where no chemical additions were made to the LiOD/D$_2$O electrolyte were also examined by XPS. Survey spectra taken from three different positions on an excess heat producing and non-excess heat producing NRL Pd-0.62 wt.%B, 0.2 cm diameter cathodes are shown in Figures 42 and 43. Both samples were treated the same and electrolyzed at the same time. Misalignment of the one electrode was believed to be the cause of its failure to produce excess heat presumably due to uneven current distribution. Different areas of the cathodes were analyzed since the surface retained a very heterogeneous appearance; some areas were very black while others retained a grayish metallic appearance. All the spectra, except the top spectrum in Figure 43, which was obtained from a thick salt deposit near the top of the electrode, contain many similarities. All show various levels of O, C, Si, Ca, Mg, Pt, Na and Zn. Trace amounts of Cu and Fe are also seen in several spectra. (The drawing die was the source of the Fe as unused samples examined by SEM/EDAX verified its presence in large amounts in selective areas where the sample had been scored in the die.) One obvious difference between the samples is the detection of Pd in all the scans of the heat producing electrode suggesting the overlayer is thinner on this electrode. Depth profiling was only performed on the non-excess heat producing electrode and is shown in Figure 44 for a metallic looking area. The presence of Pd is not obvious until 60s of sputtering is reached. Trace amounts of Si and Ca are still present on the surface
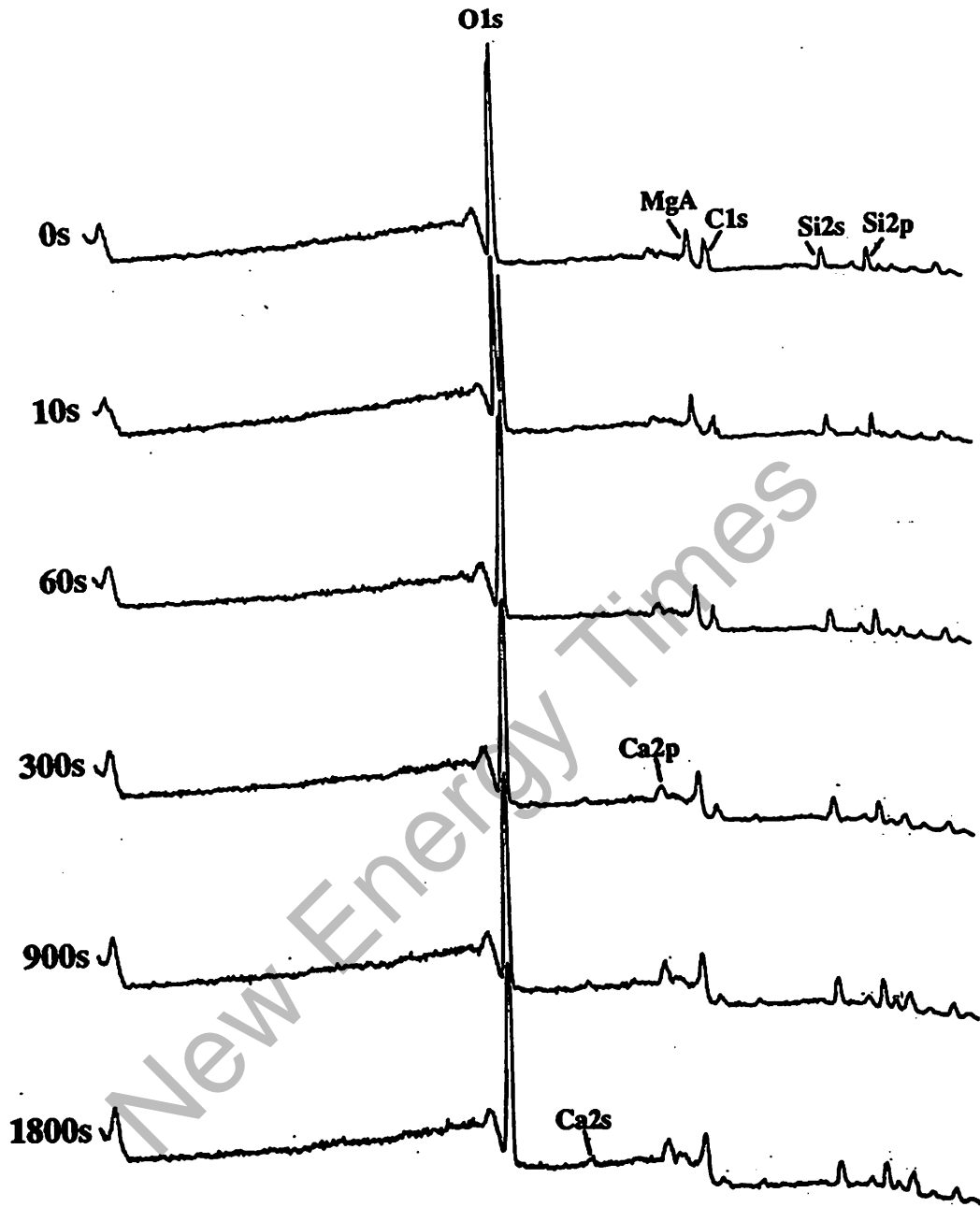
Fig. 40 - Series of XPS survey spectra obtained at various total sputter times from an NRL Pd rod, 4mm x 2cm, which produced excess heat at NAWC on the second attempt after sitting in the electrolyte after the initial electrolysis. Scans from 0 eV (right) to 1000 eV (left) binding energy
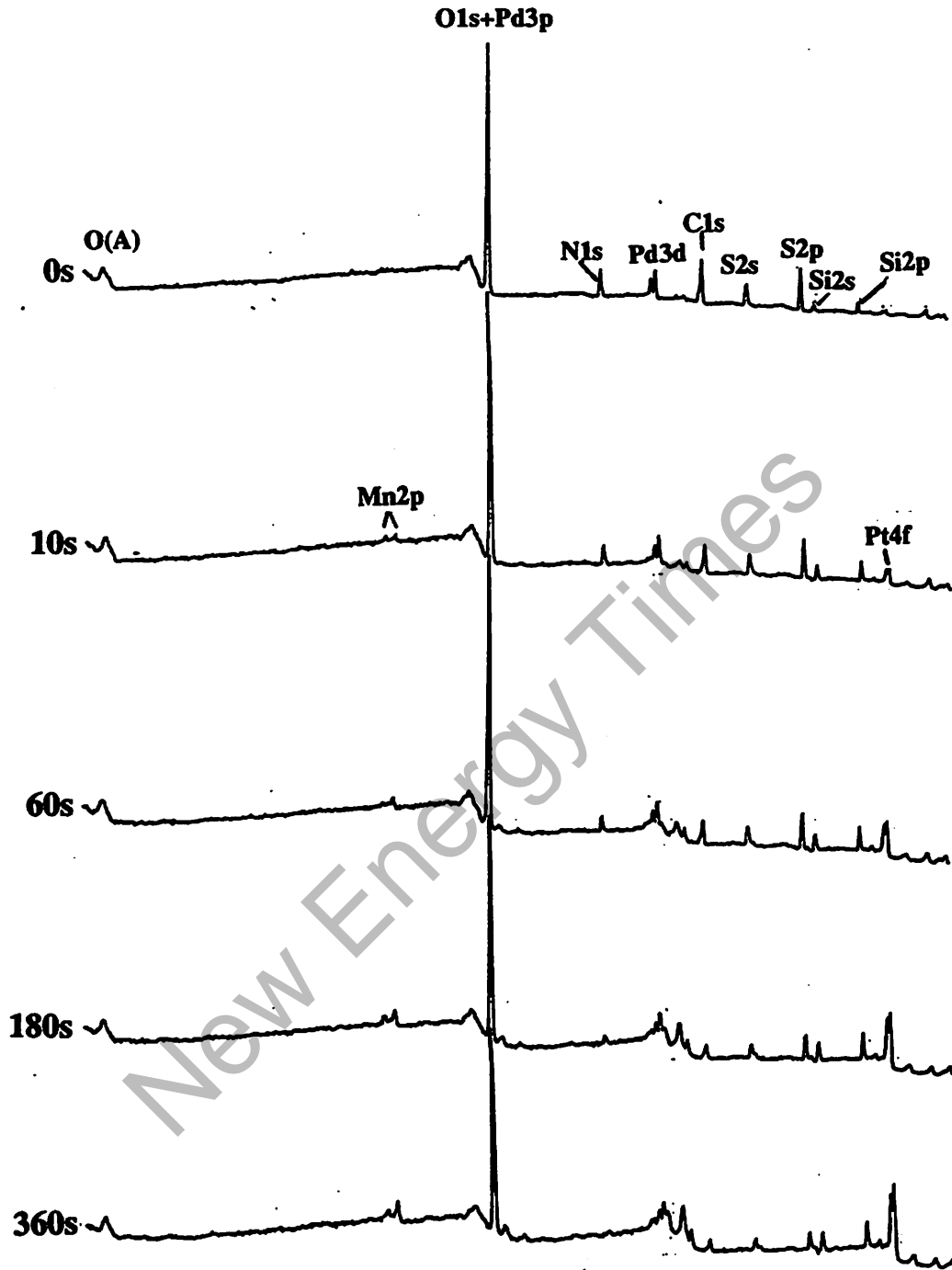
Fig. 41 - Series of XPS survey spectra obtained at various total sputter times from a NAWC Johnson Matthey 1mm Pd wire (#10960, Lot W12954, 99.997% purity) which produced excess heat. Scans from 0 ev (right) to 1000 eV (left) binding energy

600s

1200s ÷2

Pt4d

2100s ÷2
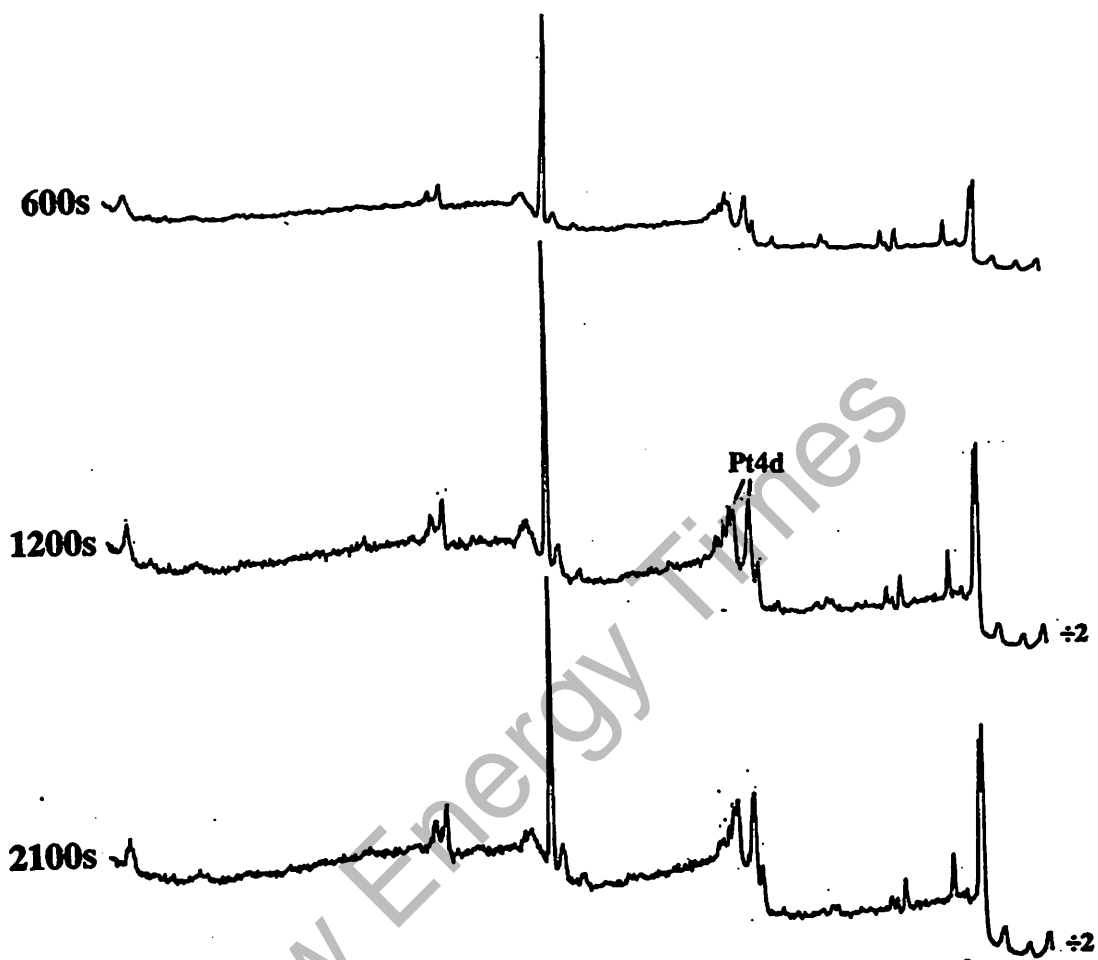
Fig. 41 - continued
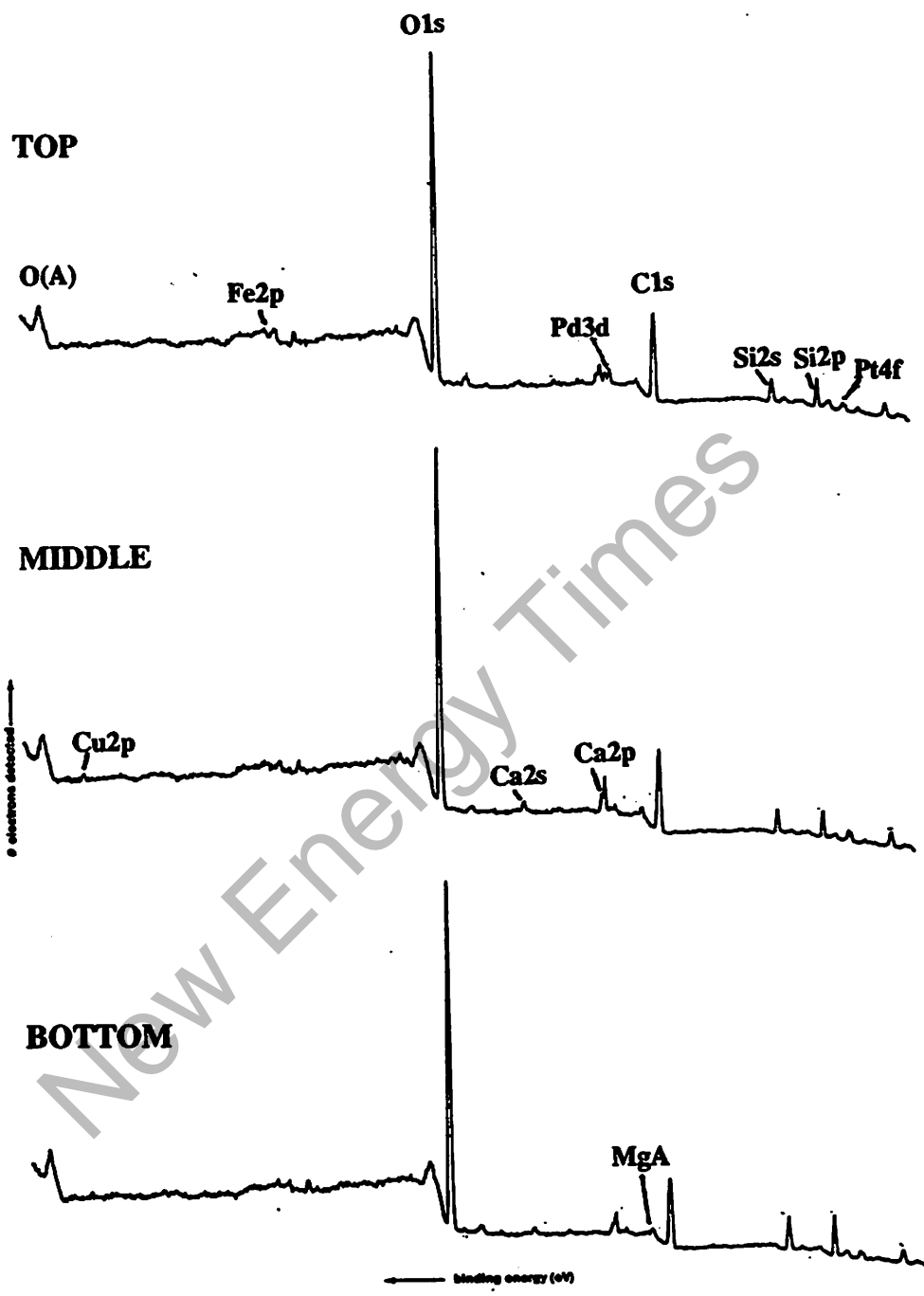
Fig. 42 - XPS survey spectra obtained from various positions on a NRL Pd-0.62B rod (#94090601) which produced excess heat at NAWC. Scans from 0 eV (right) to 1000 eV (left) binding energy
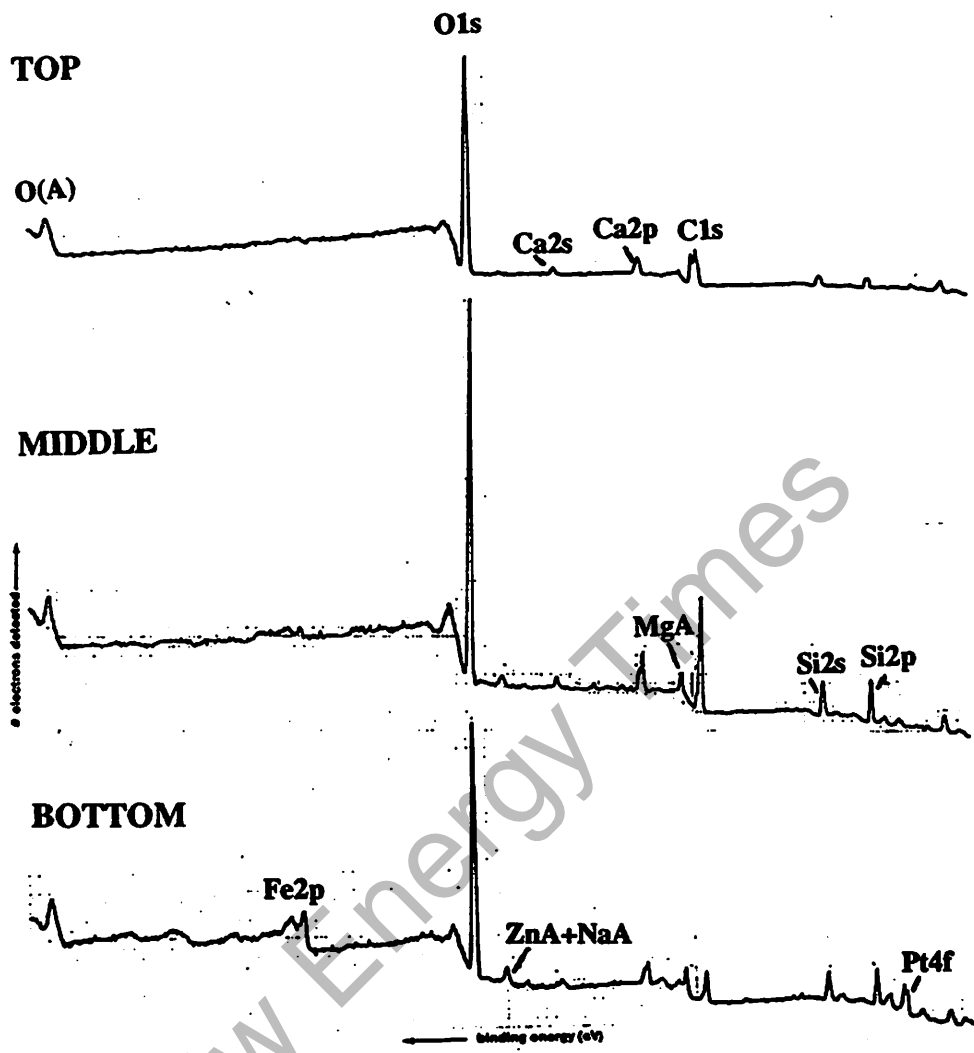
Fig. 43 - XPS survey spectra obtained from various positions on a NRL Pd-0.62B rod (#94090602) which did not produce excess heat at NAWC. Scans from 0 eV (right) to 1000 eV (left) binding energy
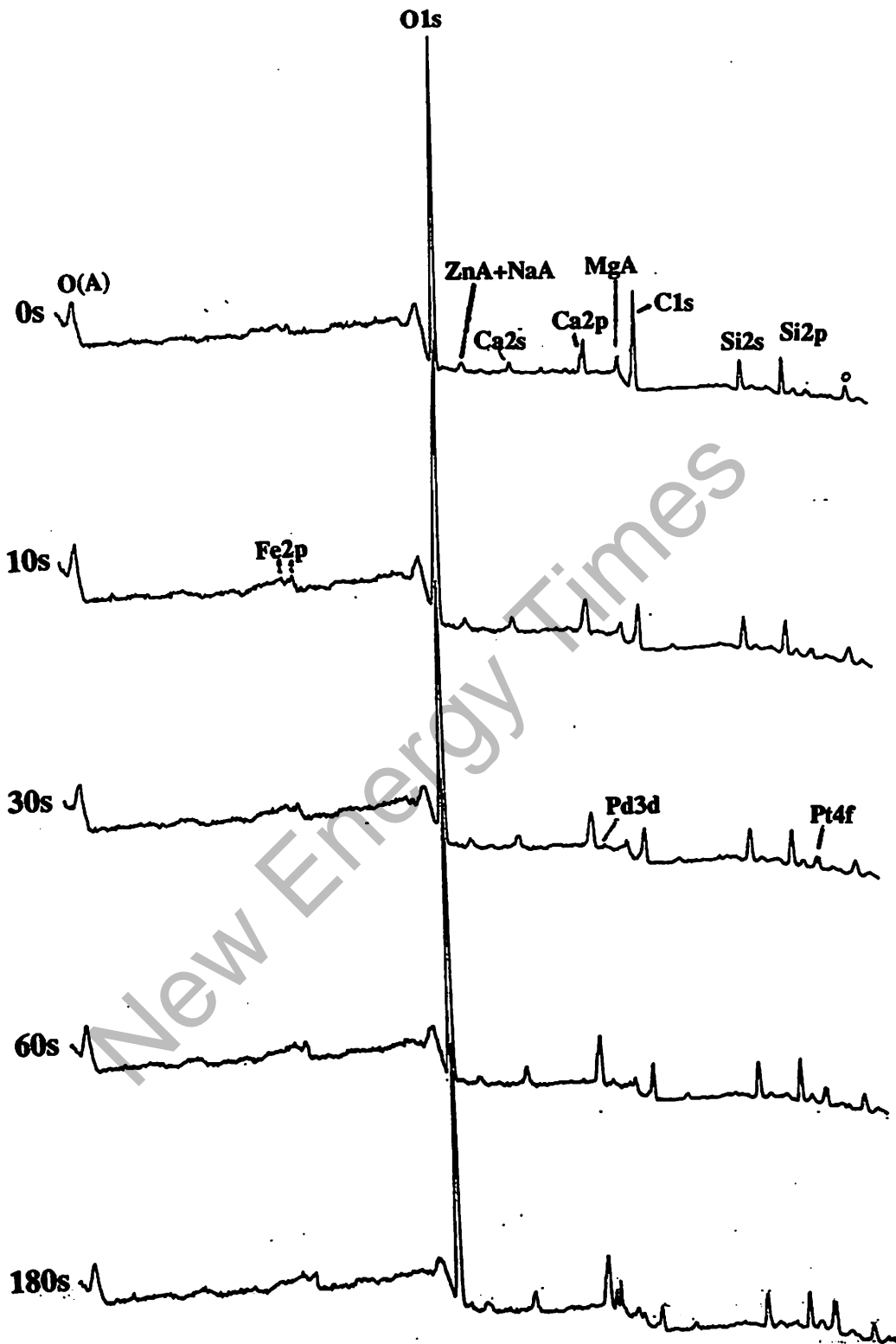
Fig. 44 - XPS survey spectra obtained at various total sputter times from a metallic gray area of the electrode in Figure 43. Scans from 0 eV (right) to 1000 eV (left) binding energy

300s Cu2p

600s

1200s x2.5

1800s x2.5

2400s x2.5

3600s x2.5
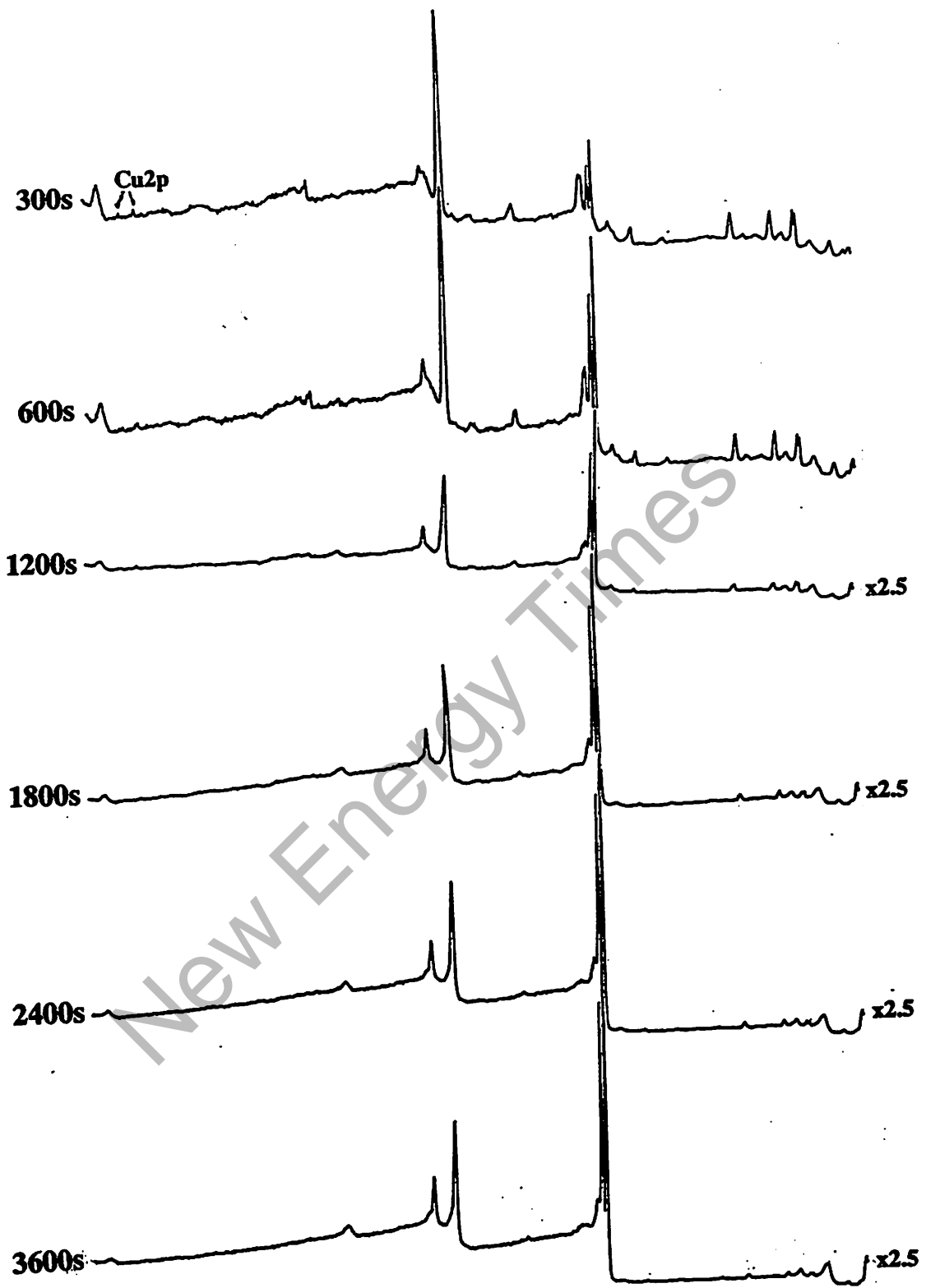
Fig. 44 - continued

after 3600s of sputtering. In Figures 45 and 46 are profiles of a Pd-0.18 wt.%B excess heat producing cathode from two different areas, one black the other gray. The gray area clearly has Pd present on the surface and sputtering removes most of the impurities relatively rapidly. The dark area contains much more Pt and the Pd peaks develop much slower with sputter time indicating a thicker layer is present. In addition, Cu and Ni are also found in the overlayer. The Ni comes from the cathode electrical connection which was apparently exposed in this experiment.

With the data presented above several observations can be made concerning excess heat-producing electrodes. All contain layers on part or all of the electrode which are relatively thin in the sense that Pd is either observed on the surface or very early in the sputter profile and the peaks due to Pd rise rapidly with continued sputtering. Pt is always observed on these electrodes and it is always visible on the surface. The electrodes, except the high purity Johnson Matthey used at NAWC (2.2 ppm by GDMS), generally have a large Pt impurity concentration in the bulk. Pt and Pd are in the metallic state when found on the surface. A silicate layer is observed on the surface but this can be sputtered away fairly rapidly. There is usually a graphitic component to the carbon which appears to extend, along with the Pt, into the bulk. Copper is a small impurity as are Zn, Na, Ca and Mg. Many of these observations can also be made for the cathode materials run at NRL. Since, however, the excess heat observed in the analyzed samples generally did not exceed 10% of the input power and the sensitivity of the NRL calorimeters was in the range of 10% and above, using the XPS data for NRL-run samples as representative of non-excess heat producing electrodes may not be correct. As a final note, many impurities found in the surface layers are also present in the bulk of the cathode at the ppm level (see Table 7 with the GDMS results for the high purity Johnson Matthey wire used at NAWC, NRL Pd and the NRL Pd-B alloys). Certainly the source of all the impurites found on the surface is not the bulk: however, as discussed above there is data to suggest that loading and deloading H-storage materials can greatly increase the room temperature diffusion rates of bulk elements.
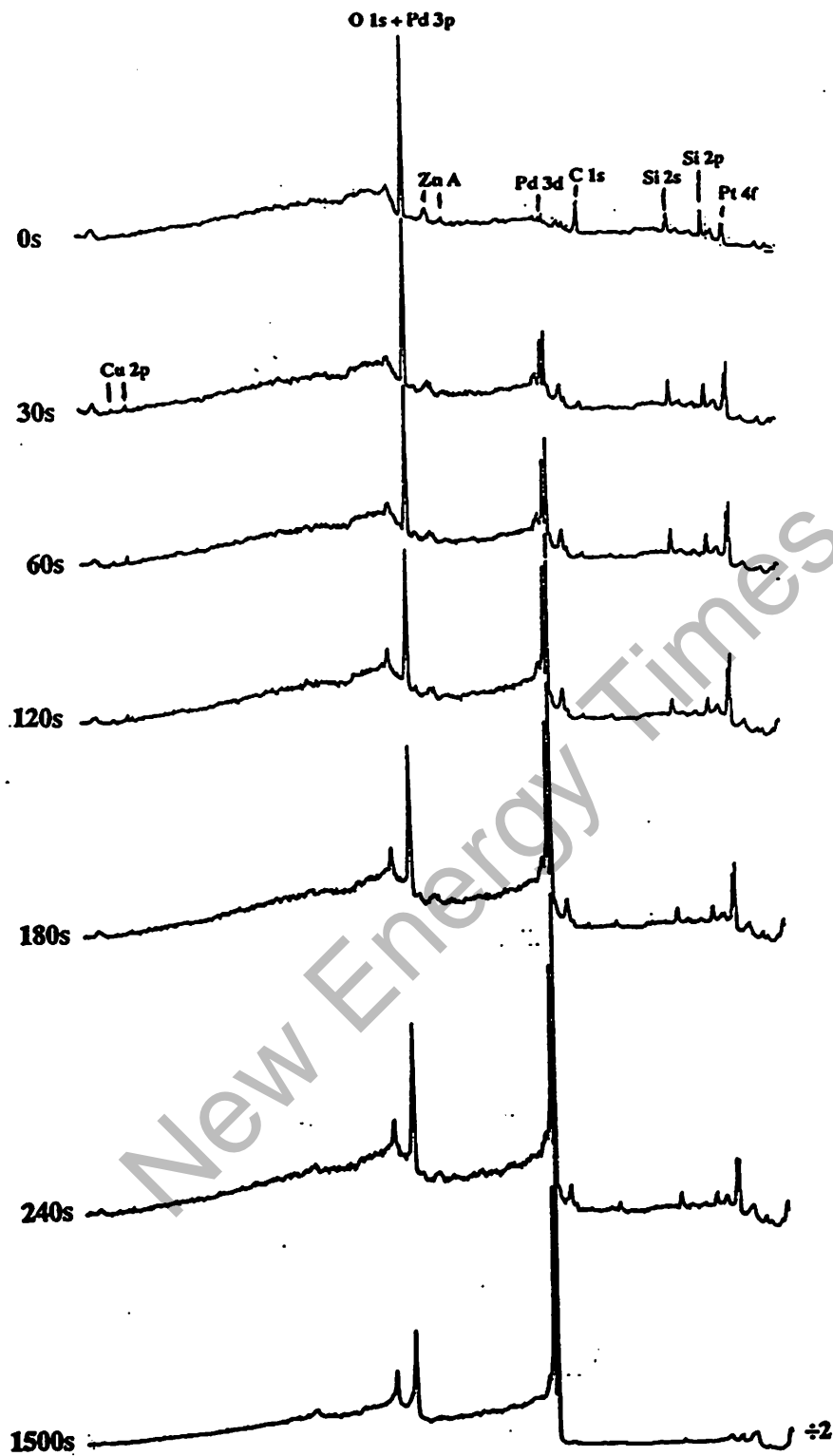
Fig. 45 - XPS survey spectra obtained at various total sputter times from a metallic gray area of a Pd-0.18B rod (#94081801) which produced excess heat at NAWC. Scans from 0 eV (right) to 1000 eV (left) binding energy
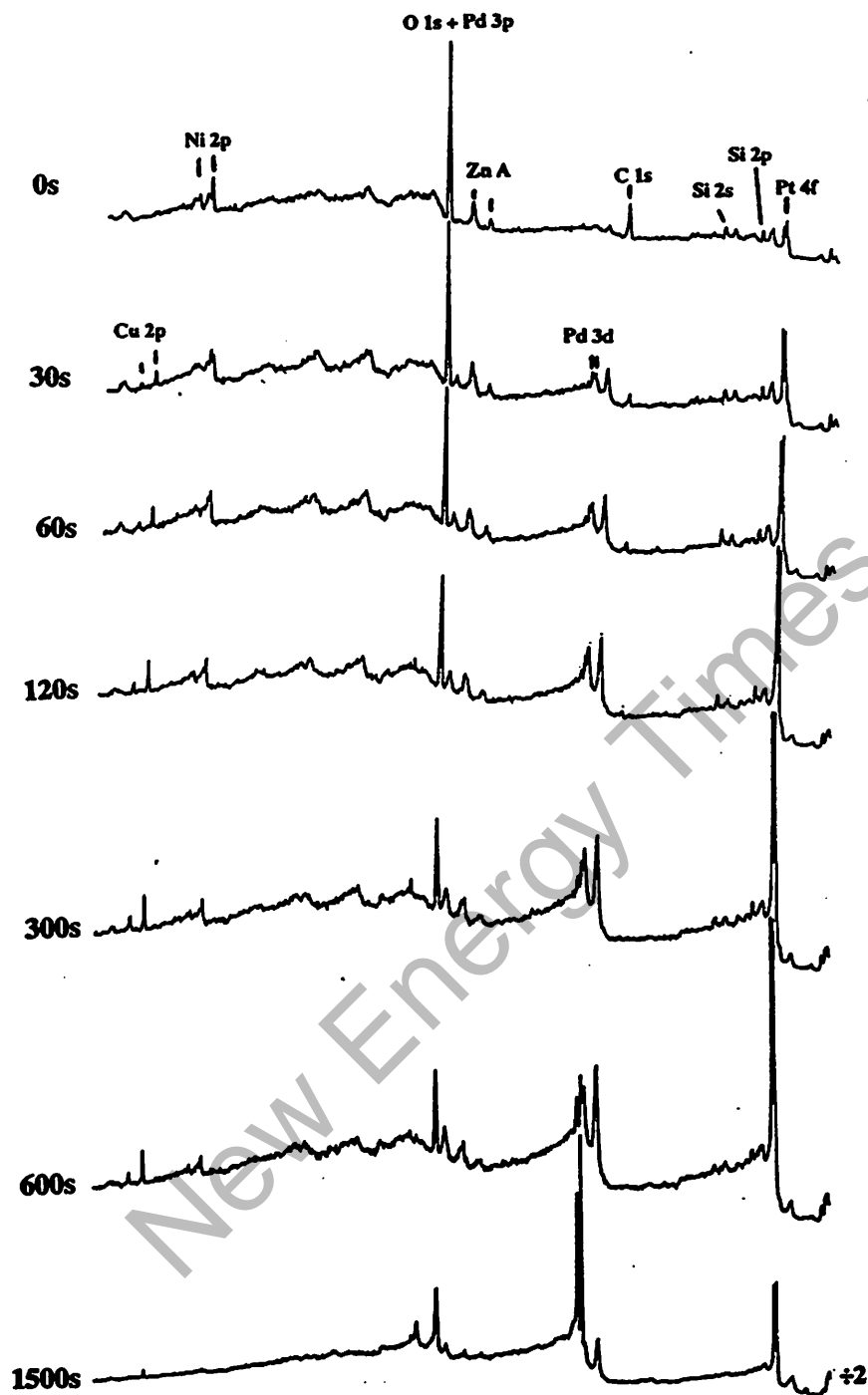
Fig. 46 - As in Figure 45 but Taken from a Black Colored Area of the Electrode

Table 7 - Glow-Discharge Mass Spectroscopic Analyses of Various Cathode Materials
(concentration in ppm by weight)

Element	NAWC Wire	NRL Pd	Pd-0.62B	Pd-0.38B	Pd-0.18B
B	0.007	<0.001	6200	3800	1760
C	<1	0.02	<1	<5	<1
N	<3	0.03	<0.1	<0.1	<5
O	<10	0.45	<10	<10	<20
Mg	0.009	1.2	3.5	2.7	2.9
Al	0.63	0.53	4.1	3.3	1.5
Si	3.5	0.31	15	11	6.8
Ca	0.29	0.58	7.9	2.9	2.4
Cr	0.21	1.2	0.98	1.1	1.1
Mn	0.004	0.75	8.2	5.9	2.6
Fe	2.9	33	56	47	36
Ni	0.03	0.85	1.4	1.7	0.98
Cu	0.76	27	26	25	16
Zn	0.02	1.2	2.3	1.7	1.6
Zr	0.04	0.3	3.9	0.79	0.84
Rh	4.2	11	11	9.6	8.5
Ag	0.45	0.71	0.75	1.4	1.5
W	0.10	3.8	2.2	1.0	0.67
Pt	2.2	30	47	38	18
In	<0.05	<0.05	<0.05	1.9	1.2
Au	1.0	0.17	0.2	0.65	0.22
Ir	1.1	0.4	0.33	0.23	0.18

Table 8 shows a comparison between the NRL heat-conduction calorimeters and isoperibol calorimeters. The main reason for acquiring the heat-conduction calorimeters was for a hundred fold increase in sensitivity. In addition, the heat-conduction calorimeters gave a faster response and were more accurate. Accuracy was increased because the heat-conduction calorimeters gave an absolute measure of heat flow (assuming no heat loss by radiation or convection) whereas the measurement in isoperibol calorimeters is relative to the temperature of the surroundings.

Table 8 - Comparison of NRL Calorimeters

	Isoperibol	Heat Conduction
Electrolytic Cell	Open	Open
Sensitivity	± 200 mW	± 2 mW
Bath Stability	± 0.02 °C	± 0.002 °C
Time Constant	40 min.	500 s
Temperature Sensor	Thermistor	Thermoelectric Device
Sensor Temp. Range	To 70 °C	To 90 °C
Temperature Response	3°C/W	0.5°C/W
Calibration Constant	0.2 W/°C	10 W/V

Calorimeter calibration constants, determined by Joule heating in a reference cell, are shown in Table 9. As noted in the Table, the constants range from 9.19-9.30 W/V using this calibration procedure. Constants were determined from the slopes of linear regression lines in plots of heat sensor response (volts) vs. input power (watts) as shown in Figure 6. Eight data points were plotted at each input power level after allowing three hours for the system to equilibrate following a change in input power. Multiple entries in the Table are the result of independent determinations of K.

Calorimeter calibration measurements were also made in electrolytic cells containing either a 0.2 cm diameter silver rod cathode or a 0.1 cm diameter palladium rod cathode in 0.1M LiOH with input powers of 0.2-10 Watts. These measurements were made to compare K values determined in an "electrolysis configuration" with those determined in a non-electrolyzing reference cell. Calibration with the non-hydrogen-absorbing silver rod cathode was compared to calibration of a palladium rod cathode after loading with hydrogen. Calibration with the palladium rod cathode was done with platinum wires for *in situ* resistance measurements attached to the cathode. As before, calibration constants were determined from the slopes of linear regression lines in plots of heat sensor response (volts) vs. input power (watts). Results of these measurements are also shown in Table 9.

Table 9 - Calorimeter Calibration Constants (Watts/Volt)

———————— Calorimeter Position/Sensor Channel ————————

Cell	LF/CH11	RR/CH12	RF/CH13	LR/CH14
100 Ohm Reference/Oil	9.269±0.004 9.295±0.003 9.267±0.004	9.304±0.006	9.302±0.001	9.196±0.001 9.192±0.001
100 Ohm Reference/0.1M LiOH		9.300±0.015 9.280±0.002		
Ag Wire/0.1M LiOH	9.232±0.011	9.305±0.017 9.250±0.027 9.284±0.029	9.280±0.029	9.174±0.014
Pd Wire/0.1M LiOH			9.225±0.015***	
Average	9.266	9.287	9.291	9.187

***not included in average for RF calorimeter position (see text for explanation)

As seen from the Table, calorimeter calibration constants determined in electrolyzing cells range from 9.17-9.28 W/V. Overall average K values for three of the four calorimeter positions (LF, RR and RF) are 9.281±0.013 W/V while the average K value for the fourth position (LR) is 9.187±0.012 W/V. While more accurate determinations of K would be beneficial, K values accurate to 1 part in 10^3 were measured. As such, assuming a 1 V sensor response at 10 W input power, a 10 mW/V uncertainty in the calibration constant would result in a 10 mW uncertainty in excess power at 10 W input power. This represents a 0.1% uncertainty in the excess power calculation.

A closer look at Table 9 shows that the uncertainties associated with the K values for electrolytic cells were generally several times larger than the uncertainties associated with the K values for reference cells. These uncertainties were due to fluctuations in cell voltage and, hence, input power resulting from the bubbling that occurs in an electrolysis cell. Also noted in the Table is the smaller K value calculated for an electrolysis cell with a palladium wire cathode. It is not clear whether the difference is significant since only one determination of K was made with this cell. A lower value of K for the palladium electrolysis cell might be caused by hydrogen loading of the cathode that is exothermic below H/Pd=0.6 [42] although palladium resistance measurements indicated that the cathode was loaded above 0.8. Another possible cause of a lower K may be recombination of H_2 and O_2. Clearly, more determinations of K with palladium cathodes are needed along with more measurements of hydrogen loading and electrolysis gas evolution rates. Note, because of the uncertainty in its significance, the K value for the cell with the palladium cathode was not included in the calculation of the average K for the right front calorimeter position.

The accuracy of the calorimeter calibration constants is certainly an important issue in the determination of excess power. Another issue is whether K could be considered constant in the range of interest. To address this issue, individual K values were calculated for a reference cell filled with 0.1 M LiOH located in the right rear calorimeter position. Input powers in the range of 0.003 W to 8.682 W were used in the calculations. The calculation assumes that the intercept in the plot of input power vs. sensor response equals zero so that $P_{out}=KV_{TED}$. As seen in Figure 7, this assumption is valid for reference cells (the mean of intercepts in electrolysis cells was 20 ± 8 mW).

Results of the individual calculations of K are shown in Table 10. All calculations were averages of 3-4 measurements obtained after allowing at least three hours for the system to equilibrate after a change in input power was made. Voltages were measured to 5 significant digits while results are reported to 4 significant digits as K was always reproducible to 3 significant digits at each power level. A variation in the calorimeter calibration constant, K, with input power levels was noted for the reference cell. The calibration constant decreased from 11.48 W/V at 0.003 W input power to 9.287 W/V at 0.85 W input power. However, from 1.07-8.68 W the calibration constant was 9.280 ± 0.002 W/V. As such, K for this reference cell could be considered constant in the range where calorimetric measurements are made (input power $\geq$ 1 watt).

Table 10 - Reference Cell Calibration

Input Power (Watts)	Calibration Constant (Watts/Volt)
0.003480	11.48
0.01155	9.927
0.04541	9.419
0.06857	9.341
0.09495	9.340
0.1314	9.317
0.1734	9.316
0.2646	9.289
0.5184	9.289
0.8472	9.287
1.067	9.282
2.352	9.282
4.134	9.280
5.231	9.278
6.484	9.279
7.883	9.279
8.143	9.278
8.682	9.279

Calculations show that at low input powers using different values for K lead to small errors in excess power. For example, at low input power levels where K is largest (i.e., at 3.480 and 11.55 mW) using a value for K of 9.5 W/V instead of 11.48 and 9.927 W/V produces errors of less than 10%. However, excess power calculations are much more sensitive to the accuracy of K at high input powers.

The importance of this is illustrated in Figure 47 for a reference cell (actual K=9.280 W/V) that produces zero excess power. As seen in the Figure, at 8.68 W input power, using a K value of 9.5 W/V in an excess power calculation results in about a 200 mW excess power determination for the cell (top curve). Reducing the value of K to 9.3 W/V lowers the excess power calculated for the cell to about 25 mW (bottom curve). Thus, K values accurate to at least 3 significant figures must be used to avoid erroneous calculations of excess power at high input powers.

K values were also calculated from an average input power and an average sensor response using the eight data points at each input power. The data used in these determinations show some interesting trends. For example, when the data from the eight data points at a given input power are averaged, the standard deviation of the input power varies 10-100x more than the standard deviation of the sensor response. (As mentioned earlier, variations in input power result almost exclusively from fluctuations in cell voltage. The cell voltage fluctuations increase at higher input powers due to bubbling in the cell.) Thus, more uncertainty is associated with the electrochemical input power to the cell than in the heat sensor response of the calorimeter. Secondly, more variation (10x) was noted in the input power and in the sensor response at high input powers (i.e., 10 W vs. 1 W). The latter is extremely important since large variations in input power and in sensor voltage lead to larger uncertainties in K. To overcome the uncertainties in K, many measurements of cell voltage and sensor response need to be measured and the appropriate statistics need to be applied to the measurements.

Experiments in the heat-conduction calorimeters were begun in October 1994 with cells containing two NRL 0.4 cm diameter Pd-0.62% B rod cathodes, one Johnson Matthey 0.1 cm diameter wire cathode, and one 100 ohm resistance heater as a reference. Details of these experiments can be found in NRL laboratory notebook # N-7818 assigned to Dr. Dawn Dominguez. The notebook covers the time from 10-24-94 to 6-30-95. Negative "excess powers" were found in the electrolytic cells. The magnitude of the "excess power" increased with increases in electrochemical input power to the cell. No excess power was seen in the reference cell. Negative "excess power" seemed to result from smaller than expected voltage responses of the thermoelectric sensors.

When the electrolysis cells were disassembled, corrosion of the anodized-aluminum cell holders was evident. The corrosion resulted from electrolyte leakage from the cells at the point where the Teflon-coated platinum lead wires exited through the Teflon cell tops (see Figure 3). Viton o-rings had been used to seal the wires in the cell top. The o-rings were pushed out of position presumably due to a build up of pressure in the cell. To eliminate the pressure build up, cell tops were redesigned to accommodate a larger diameter Teflon tubing for the exit gases. O-rings were also replaced by a Viton septum for sealing around the Teflon-coated lead wires. With the cell top design changes in place, the calorimeters were recalibrated as a check on their performance. The resistance heaters in the calorimeter walls were used in these calibrations. The calibration constants of the four calorimeters were again 9.5 W/V.

Five more calorimetric experiments were set up between January and June 1995 using the redesigned cell tops. Some of these electrochemical cells were set up by Dr. Melvin Miles (NAWC). These cells contained two NRL 0.4 cm diameter Pd-0.62% B cathodes and one 100 ohm resistance heater as a reference. Other cells contained 0.1 cm diameter Johnson Matthey 99.997% Pd wire and 0.2 cm diameter silver rod as cathodes. Again negative "excess powers" that increased with input power were observed in the electrolytic cells and, again, the voltage responses of the thermal electric sensors were smaller than expected. There was no evidence of electrolyte leakage or corrosion of the cell holders in these experiments. Nonetheless, the experiments were terminated when no cause for the "excess powers" was apparent.
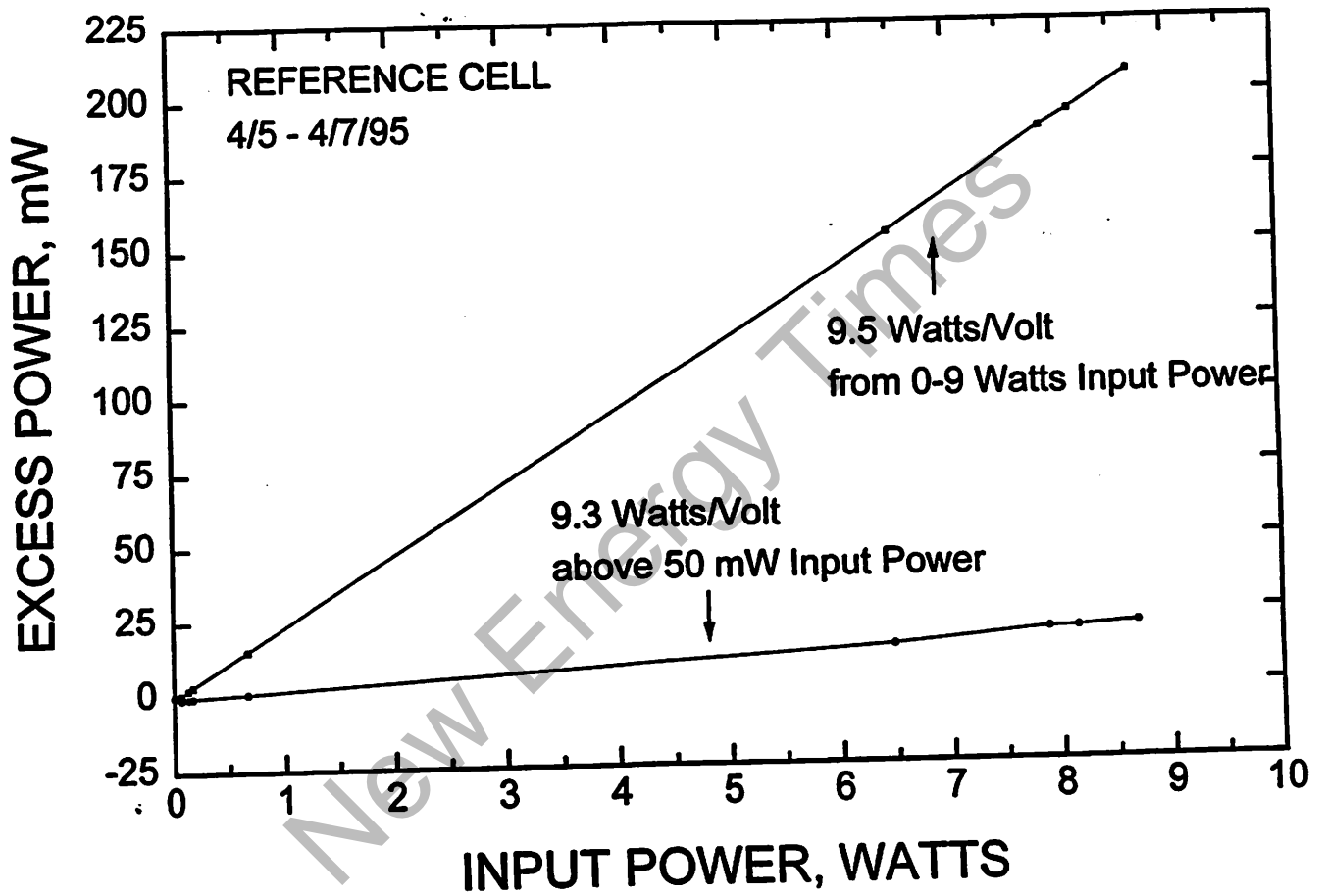
Fig. 47 - Changes in the excess power calculated for a reference cell as a function of input power. Top curve: using a calibration constant of 9.5 watts/volt from 0-9 watts input power. Bottom curve: using 9.5 watts/volt for input powers from 0-50 mW and 9.3 watts/volt for input powers from 50 mW - 9 watts

Many diagnostic tests were carried out to troubleshoot the calorimetric problem. These included alternate application of suction and pressure to various electrolytic cells, analyzing the electrolysis gas $(H_2 + O_2)$ volume produced from the cells, and leak-testing the cell tops to determine whether gas was escaping from places other than the gas exit tubes. From these tests, it was determined that electrolysis gases were leaking past the seals in the Teflon cell top. By ensuring a tight fit between the Viton o-ring around the Teflon cell top and the glass cell, and a good seal between the Viton septum and the wires and gas exit tubes the endothermic behavior was prevented. Thus, cell construction changes were implemented to prevent the gas leakage from occurring. As an additional precaution, electrolysis cells were to be pressured tested in the future before beginning a new experiment.

Gas leakage from the electrolysis cells apparently caused desorption of loosely bound water from one of the anodized-aluminum plugs at the top of the calorimeter (see Figure 3). The loosely bound water originated from the sealing of the porous anodized layer that is accomplished by boiling the part in water. This process renders the extremely porous anodic oxide film non-porous through reaction of the pore walls with water to form amorphous oxide hydroxide (AlOOH) and gelatinous boehmite. Boehmite is a crystalline form of AlOOH that contains large amounts of weakly bound water [46 and references therein]. Desorption of this loosely bound water can begin near room temperature and the process is endothermic as has been shown by thermogravimetric analysis measurements [46 and references therein].

Another problem that was noted during the experiments in the new, sensitive calorimeters was that 0.2-0.3 volts, 60 Hz ac noise contaminated most measurement channels of the data acquisition system. Those channels that measured cell voltage had an even larger background (1-3 volts ac). In addition, moving the electrical wires or the instrument rack holding the electronics often changed the measured readings. To alleviate these electronic problems, the data acquisition system was rebuilt. This revamping reduced the background noise on most channels to 0.15 mV. The background noise on the cell voltage channels was reduced to tens of mV ac at high cell currents. As an additional precaution against switching transients, the data acquisiton software was reprogrammed so that each of the scanner channels stayed closed for a full 10 seconds (previously, they were each closed for 1 s). The settle time on the measuring multimeter was also increased to 200 milliseconds before reading the dc voltage (previously, the settle time was 1 ms). The signal integration period on the multimeter remained at 100 ms.

Unfortunately, there was no time to carry out any successful calorimetric experiments in the new calorimeters before the end of the Anomalous Effects Program. Thus, the question of whether NRL researchers can reproduce the NAWC or SRI experiments that generated excess power in electrolytic cells with palladium or palladium alloy cathodes remains open.

CONCLUSIONS

The following conclusions are the results of NRL experiments on electrochemically loaded palladium and palladium alloys during the ONR-sponsored Anomalous Effects Program:

(1) Loading palladium cathodes into the β-phase with deuterium is facilitated by using material with a large grain microstructure;

(2) Most palladium cathodes with elongated or small grains didn't load deuterium into the β-phase;

(3) Hardly any grain growth occurred on annealing high purity (99.99% or better) palladium cathodes at 1100°C for 20 hours whereas lower purity (99.9%) materials readily grew large grains;

(4) Transmission electron microscopy and x-ray diffraction studies identified two distinct phases in the palladium/0.62 weight percent boron alloy; the lattice parameters for the different phases were measured;

(5) Prolonged electrolysis at high current density in basic solution resulted in the formation of a relatively thick layer on the cathode (> 1000Å) composed of a varied elemental composition with very little or no Pd identifiable on the surface. Twenty different elements have been identified from XPS analysis of over 30 different electrode surfaces. Cationic, anionic and organic species in the electrolyte have been detected as part of these surface overlayers. The anodes remained relatively film-free;

(6) Longer electrolysis times (~1000 hrs.) produced thicker films on NRL Pd cathodes compared to shorter times (<500 hrs.). In addition, the thicker films contained larger quantities of both Cu and Pt relative to Pd and in general higher loadings were obtained with these films present. This suggests that thicker films may help block the egress of D from the Pd lattice;

(7) Thinner films where Pd was present at or near the surface were found on excess heat producing electrodes obtained from SRI and NAWC (exceptions are where large quantities of certain species were added to the electrolyte to help or initiate excess heat formation). Very little copper was found in these films but appreciable amounts of Pt were present. Thin films without Cu may be necessary for excess power measurement;

(8) The source of some elements found in the cathode overlayer may be bulk diffusion of impurities such as Pt and Cu caused by the severe lattice distortion produced by absorption of large quantities of D or H;

(9) High sensitivity heat-conduction calorimeters are capable of accurately measuring ± 10 mW of excess power in electrochemical cells at high input powers provided that calibration constants are known to at least one part in 10^3, and that cell voltage and sensor voltage measurements are made frequently and treated with appropriate statistics;

(10) No excess power > 200 mW was measured in any electrolytic cells containing NRL palladium and palladium/10% silver cathodes in NRL isoperibol calorimeters;

(11) No anomalous radiation was detected with either germanium or sodium iodide gamma-ray detectors during any electrochemical experiments with deuterium or hydrogen-loaded palladium or palladium/10% silver cathodes;

(12) The palladium/deuterium codeposition experiment is inherently irreproducible;

(13) No anomalous radiation was detected during the palladium/deuterium codeposition experiment with either a germanium gamma-ray detector or an x-ray detector.

ACKNOWLEDGEMENTS

REFERENCES

1. M.H. Miles, K.H. Park, and D.E. Stilwell, "Electrochemical Calorimetric Evidence for Cold Fusion in The Palladium-Deuterium System," J. Electroanal. Chem., 296, 241-254 (1990).

2. M.H. Miles, B.F. Bush, G.S. Ostrom, and J.J. Lagowski, "Heat and Helium Production in Cold Fusion Experiments," Conference Proceedings Vol. 33, *The Science of Cold Fusion*, T. Bressani, E. Del Giudice and G. Preparata (Eds.), Bologna, 363-372 (1991).

3. B.F. Bush, J.J. Lagowski, M.H. Miles, and G.S. Ostrom, "Helium Production During Electrolysis of D_2O in Cold Fusion Experiments," J. Electroanal. Chem., 304, 271-278 (1991).

4. S. Szpak, P.A. Mosier-Boss, and J.J Smith, "Reliable Procedure for the Initiation of the Fleischmann-Pons Effect," Conference Proceedings Vol. 33, *The Science of Cold Fusion*, T. Bressani, E. Del Giudice and G. Preparata (Eds.), Bologna, 87-91 (1991).

5. S. Szpak, P.A. Mosier-Boss, and J.J. Smith, "On the Behavior of Pd Deposited in the Presence of Evolving Deuterium," J. Electroanal. Chem., 302, 255-260 (1991).

6. M. Fleischmann and S. Pons, "Electrochemically Induced Nuclear Fusion of Deuterium," J. Electroanal. Chem., 261, 301-308 (1989).

7. M.H. Miles and B.F. Bush, unpublished results.

8. D. Hodko and J.O'M. Bockris, "Possible Excess Tritium Production on Pd Codeposited With Deuterium," J. Electroanal. Chem., 353, 33-41 (1993).

9. S. Pons, "Calorimetry of the Palladium-Deuterium System," Conference Proceedings - The First Annual Conference on Cold Fusion, Salt Lake City, UT, 1-19 (1990).

10. S. Pons and M. Fleischmann, "The Calorimetry of Electrode Reactions and Measurements of Excess Enthalpy Generation in the Electrolysis of D_2O Using Pd-Based Cathodes," Conference Proceedings Vol. 33, *The Science of Cold Fusion*, T. Bressani, E. Del Giudice and G. Preparata (Eds.), Bologna, 349-362 (1991).

11. M.H. Miles, B.F. Bush, and D.E. Stilwell, "Calorimetric Principles and Problems in Measurements of Excess Power During Pd-D_2O Electrolysis," J. Phys. Chem., 98, 1948-1952 (1994).

12. F.G. Will, K. Cedzynska, M-C Yang, J.R. Peterson, H.E. Bergeson, S.C. Barrowes, W.J. West and D.C. Linton, "Studies of Electrolytic and Gas Phase Loading of Palladium With Deuterium," Conference Proceedings Vol. 33, *The Science of Cold Fusion*, T. Bressani, E. Del Giudice and G. Preparata (Eds.), Bologna, 337-383 (1991).

13. F.G. Will K. Cedzynska and D.C. Linton, "Reproducible Tritium Generation in Electrochemical Cells Employing Palladium Cathodes With High Deuterium Loading," J. Electroanal. Chem., 360, 161-176 (1993).

14. M.C.H. McKubre, R.C. Rocha-Filho, S. Smedley, F. Tanzella, J. Chao, B. Chexal, T. Passell and J. Santucci, "Calorimetry and Electrochemistry in the D/Pd System," Proceedings of the First Annual Conference on Cold Fusion, The National Cold Fusion Institute, Salt Lake City, UT, 20-31 (1990).

15. D.R. Rolison and P.P. Trzaskoma, "Morphological Differences Between Hydrogen-Loaded and Deuterium-Loaded Palladium As Observed by Scanning Electron Microscopy," J. Electroanal. Chem., 287, 375-383 (1990).

16. M Fleischmann and S. Pons, "Electrochemically Induced Nuclear Fusion of Deuterium," J. Electroanal. Chem., 261, 301-308 (1989).

17. M.C.H. McKubre, S. Crouch-Baker, A.M. Riley, S.I. Smedley and F.L. Tanzella, "Excess Power Observations in Electrochemical Studies of the D/Pd System: The Influence of Loading," Proceedings of the Third International Conference on Cold Fusion, " Frontiers of Cold Fusion," H. Ikegami, Ed., Universal Academy Press, Inc., Tokyo, 5-19 (1993).

18. M. Fleischmann, S. Pons, M.W. Anderson, L.J. Li and M. Hawkins, "Calorimetry of the Palladium-Deuterium-Heavy Water System," J. Electroanal. Chem., 287, 293-348 (1990).

19. M.C.H. McKubre, R. Rocha-Filho, S.I. Smedley, F.L. Tanzella, S. Crouch-Baker, T.O. Passell, and J. Santucci, "Isothermal Flow Calorimetric Investigations of the D/Pd System," Conference Proceedings Vol. 33, The Science of Cold Fusion, T. Bressani, E. Del Giudice and G. Preparata (Eds.), Bologna, 419-443 (1991).

20. T.A. Green and T.I. Quickenden, "Electrolytic Preparation of Highly Loaded Deuterides of Palladium," J. Electroanal. Chem., 368, 121-131 (1994).

21. D.J. Gillespie, G.N. Kamm and A.C. Ehrlich, "A Search For Anomalies in the Palladium-Deuterium System," Fusion Technology, 16, 526-528 (1989).

22. The Handbook of Chemistry and Physics, 49th Edition, The Chemical Rubber Co., Weast (Ed.) E-80 (1968).

23. M.C.H. McKubre, S. Crouch-Baker, R.C. Rocha-Filho, S.I. Smedley, F.L. Tanzella, T.O. Passell and J. Santucci, "Isothermal Flow Calorimetric Investigations of the D/Pd and H/Pd systems," J. Electroanal. Chem., 368, 55-66 (1994).

24. B. Baranowski, and R. Wisniewski, "The Electrical Resistance of Palladium and Palladium-Gold Alloy (50 wt % Au and Pd) in Gaseous Hydrogen Up to 24000 at at 25°C," Phys. Status Solidi, 35, 593-597 (1969).

25. A.W. Szafranski and B. Baranowski, "The Electrical Resistance of The Pd-Ag-H System at 25°C in a Wide Range of Hydrogen Pressure," Phys. Status Solidi A, 9, 435-447 (1972).

26. B. Baranowski, S.M. Filipek, M. Szustakowski, J. Farny, and W. Woryna, "Search For "Cold-Fusion" In Some Me-D Systems at High Pressures of Gaseous Deuterium," J. Less-Common Met., 158, 347-357 (1990).

27. G. Bambakidis, R.J. Smith and D.A. Otterson, "Electrical resistivity Versus deuterium Concentration in Palladium," Phys. Rev., 177, 1044-1048 (1969).

28. R.J. Smith and D.A. Otterson, "Electrical Resistivity of PdH_x System for H/Pd Atom Ratios to 0.97," J. Phys. Chem. Solids, **31**, 187-189 1970.

29. T.B. Flanagan and W.A. Oates, "The Palladium-Hydrogen System," Annual Rev. Mater. Sci., **21**, 269-304 (1991).

30. Abstract of patent application submitted by Johnson Matthey "Modified Palladium Cathode for Cold Fusion Type Electrochemical Process," *World Appl.* 90/15,415A in Platinum Metals Rev., **35**, 166 (1991).

31. J.P. Hoare, "Surface to Volume Considerations in the Palladium-Hydrogen-Acid System," J. Electrochem. Soc., **106**, 640-643 (1959).

32. A.M. Riley, J.D. Seader, D.W. Pershing and C. Walling, "An *In-Situ* Volumetric Method for Dynamically Measuring the Absorption of Deuterium in Palladium During Electrolysis," J. Electrochem., Soc., **139**, 1342-1347 (1992).

33. M.C.H. McKubre, S. Crouch-Baker, A.K. Hauser, S.I. Smedley, F.L. Tanzella, M.S. Williams and S.S. Wing, "Concerning Reproducibility of Excess Power Production," submitted for publication in the Proceedings of the Fifth International Conference on Cold Fusion, Monte-Carlo (1995).

34. D.R. Rolison, W.E. O'Grady, R.J. Doyle, Jr., and P.P. Trzaskoma, "Anomalies in the Surface Analysis of Deuterated Palladium," Proceedings of the First Annual Conference on Cold Fusion, The National Cold Fusion Institute, Salt Lake City, UT, 272-280 (1990).

35. C.T. Dillon and B.J. Kennedy, "The Electrochemically Formed Palladium-Deuterium System. I. Surface Composition and Morphology," Aust. J. Chem., **46**, 663-679 (1993).

36. C.J. Lihn, C.C. Wan, C.M. Wan and T.P. Perng, "The Influence of Deposits on Palladium Cathodes in D_2O Electrolysis," Fusion Technology, **24**, 324-331 (1993).

37. M. Fleischmann and S. Pons, private communication.

38. D. Cravens, "Factors Affecting Success Rate of Heat Generation in Cold Fusion Cells," Cold Fusion, **1**, 58-61 (1994).

39. E.M. Savitskii, V.P. Polyakova and M.A. Tylkina, *Palladium Alloys*, Primary Sources, New York, 48 (1969).

40. S. Arajs, K.V. Rao, Y.D. Yao and W. Teoh, "Electrical Resistivity of Palladium-Silver Alloys At High Temperatures," Phys. Rev. B, **15**, 2429-2431 (1977).

41. T.B. Flanagan and Y. Sakamoto, "Hydrogen in Disordered and Ordered Palladium Alloys," Platinum Metals Rev., **37**, 26-37 (1993).

42. J. Balej and J. Divisek, "Energy Balance of D_2O Electrolysis With a Palladium Cathode; Part I. Theoretical Relations," J. Electroanal. Chem., **278**, 85-98 (1989).

43. S.B. Ziemecki, G.A. Jones and D.G. Swartzfager, "Coexistence of Hydrogen and Carbon Solutes in the Palladium Lattice," J. Less-Common Metals, **131**, 157-162 (1987).

44. R. Burch and F.A. Lewis, "Absorption of Hydrogen by Palladium + Boron and Palladium + Silver + Boron Alloys," Trans. Faraday Soc., **66**, 727-735 (1970).

45. J.J. Willems and K.H.J. Buschow, "From Permanent Magnets to Rechargeable Hydride Electrodes," J. Less-Common Metals, **129**, 13-30 (1987).

46. K. Wefers and C. Misra, *Oxides and Hydroxides of Aluminum*, Alcoa Laboratories (1987).

Appendix A

GLOW-DISCHARGE MASS SPECTROSCOPIC ANALYSES
OF PALLADIUM CATHODE MATERIALS

(1) Palladium sponge (Johnson Matthey, 99.999%), as received

(2) Palladium sponge (Johnson Matthey, 99.999%), as received

(3) Palladium rod processed at NRL

(4) Palladium rod processed at NRL - 3 pieces

(5) Palladium plate processed at NRL

(6) Palladium/0.62 wt.% boron rod processed at NRL

(7) Palladium/0.38 wt.% boron rod processed at NRL

(8) Palladium/0.18 wt.% boron rod processed at NRL

(9) Palladium rod (Johnson Matthey "special batch") from SRI

(10) Palladium rod (Johnson Matthey, 99.9% - stock #98529, lot #13E05)

(11) Palladium wire (Johnson Matthey, 99.9% - stock #10280, lot #K11C06)

(12) Palladium wire (Johnson Matthey, 99.997% - stock #10960, lot #7403)

(13) Palladium wire (Johnson Matthey, 99.997% - stock #10960, lot #W12954) from NAWC

(14) Palladium wire (Goodfellow, 99.95% - stock #005150/11)

(15) Palladium wire (Goodfellow, 99.99+% - stock #005155/11)

(1)   Palladium sponge (Johnson Matthey, 99.999%), as received

Client	Naval Research Labs.		P.O. #	
Date	September 16, 1992		Job #	B347
	Client ID	Palladium # 1		
	Shiva ID	92091403		
	Element	Concentration	Element	Concentration
	Li	< 0.01	Pd	Matrix
	Be	< 0.005	Ag	1.5
	B	0.1	Cd	< 0.1
	C	5	In	< 0.05
	N	1	Sn	0.8
	O	10	Sb	< 0.1
	F	0.05	Te	< 0.01
	Na	1	I	< 0.005
	Mg	0.1	Cs	< 0.005
	Al	0.5	Ba	< 0.005
	Si	0.6	La	< 0.005
	P	0.06	Ce	< 0.005
	S	0.1	Pr	< 0.005
	Cl	0.2	Nd	< 0.005
	K	0.1	Sm	< 0.005
	Ca	0.5	Eu	< 0.005
	Sc	< 0.001	Gd	< 0.005
	Ti	4	Tb	< 0.005
	V	0.006	Dy	< 0.005
	Cr	2.5	Ho	< 0.005
	Mn	0.9	Er	< 0.005
	Fe	45	Tm	< 0.005
	Co	0.3	Yb	< 0.005
	Ni	1.3	Lu	< 0.005
	Cu	0.8	Hf	< 0.01
	Zn	0.9	Ta	< 3
	Ga	0.3	W	1
	Ge	< 0.05	Re	< 0.005
	As	0.1	Os	< 0.01
	Se	< 0.05	Ir	0.55
	Br	< 0.01	Pt	12
	Rb	< 0.01	Au	1
	Sr	< 0.01	Hg	< 0.1
	Y	< 0.01	Tl	< 0.01
	Zr	0.05	Pb	0.2
	Nb	< 0.01	Bi	< 0.01
	Mo	0.5	Th	0.01
	Ru	0.6	U	0.002
	Rh	8		

(All concentrations are expressed as PPM WT)

104   Analyzed by:

(2) Palladium sponge (Johnson Matthey, 99.999%), as received

Client	Naval Research Labs.		P.O. #	
Date	March 31, 1994		Job #	D262
	Client ID	Palladium		
		#1 sponge		
	Shiva ID	94032807		
	Element	Concentration	Element	Concentration
		[ppmwt]		[ppmwt]
	Li	< 0.01	Pd	Matrix
	Be	< 0.005	Ag	1.6
	B	0.007	Cd	< 0.1
	C	< 10	In	< 0.05
	N	< 0.1	Sn	0.8
	O	< 20	Sb	0.2
	F	< 0.01	Te	< 0.01
	Na	0.1	I	< 0.005
	Mg	< 0.01	Cs	< 0.005
	Al	0.06	Ba	< 0.005
	Si	0.15	La	< 0.005
	P	< 0.01	Ce	< 0.005
	S	0.1	Pr	< 0.005
	Cl	< 0.01	Nd	< 0.005
	K	0.03	Sm	< 0.005
	Ca	< 0.05	Eu	< 0.005
	Sc	< 0.001	Gd	< 0.005
	Ti	0.4	Tb	< 0.005
	V	< 0.005	Dy	< 0.005
	Cr	2.8	Ho	< 0.005
	Mn	1.3	Er	< 0.005
	Fe	31	Tm	< 0.005
	Co	0.01	Yb	< 0.005
	Ni	1.1	Lu	< 0.005
	Cu	0.44	Hf	< 0.01
	Zn	0.3	Ta	< 1
	Ga	< 0.01	W	< 0.01
	Ge	< 0.05	Re	< 0.005
	As	0.2	Os	< 0.01
	Se	< 0.05	Ir	0.28
	Br	< 0.01	Pt	6.3
	Rb	< 0.01	Au	0.06
	Sr	< 0.01	Hg	< 0.1
	Y	< 0.01	Tl	< 0.01
	Zr	0.02	Pb	0.11
	Nb	< 0.01	Bi	< 0.01
	Mo	0.05	Th	< 0.001
	Ru	0.35	U	< 0.001
	Rh	6.3		

105

ANALYZED BY: _____

(3)   Palladium rod processed at NRL

Client	Naval Research Labs.	P.O. #	
Date	March 31, 1994	Job #	D262
	Client ID	Palladium	
		#2 processed	
	Shiva ID	94032808	
	Element	Concentration	Element	Concentration
		[ppmwt]		[ppmwt]

Element	Concentration [ppmwt]	Element	Concentration [ppmwt]
Li	0.06	Pd	Matrix
Be	< 0.005	Ag	1.1
B	< 0.005	Cd	< 0.1
C	< 1	In	< 0.05
N	< 0.1	Sn	0.54
O	< 0.5	Sb	< 0.01
F	< 0.01	Te	< 0.01
Na	0.01	I	< 0.005
Mg	1.2	Cs	< 0.005
Al	0.3	Ba	< 0.005
Si	1	La	< 0.005
P	0.03	Ce	< 0.005
S	0.25	Pr	< 0.005
Cl	< 0.01	Nd	< 0.005
K	< 0.01	Sm	< 0.005
Ca	0.8	Eu	< 0.005
Sc	< 0.001	Gd	< 0.005
Ti	0.36	Tb	< 0.005
V	0.003	Dy	< 0.005
Cr	1.1	Ho	< 0.005
Mn	0.75	Er	< 0.005
Fe	30	Tm	< 0.005
Co	0.01	Yb	< 0.005
Ni	0.84	Lu	< 0.005
Cu	31	Hf	0.3
Zn	1	Ta	< 1
Ga	0.02	W	0.5
Ge	< 0.05	Re	< 0.005
As	0.1	Os	< 0.01
Se	< 0.05	Ir	0.4
Br	< 0.01	Pt	31
Rb	< 0.01	Au	0.17
Sr	< 0.01	Hg	< 0.1
Y	< 0.01	Tl	< 0.01
Zr	0.3	Pb	0.2
Nb	< 0.01	Bi	0.01
Mo	0.03	Th	< 0.001
Ru	0.36	U	< 0.001
Rh	9.3		

106

ANALYZED BY: _____

SH1...A TECHNOLOGIES, INC.
6260 South Bay Rd • Cicero, New York 13039
315-699-5332 • FAX: 315-699-0349

(4)   Palladium rod processed at NRL - 3 pieces

Client	Naval Research Labs.		P.O. #	
Date	November 28, 1994		Job #	DB13
Client ID	Pd shiny rod	Pd shiny rod	Pd shiny rod	
	#2 - E	#2 - F	#2 - G	
Shiva ID	94112112-E	94112112-F	94112112-G	
Element	Concentration	Concentration	Concentration	
	[ppmwt]	[ppmwt]	[ppmwt]	
B	< 0.001	< 0.001	< 0.001	
C	0.02	0.01	0.01	
N	0.03	0.03	0.03	
O	0.45	0.36	0.42	
Al	0.53	0.52	0.51	
Si	0.31	0.32	0.43	
Ca	0.58	0.67	0.66	
Ti	0.29	0.28	0.27	
Cr	1.2	1.2	1.1	
Fe	33	33	32	
Ni	0.85	0.96	0.81	
Cu	27	24	23	
Zn	1.2	1.1	1.2	
Mo	0.06	0.01	0.05	
Ru	0.36	0.35	0.32	
Rh	11	10.5	10.5	
Ag	0.71	1.1	1.1	
Sn	0.61	0.59	0.56	
W	3.8	3.4	3.7	
Ir	0.27	0.27	0.25	
Pt	30	29	30	
Au	0.21	0.16	0.19	
Pb	0.24	0.2	0.21	

107

ANALYZED BY: _____
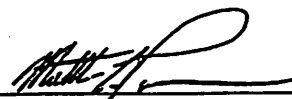
(5)   Palladium plate processed at NRL

Client	Naval Research Labs.		P.O. #	
Date	March 31, 1994		Job #	D262
	Client ID	Palladium		
		#4 plate		
	Shiva ID	94032810		
	Element	Concentration [ppmwt]	Element	Concentration [ppmwt]
	Li	0.07	Pd	Matrix
	Be	< 0.005	Ag	1.7
	B	< 0.005	Cd	< 0.1
	C	< 0.1	In	< 0.05
	N	< 0.1	Sn	0.8
	O	< 1	Sb	< 0.01
	F	< 0.01	Te	< 0.01
	Na	0.07	I	< 0.005
	Mg	1.7	Cs	< 0.005
	Al	0.3	Ba	< 0.005
	Si	9.6	La	< 0.005
	P	0.95	Ce	< 0.005
	S	< 0.01	Pr	< 0.005
	Cl	< 0.01	Nd	< 0.005
	K	< 0.01	Sm	< 0.005
	Ca	1.1	Eu	< 0.005
	Sc	< 0.001	Gd	< 0.005
	Ti	0.69	Tb	< 0.005
	V	0.006	Dy	< 0.005
	Cr	1.8	Ho	< 0.005
	Mn	1.1	Er	< 0.005
	Fe	50	Tm	< 0.005
	Co	0.07	Yb	< 0.005
	Ni	1.3	Lu	< 0.005
	Cu	12	Hf	< 0.01
	Zn	2	Ta	< 1
	Ga	0.03	W	3
	Ge	< 0.05	Re	< 0.005
	As	0.2	Os	< 0.01
	Se	< 0.05	Ir	0.1
	Br	< 0.01	Pt	26
	Rb	< 0.01	Au	0.2
	Sr	< 0.01	Hg	< 0.1
	Y	< 0.01	Tl	< 0.01
	Zr	1.2	Pb	0.4
	Nb	< 0.01	Bi	0.03
	Mo	0.28	Th	< 0.001
	Ru	0.56	U	< 0.001
	Rh	11		

108

ANALYZED BY: _____

(6) Palladium/0.62 wt.% boron rod processed at NRL

Client	Naval Research Labs.		P.O. #	
Date	July 31, 1994		Job #	D662
	Client ID	Palladium #3		
	Shiva ID	94072623		
	Element	Concentration [ppmwt]	Element	Concentration [ppmwt]
	Li	0.01	Pd	Matrix
	Be	< 0.005	Ag	0.75
	B	6200	Cd	< 0.1
	C	< 1	In	< 0.05
	N	< 0.1	Sn *	< 0.5
	O	< 10	Sb	< 0.05
	F	< 0.01	Te	0.35
	Na	0.05	I	< 0.05
	Mg	3.5	Cs	< 0.005
	Al	4.1	Ba	0.09
	Si	15	La	< 0.005
	P	0.15	Ce	< 0.005
	S	0.59	Pr	< 0.005
	Cl	< 0.01	Nd	< 0.005
	K	< 0.01	Sm	< 0.005
	Ca	7.9	Eu	< 0.005
	Sc	< 0.001	Gd	< 0.005
	Ti	0.95	Tb	< 0.005
	V	0.57	Dy	< 0.005
	Cr	0.98	Ho	< 0.005
	Mn	8.2	Er	< 0.005
	Fe	56	Tm	< 0.005
	Co	0.06	Yb	< 0.005
	Ni	1.4	Lu	< 0.005
	Cu	26	Hf	0.09
	Zn	2.3	Ta	< 1
	Ga	0.02	W	2.2
	Ge	< 0.05	Re	< 0.005
	As	0.11	Os	< 0.01
	Se	0.22	Ir	0.33
	Br	< 0.01	Pt	47
	Rb	< 0.01	Au	0.2
	Sr	0.05	Hg	< 0.1
	Y	0.01	Tl	< 0.01
	Zr	3.9	Pb	0.38
	Nb	0.02	Bi	0.02
	Mo	0.33	Th	0.002
	Ru	0.45	U	0.003
	Rh	11		-

(* – PdB+ Interference)

109

Aɴᴀʟʏᴢᴇᴅ ʙʏ: _____

(7)   Palladium/0.38 wt.% boron rod processed at NRL

Client	Naval Research Labs.		P.O.#:	N00173 4278-5002
Date	October 7, 1994		Job #	D921
	Client ID	Palladium #1		
	Shiva ID	94100602		
	Element	Concentration [ppmwt]	Element	Concentration [ppmwt]
	Li	< 0.005	Pd	Matrix
	Be	< 0.005	Ag	1.4
	B	3800	Cd	< 0.1
	C	< 5	In	1.9
	N	< 0.1	Sn	22
	O	< 10	Sb	0.42
	F	< 0.01	Te	0.15
	Na	0.06	I	< 0.05
	Mg	2.7	Cs	< 0.005
	Al	3.3	Ba	0.15
	Si	11	La	< 0.005
	P	0.08	Ce	< 0.005
	S	0.38	Pr	< 0.005
	Cl	0.01	Nd	< 0.005
	K	< 0.01	Sm	< 0.005
	Ca	2.9	Eu	< 0.005
	Sc	< 0.001	Gd	< 0.005
	Ti	0.47	Tb	< 0.005
	V	0.27	Dy	< 0.005
	Cr	1.1	Ho	< 0.005
	Mn	5.9	Er	< 0.005
	Fe	47	Tm	< 0.005
	Co	0.06	Yb	< 0.005
	Ni	1.7	Lu	< 0.005
	Cu	25	Hf	< 0.01
	Zn	1.7	Ta	< 1
	Ga	< 0.05	W	1.0
	Ge	< 0.05	Re	< 0.005
	As	0.07	Os	< 0.01
	Se	0.07	Ir	0.23
	Br	0.04	Pt	38
	Rb	< 0.01	Au	0.65
	Sr	< 0.01	Hg	< 0.1
	Y	< 0.01	Tl	< 0.01
	Zr	0.79	Pb	0.16
	Nb	0.02	Bi	0.009
	Mo	0.34	Th	0.002
	Ru	0.27	U	< 0.001
	Rh	9.6		

110

ANALYZED BY:

(8)   Palladium/0.18 wt.% boron rod processed at NRL

Client	Naval Research Labs.		P.O.#:	N00173 4278-5002
Date	October 7, 1994		Job #	D921
	Client ID	Palladium		
		#2		
	Shiva ID	94100603		
	Element	Concentration	Element	Concentration
		[ppmwt]		[ppmwt]
	Li	0.004	Pd	Matrix
	Be	< 0.005	Ag	1.5
	B	1760	Cd	< 0.1
	C	< 1	In	1.2
	N	< 5	Sn	13
	O	< 20	Sb	2.4
	F	< 0.01	Te	0.19
	Na	0.12	I	<-0.05
	Mg	2.9	Cs	< 0.005
	Al	1.5	Ba	< 0.005
	Si	6.8	La	< 0.005
	P	0.07	Ce	< 0.005
	S	0.37	Pr	< 0.005
	Cl	< 0.005	Nd	< 0.005
	K	< 0.01	Sm	< 0.005
	Ca	2.4	Eu	< 0.005
	Sc	< 0.001	Gd	< 0.005
	Ti	0.44	Tb	< 0.005
	V	0.14	Dy	< 0.005
	Cr	1.1	Ho	< 0.005
	Mn	2.6	Er	< 0.005
	Fe	36	Tm	< 0.005
	Co	0.02	Yb	< 0.005
	Ni	0.98	Lu	< 0.005
	Cu	16	Hf	< 0.01
	Zn	1.6	Ta	< 1
	Ga	1.1	W	0.67
	Ge	< 0.05	Re	< 0.005
	As	< 0.01	Os	< 0.01
	Se	.0.05	Ir	0.18
	Br	0.68	Pt	18
	Rb	< 0.01	Au	0.22
	Sr	< 0.01	Hg	< 0.1
	Y	< 0.001	Tl	< 0.01
	Zr	0.84	Pb	0.20
	Nb	0.02	Bi	< 0.01
	Mo	0.06	Th	0.004
	Ru	0.26	U	< 0.001
	Rh	8.5		

111

ANALYZED BY: _____

(9) Palladium rod (Johnson Matthey "special batch") from SRI

Client	Naval Research Labs.		P.O. #	
Date	July 31, 1994		Job #	D662
	Client ID	Palladium		
		#4		
	Shiva ID	94072624		
	Element	Concentration	Element	Concentration
		[ppmwt]		[ppmwt]
	Li	0.008	Pd	Matrix
	Be	< 0.005	Ag	1.6
	B	23	Cd	< 0.1
	C	< 1	In	< 0.05
	N	< 0.1	Sn	0.28
	O	< 20	Sb	< 0.05
	F	< 0.01	Te	< 0.05
	Na	0.03	I	< 0.05
	Mg	0.09	Cs	< 0.005
	Al	1.1	Ba	< 0.005
	Si	1.8	La	< 0.005
	P	0.09	Ce	< 0.005
	S	0.42	Pr	< 0.005
	Cl	< 0.01	Nd	< 0.005
	K	< 0.01	Sm	< 0.005
	Ca	7.5	Eu	< 0.005
	Sc	< 0.001	Gd	< 0.005
	Ti	0.11	Tb	< 0.005
	V	< 0.005	Dy	< 0.005
	Cr	1.3	Ho	< 0.005
	Mn	0.22	Er	< 0.005
	Fe	14	Tm	< 0.005
	Co	0.04	Yb	< 0.005
	Ni	0.58	Lu	< 0.005
	Cu	2.6	Hf	< 0.01
	Zn	0.55	Ta	< 1
	Ga	0.01	W	0.06
	Ge	< 0.05	Re	< 0.005
	As	0.19	Os	< 0.01
	Se	0.15	Ir	0.75
	Br	< 0.01	Pt	28
	Rb	< 0.01	Au	0.3
	Sr	< 0.01	Hg	< 0.1
	Y	< 0.01	Tl	< 0.01
	Zr	0.95	Pb	0.26
	Nb	< 0.01	Bi	< 0.01
	Mo	0.02	Th	< 0.001
	Ru	0.87	U	< 0.001
	Rh	24		-

112

ANALYZED BY: _____

(10)   Palladium rod (Johnson Matthey, 99.9% - stock #98529, lot #13E05)

Client	Naval Research Labs.		P.O.#:	N00173-95-P-0058
Date	October 11, 1994		Job #	D939
	Client ID	Palladium #1		
	Shiva ID	94101109		
	Element	Concentration [ppmwt]	Element	Concentration [ppmwt]
	Li	< 0.005	Pd	Matrix
	Be	< 0.005	Ag	0.7
	B	4.1	Cd	< 0.1
	C	< 0.1	In	< 0.05
	N	< 0.05	Sn	0.22
	O	< 6	Sb	< 0.05
	F	< 0.01	Te	< 0.05
	Na	0.02	I	< 0.05
	Mg	0.09	Cs	< 0.005
	Al	7.6	Ba	< 0.005
	Si	16	La	< 0.005
	P	0.11	Ce	< 0.005
	S	1.5	Pr	< 0.005
	Cl	< 0.001	Nd	< 0.005
	K	< 0.01	Sm	< 0.005
	Ca	5.1	Eu	< 0.005
	Sc	< 0.001	Gd	< 0.005
	Ti	0.52	Tb	< 0.005
	V	0.05	Dy	< 0.005
	Cr	1.6	Ho	< 0.005
	Mn	0.84	Er	< 0.005
	Fe	37	Tm	< 0.005
	Co	0.07	Yb	< 0.005
	Ni	1.4	Lu	< 0.005
	Cu	6.5	Hf	< 0.01
	Zn	3.6	Ta	< 2
	Ga	0.10	W	0.91
	Ge	< 0.05	Re	< 0.005
	As	1.5	Os	< 0.005
	Se	0.23	Ir	1.6
	Br	0.01	Pt	960
	Rb	< 0.01	Au	1.2
	Sr	< 0.01	Hg	< 0.1
	Y	< 0.01	Tl	< 0.01
	Zr	0.05	Pb	1.8
	Nb	< 0.01	Bi	0.03
	Mo	0.56	Th	< 0.001
	Ru	1.1	U	< 0.001
	Rh	71		

113

Analyzed by: _____

(11) Palladium wire (Johnson Matthey, 99.9% - stock #10280,
lot #K11C06)

Client	Naval Research Labs.		P.O. #	
Date	September 5, 1994		Job #	D796
	Client ID	Palladium		
		#1		
	Shiva ID	94090108		
	Element	Concentration	Element	Concentration
		[ppmwt]		[ppmwt]
	Li	0.009	Pd	Matrix
	Be	< 0.005	Ag	29
	B	17	Cd	< 0.1
	C	< 5	In	0.38
	N	< 0.1	Sn	11
	O	< 10	Sb	0.31
	F	< 0.01	Te	0.09
	Na	0.03	I	< 0.05
	Mg	0.29	Cs	< 0.005
	Al	59	Ba	0.11
	Si	67	La	< 0.005
	P	1.1	Ce	< 0.005
	S	3.0	Pr	< 0.005
	Cl	0.17	Nd	< 0.005
	K	< 0.01	Sm	< 0.005
	Ca	7.3	Eu	< 0.005
	Sc	< 0.001	Gd	< 0.005
	Ti	5.5	Tb	< 0.005
	V	0.29	Dy	< 0.005
	Cr	5.3	Ho	< 0.005
	Mn	1.6	Er	< 0.005
	Fe	95	Tm	< 0.005
	Co	0.21	Yb	< 0.005
	Ni	54	Lu	< 0.005
	Cu	24	Hf	< 0.01
	Zn	5.2	Ta	< 1
	Ga	0.26	W	1.4
	Ge	< 0.05	Re	< 0.005
	As	0.10	Os	< 0.01
	Se	0.73	Ir	12
	Br	< 0.01	Pt	1100
	Rb	< 0.01	Au	36
	Sr	0.02	Hg	< 0.1
	Y	< 0.01	Tl	< 0.01
	Zr	0.16	Pb	48
	Nb	0.05	Bi	0.52
	Mo	9.1	Th	< 0.001
	Ru	36	U	< 0.001
	Rh	110		

114

ANALYZED BY: _____

(12) Palladium wire (Johnson Matthey, 99.997% - stock #10960, lot #7403).

Client	Naval Research Labs.	P.O. #	
Date	September 5, 1994	Job #	D796
	Client ID	Palladium	
	#2		
	Shiva ID	94090109	
	Element	Concentration [ppmwt]	Element	Concentration [ppmwt]
	Li	< 0.001	Pd	Matrix
	Be	< 0.005	Ag	< 0.1
	B	0.01	Cd	< 0.1
	C	< 1	In	< 0.05
	N	< 5	Sn	0.02
	O	< 20	Sb	< 0.05
	F	< 0.01	Te	< 0.01
	Na	0.15	I	< 0.05
	Mg	0.008	Cs	< 0.005
	Al	0.34	Ba	< 0.005
	Si	43	La	< 0.005
	P	0.01	Ce	< 0.005
	S	0.33	Pr	< 0.005
	Cl	0.17	Nd	< 0.005
	K	< 0.01	Sm	< 0.005
	Ca	0.11	Eu	< 0.005
	Sc	< 0.001	Gd	< 0.005
	Ti	0.09	Tb	< 0.005
	V	0.008	Dy	< 0.005
	Cr	0.25	Ho	< 0.005
	Mn	0.01	Er	< 0.005
	Fe	1.1	Tm	< 0.005
	Co	0.02	Yb	< 0.005
	Ni	0.05	Lu	< 0.005
	Cu	0.11	Hf	< 0.01
	Zn	0.10	Ta	< 1
	Ga	< 0.01	W	0.15
	Ge	< 0.05	Re	< 0.005
	As	< 0.01	Os	< 0.01
	Se	0.02	Ir	0.86
	Br	0.68	Pt	1.9
	Rb	< 0.01	Au	1.2
	Sr	< 0.01	Hg	< 0.1
	Y	< 0.001	Tl	< 0.01
	Zr	0.01	Pb	0.05
	Nb	0.04	Bi	< 0.01
	Mo	0.08	Th	< 0.001
	Ru	0.34	U	< -0.001
	Rh	0.56		

115

ANALYZED BY: _____

(13) Palladium wire (Johnson Matthey, 99.997% - stock #10960, lot #W12954) from NAWC

Date	July 31, 1994		P.O. #	
			Job #	D662
	Client ID	Palladium #5		
	Shiva ID	94072625		
	Element	Concentration [ppmwt]	Element	Concentration [ppmwt]
	Li	0.005	Pd	Matrix
	Be	< 0.005	Ag	0.45
	B	0.007	Cd	< 0.1
	C	< 1	In	< 0.05
	N	< 3	Sn	< 0.05
	O	< 10	Sb	< 0.05
	F	< 0.01	Te	< 0.05
	Na	0.20	I	< 0.05
	Mg	0.009	Cs	<·0.005
	Al	0.63	Ba	< 0.005
	Si	3.5	La	< 0.005
	P	0.09	Ce	< 0.005
	S	0.39	Pr	< 0.005
	Cl	0.49	Nd	< 0.005
	K	0.04	Sm	< 0.005
	Ca	0.29	Eu	< 0.005
	Sc	< 0.001	Gd	< 0.005
	Ti	0.05	Tb	< 0.005
	V	< 0.005	Dy	< 0.005
	Cr	0.21	Ho	< 0.005
	Mn	0.004	Er	< 0.005
	Fe	2.9	Tm	< 0.005
	Co	0.01	Yb	< 0.005
	Ni	0.03	Lu	< 0.005
	Cu	0.76	Hf	0.02
	Zn	0.02	Ta	< 10
	Ga	< 0.01	W	0.10
	Ge	< 0.05	Re	< 0.005
	As	0.01	Os	< 0.01
	Se	< 0.01	Ir	1.1
	Br	0.48	Pt	2.2
	Rb	< 0.01	Au	1.0
	Sr	< 0.01	Hg	< 0.1
	Y	< 0.01	Tl	< 0.01
	Zr	0.04	Pb	0.01
	Nb	0.05	Bi	< 0.01
	Mo	< 0.01	Th	< 0.001
	Ru	0.48	U	< 0.001
	Rh	4.2		-

116

ANALYZED BY: _____

(14)   Palladium wire (Goodfellow, 99.95% - stock #005150/11)

Client	Naval Research Labs.	P.O. #	
Date	September 5, 1994	Job #	D796
	Client ID	Palladium	
	#6		
	Shiva ID	94090113	
	Element	Concentration [ppmwt]	Element	Concentration [ppmwt]
	Li	< 0.005	Pd	Matrix
	Be	< 0.005	Ag	13
	B	2.5	Cd	< 0.1
	C	< 1	In	< 0.05
	N	< 0.1	Sn	< 0.05
	O	< 10	Sb	0.78
	F	< 0.01	Te	< 0.05
	Na	0.01	I	< 0.05
	Mg	0.04	Cs	< 0.005
	Al	2.3	Ba	< 0.005
	Si	6.6	La	< 0.005
	P	1.3	Ce	< 0.005
	S	2.5	Pr	< 0.005
	Cl	0.03	Nd	< 0.005
	K	< 0.01	Sm	< 0.005
	Ca	< 0.05	Eu	< 0.005
	Sc	< 0.001	Gd	< 0.005
	Ti	0.05	Tb	< 0.005
	V	0.02	Dy	< 0.005
	Cr	0.68	Ho	< 0.005
	Mn	0.17	Er	< 0.005
	Fe	30	Tm	< 0.005
	Co	0.45	Yb	< 0.005
	Ni	1.4	Lu	< 0.005
	Cu	22	Hf	0.01
	Zn	2.5	Ta	< 10
	Ga	0.23	W	0.2
	Ge	< 0.05	Re	< 0.005
	As	0.35	Os	< 0.01
	Se	0.18	Ir	0.59
	Br	0.11	Pt	80
	Rb	< 0.01	Au	0.9
	Sr	< 0.01	Hg	< 0.1
	Y	< 0.01	Tl	< 0.01
	Zr	< 0.01	Pb	0.13
	Nb	< 0.01	Bi	0.08
	Mo	0.13	Th	< 0.001
	Ru	0.06	U	< 0.001
	Rh	6		

ANALYZED BY: _____

GDMS ANALYTICAL REPORT

(15) Palladium wire (Goodfellow, 99.99+% - stock #005155/11)

Client	Naval Research Labs.		P.O. #	
Date	September 5, 1994		Job #	D796
	Client ID	Palladium #5		
	Shiva ID	94090112		
	Element	Concentration [ppmwt]	Element	Concentration [ppmwt]
	Li	0.007	Pd	Matrix
	Be	< 0.005	Ag	0.55
	B	0.01	Cd	< 0.1
	C	< 1	In	< 0.05
	N	< 3	Sn	< 0.05
	O	< 3	Sb	< 0.05
	F	< 0.01	Te	< 0.05
	Na	0.4	I	< 0.05
	Mg	0.05	Cs	< 0.005
	Al	0.27	Ba	< 0.005
	Si	6.8	La	< 0.005
	P	0.01	Ce	< 0.005
	S	0.03	Pr	< 0.005
	Cl	0.15	Nd	< 0.005
	K	0.05	Sm	< 0.005
	Ca	0.2	Eu	< 0.005
	Sc	< 0.001	Gd	< 0.005
	Ti	0.16	Tb	< 0.005
	V	< 0.005	Dy	< 0.005
	Cr	0.04	Ho	< 0.005
	Mn	0.01	Er	< 0.005
	Fe	2.8	Tm	< 0.005
	Co	0.03	Yb	< 0.005
	Ni	0.21	Lu	< 0.005
	Cu	0.11	Hf	< 0.005
	Zn	0.02	Ta	< 10
	Ga	< 0.01	W	0.10
	Ge	< 0.05	Re	< 0.005
	As	< 0.01	Os	< 0.01
	Se	< 0.01	Ir	0.65
	Br	< 0.01	Pt	0.59
	Rb	< 0.01	Au	1.3
	Sr	< 0.01	Hg	< 0.1
	Y	< 0.01	Tl	< 0.01
	Zr	< 0.01	Pb	< 0.01
	Nb	< 0.01	Bi	< 0.01
	Mo	< 0.01	Th	< 0.001
	Ru	0.07	U	< 0.001
	Rh	0.2		

ANALYZED BY:

Appendix B

REPORT ON THE ELECTROCHEMICAL LOADING OF DEUTERIUM AND HYDROGEN INTO PALLADIUM ELECTRODES

Dawn D. Dominguez, Patrick L. Hagans and M. Ashraf Imam
Naval Research Laboratory, Washington, D.C. 20375

This report will summarize the experimental details in a Table from a series of electrochemical loading/calorimetric experiments on palladium electrodes. The Table will include experiments run at NRL from the start of the ONR-sponsor Anomalous Effects Program in September of 1992 through December of 1994.

The majority of the experiments were attempts to electrolytically load palladium cathodes with deuterium and then to measure excess power produced in the electrolytic cell. Palladium cathodes loaded electrolytically with hydrogen were designed to serve as controls. The loading progress was monitored in situ by measuring the change in the axial resistance of the cathode. The D/Pd or H/Pd ratio was then determined from known relationships between the resistance and the atomic ratios (McKubre 1994). Resistance measurements were made by the four-point probe method with 0.5 A applied current.

Generally, the loading/calorimetric experiments were carried out by running two open, electrochemical cells in series under galvanostatic control. Electrolysis cells were made of borosilicate-glass or quartz. Other cell components were made of Teflon. Cathodes were either palladium (99.9 or 99.99%) or a palladium-10% silver alloy and anodes were platinum (99.9%) or a platinum-clad niobium. Platinum lead wires (99.9%) were spot-welded to the cathode and anode and then covered with heat-shrink Teflon. Electrolyte was made by the reaction of 99.9% lithium foil with either D_2O or H_2O. Effluent gases evolved through an oil bubbler.

The isoperibol calorimeters used in these experiments were similar to those described by *Miles et al. (1990)*. Temperature was measured by two thermistor thermometers (calibrated within $\pm0.01\,°C$) located in a secondary compartment containing water surrounding the electrolysis cell. The calorimeters were held in a constant temperature bath set at $27.00\pm0.02\,°C$ and were calibrated by Joule heating over the power range used. Calorimetric cell constants were on the order of $0.200\ W/°C$. The sensitivity of the calorimeters was generally $\pm10\%$ (thus, with 2 W input power, only excess power greater than 200 mW could be detected). No excess power greater than 200 mW was measured in any of the experiments listed in the Table.

Anomalous Effects Table for NRL Experiments Run 9/92-12/94

A.) CATHODE DESCRIPTION

Expt.	Cathode	Cathode Code Name	Cathode Source	Cathode Purity	Cathode Geometry	Cathode Dimens. (l x d) cm x cm	Cathode Area/cm2	Cathode Grooves
12_1	Pd_A'	94061001	GF	3N	rod	3.0 x 0.4	3.8	no
12_2	Pd_B'	94061201	JM	3N	rod	3.0 x 0.4	3.8	no
12_3	Pd_C'	93101904	NRL-9_D	4N	rod	3.5 x 0.4	4.4	yes
12_4	Pd_D'	93101906	NRL-9_F	4N	rod	3.5 x 0.4	4.4	yes
12_5	Pd_E'	94061005	NRL	4N	rod	3.5 x 0.4	4.4	yes
12_6	Pd_F'	94061006	NRL	4N	rod	3.5 x 0.4	4.4	yes
12_7	Pd_G'	94063001	JM	4N	wire	3.0 x 0.1	0.9	no
12_8	Pd_H'	94063002	JM	4N	wire	3.0 x 0.1	0.9	no
12_9	Pd_I'	94061101	GF	3N	wire	3.0 x 0.1	0.9	no
12_10	Pd_J'	93021603	JM	3N	wire	3.0 x 0.1	0.9	no
11_1	Pd_G'	94061001	NRL	4N	rod	3.5 x 0.4	4.4	yes
11_2	Pd_H'	94061002	NRL	4N	rod	3.5 x 0.4	4.4	yes
11_3	Pd_I'	94061003	NRL	4N	rod	3.5 x 0.4	4.4	yes
11_4	Pd_J'	94061004	NRL	4N	rod	3.5 x 0.4	4.4	yes
11_5	Pd_M'	93091001	E#3	3N	rod	3.0 x 0.3	2.8	yes
11_6	Pd_N'	93091002	E#3	3N	rod	3.0 x 0.3	2.8	yes
11_7	Pd_O'	93021601	JM	3N	wire	3.5 x 0.1	1.1	no
11_8	Pd_P'	93021602	JM	3N	wire	3.5 x 0.1	1.1	no
11-9	Pd_Q'	94052501	JM_SB	4N	rod	3.0 x 0.4	3.8	no
11_10	Pd_R'	94052502	JM_SB	4N	rod	3.0 x 0.4	3.8	no
10_1	Pd_G	94021001	NRL	4N	rod	3.5 x 0.4	4.4	yes
10_2	Pd_H	94021002	NRL	4N	rod	3.5 x 0.4	4.4	yes
10_3	Pd_I	94021003	NRL	4N	rod	3.5 x 0.4	4.4	yes
10_4	Pd_J	94021004	NRL	4N	rod	3.5 x 0.4	4.4	yes
10_5	Pd_M	94021005	NRL	4N	rod	3.5 x 0.4	4.4	yes
10_6	Pd_N	94021006	NRL	4N	rod	3.5 x 0.4	4.4	yes
10_7	Pd_O	94021007	NRL	4N	rod	3.5 x 0.4	4.4	yes
10_8	Pd_P	94021008	NRL	4N	rod	3.5 x 0.4	4.4	yes
9_1	Pd_A	93101901	NRL	4N	plate	3.5 x 0.7 x 0.07	5.4	yes
9_2	Pd_B	93101902	NRL	4N	plate	3.5 x 0.7 x 0.07	5.4	yes
9_3	Pd_C	93102001	NRL	4N	rod	3.5 x 0.4	4.4	yes
9_4	Pd_D	93102002	NRL	4N	rod	3.5 x 0.4	4.4	yes
9_5	Pd_E	93102003	NRL	4N	rod	3.5 x 0.4	4.4	yes
9_6	Pd_F	93102004	NRL	4N	rod	3.5 x 0.4	4.4	yes
8_1	Pd_U	93090301	NRL	4N	rod	3.5 x 0.4	4.4	yes
8_2	Pd_V	93090302	NRL	4N	rod	3.5 x 0.4	4.4	yes
8_3	Pd_W	93090401	NRL	4N	plate	3.5 x 0.7 x 0.07	5.4	yes
8_4	Pd_X	93090402	NRL	4N	plate	3.5 x 0.7 x 0.07	5.4	yes
8_5	Pd_Y	93090303	NRL	4N	rod	3.5 x 0.4	4.4	yes
8_6	Pd_Z	93090403	NRL	4N	plate	3.5 x 0.7 x 0.07	5.4	yes
7_1	Pd_O	93080601	NRL	4N	plate	3.5 x 0.7 x 0.07	5.4	yes
7_2	Pd_P	93080602	NRL	4N	plate	3.5 x 0.7 x 0.07	5.4	yes
7_3	Pd_Q	93080603	NRL	4N	plate	3.5 x 0.7 x 0.07	5.4	yes
7_4	Pd_R	93080604	NRL	4N	plate	3.5 x 0.7 x 0.07	5.4	yes
7_5	Pd_S	93080605	NRL	4N	plate	3.5 x 0.7 x 0.07	5.4	yes
7_6	Pd_T	93080606	NRL	4N	plate	3.5 x 0.7 x 0.07	5.4	yes
6_1	Pd_I	93060301	NRL	4N	rod	3.5 x 0.4	4.4	yes
6_2	Pd_J	93060302	NRL	4N	rod	3.5 x 0.4	4.4	yes
6_3	Pd_K	93060303	NRL	4N	rod	3.5 x 0.4	4.4	yes
6_4	Pd_L	93060304	NRL	4N	rod	3.5 x 0.4	4.4	yes
6_5	Pd_M	93060305	NRL	4N	rod	3.5 x 0.4	4.4	yes
6_6	Pd_N	93060306	NRL	4N	rod	3.5 x 0.4	4.4	yes
5_1	Pd_E	93021701	NRL	4N	rod	3.5 x 0.4	4.4	yes
5_2	Pd_C	93021702	NRL	4N	rod	3.5 x 0.4	4.4	yes
4_1	Pd_G	93020901	NRL	4N	rod	3.5 x 0.4	4.4	yes
4_2	Pd_H	93020902	NRL	4N	rod	3.5 x 0.4	4.4	yes
3_1	Pd_E	93011501	NRL	4N	rod	3.5 x 0.4	4.4	yes
3_2	Pd_F	93011502	NRL	4N	rod	3.5 x 0.4	4.4	yes
2_1	Pd/Ag_C	92093001	NRL	4N	rod	3.5 x 0.4	4.4	yes
2_2	Pd/Ag_D	92093002	NRL	4N	rod	3.5 x 0.4	4.4	yes
1_1	Pd/Ag_A	92071401	NRL	4N	rod	3.5 x 0.4	4.4	yes
1_2	Pd/Ag_B	92071402	NRL	4N	rod	3.5 x 0.4	4.4	yes

B.) CATHODE/ANODE DESCRIPTION

Expt.	Cathode Grain Size/um	Pt Wires for Resistance Meas.	Spot Weld Electrodes	Cathode Etch w/ Aqua Regia	Anode Type	Anode Length/cm
12_1	elongated	yes	Cu/Cr	yes	Pt mesh	5
12_2	elongated	yes	Cu/Cr	yes	Pt mesh	5
12_3	large, 600	yes	Cu/Cr	yes	Pt wire	5
12_4	large, 600	yes	Cu/Cr	yes	Pt wire	5
12_5	large, 600	yes	Pd/Ag	yes	Pt wire	5
12_6	large, 600	yes	Pd/Ag	yes	Pt wire	5
12_7	elongated	yes	Cu/Cr	yes	Pt wire	5
12_8	elongated	yes	Cu/Cr	yes	Pt mesh	5
12_9	large, 600	yes	Cu/Cr	yes	Pt mesh	5
12_10	large, 600	yes	Cu/Cr	yes	Pt wire	5
11_1	large, 600	yes	Pd/Ag	yes	Pt mesh	5
11_2	large, 600	yes	Pd/Ag	yes	Pt mesh	5
11_3	large, 600	yes	Pd/Ag	yes	Pt/Nb	5
11_4	large, 600	yes	Pd/Ag	yes	Pt/Nb	5
11_5	SRI	yes	Cu/Cr	yes	Pt wire	5
11_6	SRI	yes	Cu/Cr	yes	Pt wire	5
11_7	elongated	yes	Cu/Cr	yes	Pt wire	5
11_8	elongated	yes	Cu/Cr	yes	Pt wire	5
11-9	large, 600	yes	Cu/Cr	yes	Pt wire	5
11_10	large, 600	yes	Cu/Cr	yes	Pt wire	5
10_1	large, 600	yes	Pd/Ag	yes	Pt mesh	5
10_2	large, 600	yes	Pd/Ag	yes	Pt mesh	5
10_3	SRI	yes	Pd/Ag	yes	Pt/Nb	5
10_4	SRI	yes	Pd/Ag	yes	Pt/Nb	5
10_5	large, 600	yes	Pd/Ag	yes	Pt wire	5
10_6	large, 600	yes	Pd/Ag	yes	Pt wire	5
10_7	large, 600	yes	Pd/Ag	yes	Pt mesh	5
10_8	large, 600	yes	Pd/Ag	yes	Pt mesh	5
9_1	large, 600	yes	Pd/Ag	yes	Pt/Nb	5
9_2	large, 600	yes	Pd/Ag	yes	Pt/Nb	5
9_3	large, 600	yes	Pd/Ag	yes	Pt mesh	5
9_4	large, 600	yes	Pd/Ag	yes	Pt mesh	5
9_5	large, 600	yes	Pd/Ag	yes	Pt/Nb	6.5
9_6	large, 600	yes	Pd/Ag	yes	Pt/Nb	6.5
8_1	large, 600	yes	Pd/Ag	yes	Pt/Nb	5
8_2	large, 600	yes	Pd/Ag	yes	Pt/Nb	5
8_3	large, 600	yes	Pd/Ag	yes	Pt/Nb	5
8_4	large, 600	yes	Pd/Ag	yes	Pt/Nb	5
8_5	large, 600	yes	Pd/Ag	yes	Pt/Nb	5
8_6	large, 600	yes	Pd/Ag	yes	Pt/Nb	5
7_1	small, 40	yes	Pd/Ag	yes	Pt/Nb	5
7_2	small, 40	yes	Pd/Ag	yes	Pt/Nb	5
7_3	elongated	yes	Pd/Ag	yes	Pt/Nb	5
7_4	elongated	yes	Pd/Ag	yes	Pt/Nb	5
7_5	large, 600	yes	Pd/Ag	yes	Pt/Nb	5
7_6	large, 600	yes	Pd/Ag	yes	Pt/Nb	5
6_1	small, 40	yes	Pd/Ag	yes	Pt/Nb	5
6_2	small, 40	yes	Pd/Ag	yes	Pt/Nb	5
6_3	elongated	yes	Pd/Ag	yes	Pt/Nb	5
6_4	elongated	yes	Pd/Ag	yes	Pt/Nb	5
6_5	large, 600	yes	Pd/Ag	yes	Pt/Nb	5
6_6	large, 600	yes	Pd/Ag	yes	Pt/Nb	5
5_1	small, 60	yes	Pd/Ag	no	Pt/Nb	5
5_2	small, 60	yes	Pd/Ag	no	Pt/Nb	5
4_1	small, 60	yes	Pd/Ag	no	Pt/Nb	5
4_2	small, 60	yes	Pd/Ag	no	Pt/Nb	5
3_1	small, 60	yes	Pd/Ag	yes	Pt/Nb	5
3_2	small, 60	yes	Pd/Ag	yes	Pt/Nb	5
2_1	small, 40	yes	Pd/Ag	no	Pt/Nb	5
2_2	small, 40	yes	Pd/Ag	no	Pt/Nb	5
1_1	small, 40	yes	Pd/Ag	no	Pt/Nb	5
1_2	small, 40	yes	Pd/Ag	no	Pt/Nb	5

121

Expt.	Anode Description	Cell Dimens. (l x d) in x in	Cell Material/Prep.
12_1	new, acid cleaned	6.0 x 1.0	used pyrex/acid cleaned
12_2	new, acid cleaned	6.0 x 1.0	used pyrex/acid cleaned
12_3	reused set #11, more turns, acid cleaned	6.0 x 1.0	used pyrex/acid cleaned
12_4	reused set #11, more turns, acid cleaned	6.0 x 1.0	used pyrex/acid cleaned
12_5	reused set #11, more turns, acid cleaned	6.0 x 1.0	used pyrex/acid cleaned
12_6	reused set #11, more turns, acid cleaned	6.0 x 1.0	used pyrex/acid cleaned
12_7	reused set #11, more turns, acid cleaned	6.0 x 1.0	used pyrex/acid cleaned
12_8	new, acid cleaned	6.0 x 1.0	used pyrex/acid cleaned
12_9	new, acid cleaned	6.0 x 1.0	used pyrex/acid cleaned
12_10	reused set #11, more turns, acid cleaned	6.0 x 1.0	used pyrex/acid cleaned
11_1	reused, no acid clean	6.0 x 1.0	used pyrex/acid cleaned
11_2	reused, no acid clean	6.0 x 1.0	used pyrex/acid cleaned
11_3	reused, no acid clean	6.0 x 1.0	used pyrex/acid cleaned
11_4	reused, no acid clean	6.0 x 1.0	used pyrex/acid cleaned
11_5	new, acid cleaned	6.0 x 1.0	used pyrex/acid cleaned
11_6	new, acid cleaned	6.0 x 1.0	used pyrex/acid cleaned
11_7	new, acid cleaned	6.0 x 1.0	used pyrex/acid cleaned
11_8	new, acid cleaned	6.0 x 1.0	used pyrex/acid cleaned
11-9	new, acid cleaned	6.0 x 1.0	used pyrex/acid cleaned
11_10	new, acid cleaned	6.0 x 1.0	used pyrex/acid cleaned
10_1	new, acid cleaned	6.0 x 1.0	used pyrex/acid cleaned
10_2	new, acid cleaned	6.0 x 1.0	new pyrex/acid cleaned
10_3	new, acid cleaned	6.0 x 1.0	used pyrex/acid cleaned
10_4	new, acid cleaned	6.0 x 1.0	used pyrex/acid cleaned
10_5	new, acid cleaned	6.0 x 1.0	used pyrex/acid cleaned
10_6	new, acid cleaned	6.0 x 1.0	new pyrex/acid cleaned
10_7	new, acid cleaned	6.0 x 1.0	new pyrex/acid cleaned
10_8	new, acid cleaned	6.0 x 1.0	new pyrex/acid cleaned
9_1	reused set #7, acid cleaned	6.0 x 1.0	used pyrex/acid cleaned
9_2	reused set #7, acid cleaned	6.0 x 1.0	used pyrex/acid cleaned
9_3	new, acid cleaned	6.0 x 1.0	used pyrex/acid cleaned
9_4	new, acid cleaned	6.0 x 1.0	used pyrex/acid cleaned
9_5	new, acid cleaned	6.0 x 1.0	used quartz/acid cleaned
9_6	new, acid cleaned	6.0 x 1.0	used quartz/acid cleaned
8_1	reused set #6, acid cleaned	6.0 x 1.0	used pyrex/acid cleaned
8_2	reused set #6, acid cleaned	6.0 x 1.0	used pyrex/acid cleaned
8_3	reused set #7, acid cleaned	6.0 x 1.0	used pyrex/acid cleaned
8_4	reused set #7, acid cleaned	6.0 x 1.0	used pyrex/acid cleaned
8_5	reused set #6, acid cleaned	6.0 x 1.0	used quartz/acid cleaned
8_6	reused set #7, acid cleaned	6.0 x 1.0	used quartz/acid cleaned
7_1	new, acid cleaned	6.0 x 1.0	new pyrex/acid cleaned
7_2	new, acid cleaned	6.0 x 1.0	new pyrex/acid cleaned
7_3	new, acid cleaned	6.0 x 1.0	new pyrex/acid cleaned
7_4	new, acid cleaned	6.0 x 1.0	new pyrex/acid cleaned
7_5	new, acid cleaned	6.0 x 1.0	new pyrex/acid cleaned
7_6	new, acid cleaned	6.0 x 1.0	new pyrex/acid cleaned
6_1	new, acid cleaned	6.0 x 1.0	new pyrex/acid cleaned
6_2	new, acid cleaned	6.0 x 1.0	new pyrex/acid cleaned
6_3	new, acid cleaned	6.0 x 1.0	new pyrex/acid cleaned
6_4	new, acid cleaned	6.0 x 1.0	new pyrex/acid cleaned
6_5	new, acid cleaned	6.0 x 1.0	new pyrex/acid cleaned
6_6	new, acid cleaned	6.0 x 1.0	new pyrex/acid cleaned
5_1	new, acid cleaned	6.0 x 1.0	new pyrex/acid cleaned
5_2	new, acid cleaned	6.0 x 1.0	new pyrex/acid cleaned
4_1	new, acid cleaned	6.0 x 1.0	new pyrex/acid cleaned
4_2	new, acid cleaned	6.0 x 1.0	new pyrex/acid cleaned
3_1	new, acid cleaned	6.0 x 1.0	new pyrex/acid cleaned
3_2	used in calibrations, acid cleaned	6.0 x 1.0	new pyrex/acid cleaned
2_1	new, acid cleaned	6.0 x 1.0	new pyrex/acid cleaned
2_2	new, acid cleaned	6.0 x 1.0	new pyrex/acid cleaned
1_1	new, acid cleaned	6.0 x 1.0	new pyrex/acid cleaned
1_2	new, acid cleaned	6.0 x 1.0	new pyrex/acid cleaned

Expt.	Electrolyte	Sources Li/(H)D2O	Electrolyte Prep. Date	Misc. Info.
12_1	0.1 M LiOD	JM/CIL	09-08-94	cathode acid etch in plastic, new cell top, no end-caps
12_2	0.1 M LiOD	JM/CIL	09-08-94	cathode acid etch in plastic, new cell top, no end-caps
12_3	0.1 M LiOD	JM/CIL	09-08-94	cathode acid etch in plastic, new cell top, no end-caps
12_4	0.1 M LiOD	JM/CIL	09-08-94	cathode acid etch in plastic, new cell top, no end-caps
12_5	0.1 M LiOD	JM/CIL	09-08-94	cathode acid etch in plastic, new cell top, no end-caps
12_6	0.1 M LiOD	JM/CIL	09-08-94	cathode acid etch in plastic, new cell top, no end-caps
12_7	0.1 M LiOD	JM/CIL	09-14-94	cathode acid etch in plastic, new cell top, no end-caps
12_8	0.1 M LiOD	JM/CIL	09-14-94	cathode acid etch in plastic, new cell top, no end-caps
12_9	0.1 M LiOD	JM/CIL	09-14-94	cathode acid etch in plastic, new cell top, no end-caps
12_10	0.1 M LiOD	JM/CIL	09-14-94	cathode acid etch in plastic, new cell top, no end-caps
11_1	0.1 M LiOD	JM/OH	03-14-94	cathode acid etch in plastic, new cell top, no end-caps
11_2	0.1 M LiOD	JM/OH	03-14-94	cathode acid etch in plastic, new cell top, no end-caps
11_3	0.1 M LiOH	JM/3xdH2O	03-14-94	cathode acid etch in plastic, new cell top, no end-caps
11_4	0.1 M LiOD	JM/OH	03-14-94	cathode acid etch in plastic, new cell top, no end-caps
11_5	0.1 M LiOD	JM/OH	03-14-94	cathode acid etch in plastic, new cell top, no end-caps
11_6	0.1 M LiOD	JM/OH	03-14-94	cathode acid etch in plastic, new cell top, no end-caps
11_7	0.1 M LiOD	JM/OH	03-14-94	cathode acid etch in plastic, new cell top, no end-caps
11_8	0.1 M LiOD	JM/OH	03-14-94	cathode acid etch in plastic, new cell top, no end-caps
11-9	0.1 M LiOD	JM/OH	03-14-94	cathode acid etch in plastic, new cell top, no end-caps
11_10	0.1 M LiOD	JM/OH	03-14-94	cathode acid etch in plastic, new cell top, no end-caps
10_1	0.1 M LiOD	JM/OH	04-04-94	cathode acid etch in plastic, new cell top, no end-caps
10_2	0.1 M LiOD	JM/OH	04-04-94	cathode acid etch in plastic, new cell top, no end-caps
10_3	0.1 M LiOH	JM/3xdH2O	04-04-94	cathode acid etch in plastic, new cell top, no end-caps
10_4	0.1 M LiOD	JM/OH	04-04-94	cathode acid etch in plastic, new cell top, no end-caps
10_5	0.1 M LiOD	JM/OH	04-04-94	cathode acid etch in plastic, new cell top, no end-caps
10_6	0.1 M LiOD	JM/OH	04-04-94	cathode acid etch in plastic, new cell top, no end-caps
10_7	0.1 M Li2SO4	JM/H2SO4	04-04-94	cathode acid etch in plastic, new cell top, no end-caps
10_8	0.1 M Li2SO4	JM/D2SO4	04-04-94	cathode acid etch in plastic, new cell top, no end-caps
9_1	0.1 M LiOH	JM/3xdH2O	11-11-93	cathode acid etch in plastic, new cell top, no end-caps
9_2	0.1 M LiOD	JM/OH	11-11-93	cathode acid etch in plastic, new cell top, no end-caps
9_3	0.1 M LiOH	JM/3xdH2O	11-11-93	cathode acid etch in plastic, new cell top, no end-caps
9_4	0.1 M LiOD	JM/OH	11-11-93	ditto above, Pt wire to anode off at start
9_5	1.0 M LiOH	JM/3xdH2O	11-11-93	cathode acid etch in plastic, new cell top, no end-caps
9_6	1.0 M LiOD	JM/OH	11-11-93	new cell top, no end-caps
8_1	0.1 M LiOD	JM/OH	09-11-93	new cell top, no end-caps
8_2	0.1 M LiOH	JM/3xdH2O	09-11-93	Pt wire to anode off at start, no end-caps
8_3	0.1 M LiOD	JM/OH	09-11-93	no end-caps
8_4	0.1 M LiOH	JM/3xdH2O	09-11-93	no end-caps
8_5	0.1 M LiOH	JM/3xdH2O	09-11-93	no end-caps
8_6	0.1 M LiOH	JM/3xdH2O	09-11-93	rectangular anode, no end-caps
7_1	0.1 M LiOD	JM/CIL	??	rectangular anode, no end-caps
7_2	0.1 M LiOH	JM/3xdH2O	??	rectangular anode, no end-caps
7_3	0.1 M LiOD	JM/CIL	??	rectangular anode, no end-caps
7_4	0.1 M LiOH	JM/3xdH2O	??	rectangular anode, no end-caps, new cell top - bubbles
7_5	0.1 M LiOD	JM/CIL	??	rectangular anode, no end-caps, new cell top - bubbles
7_6	0.1 M LiOH	JM/3xdH2O	??	
6_1	0.1 M LiOD	JM/CIL	??	
6_2	0.1 M LiOH	JM/3xdH2O	??	new cell top design - bubbles
6_3	0.1 M LiOD	JM/CIL	??	new cell top design - bubbles
6_4	0.1 M LiOH	JM/3xdH2O	??	
6_5	0.1 M LiOD	JM/CIL	??	
6_6	0.1 M LiOH	JM/3xdH2O	??	
5_1	0.1 M LiOH	JM/3xdH2O	11-16-92	cell run independently (not in series)
5_2	0.1 M LiOD	JM/CIL	11-16-92	cell run independently (not in series)
4_1	0.1 M LiOD	JM/CIL	11-16-92	
4_2	0.1 M LiOD	JM/CIL	11-16-92	
3_1	0.1 M LiOD	JM/CIL	08-15-92	boiled off electrolyte
3_2	0.1 M LiOH	JM/3xdH2O	08-15-92	boiled off electrolyte
2_1	0.1 M LiOD	JM/CIL	08-15-92	current reversed at start, jumper wire on current card
2_2	0.1 M LiOH	JM/3xdH2O	08-15-92	current reversed at start, jumper wire on current card
1_1	0.1 M LiOH	JM/3xdH2O	08-15-92	
1_2	0.1 M LiOD	JM/CIL	08-15-92	

123

Expt.	Isoperibol Calorimeter	Bath Temp. C	Cathode R0/uohm	Experiment Start Date	Initial c.d. mA cm-2	Time/h @ Init. c.d.	Highest c.d. mA cm-2
12_1	none	27	159	09-08-94	22	100	263
12_2	none	27	156	09-08-94	22	100	263
12_3	none	27	205	09-08-94	22	100	227
12_4	none	27	207	09-08-94	22	100	227
12_5	none	27	192	09-08-94	22	100	227
12_6	none	27	194	09-08-94	22	100	227
12_7	none	27	3599	09-14-94	111	50	555
12_8	none	27	3548	09-14-94	111	50	555
12_9	none	27	2708	09-14-94	111	120	555
12_10	none	27	3081	09-14-94	111	120	555
11_1	none	27	203	06-27-94	22	60	68
11_2	none	27	188	06-27-94	22	–	–
11_3	none	27	202	06-27-94	22	60	68
11_4	none	27	196	06-27-94	22	60	68
11_5	none	27	450	07-19-94	35	100	357
11_6	none	27	412	07-19-94	35	100	357
11_7	none	27	2904	08-01-94	45	60	273
11_8	none	27	3429	08-01-94	45	60	273
11-9	none	27	166	08-02-94	26	50	79
11_10	none	27	162	08-02-94	26	50	79
10_1	G	27	197	04-04-94	22	30	455
10_2	H	27	201	04-04-94	22	30	455
10_3	I	27	214	04-04-94	22	30	455
10_4	J	27	201	04-04-94	22	30	455
10_5	M	27	194	04-04-94	22	40	455
10_6	N	27	205	04-04-94	22	40	455
10_7	–	27	208	04-05-94	22	30	455
10_8	–	27	202	04-05-94	22	30	455
9_1	I	27	459	11-11-93	18	90	139
9_2	J	27	435	11-11-93	18	90	139
9_3	C	27	207	11-12-93	22	70	170
9_4	D	27	205	11-12-93	22	70	170
9_5	–	27	–	11-12-93	–	–	–
9_6	F	27	208	11-12-93	22	70	170
8_1	I	27	209	09-11-93	22	50	455
8_2	J	27	205	09-11-93	22	50	455
8_3	W	27	468	09-11-93	–	–	370
8_4	X	27	450	09-11-93	18	50	370
8_5	Y	27	205	09-30-93	22	190	455
8_6	Z	27	478	10-02-93	18	150	370
7_1	I	27	459	08-12-93	18	125	370
7_2	J	27	454	08-12-93	18	125	370
7_3	K	27	451	08-12-93	18	125	370
7_4	L	27	459	08-12-93	18	125	370
7_5	M	27	531	08-12-93	18	125	370
7_6	N	27	509	08-12-93	18	125	370
6_1	I	27	201	06-29-93	22	300	114
6_2	J	27	205	06-29-93	22	300	114
6_3	K	27	193	06-29-93	22	300	114
6_4	L	27	209	06-29-93	22	300	114
6_5	M	27	196	06-29-93	22	300	114
6_6	N	27	200	06-29-93	22	300	114
5_1	E	27	203	02-19-93	2	750	455
5_2	C	27	194	02-19-93	2	750	455
4_1	G	27	199	02-10-93	2	450	455
4_2	H	27	204	02-10-93	11	160	455
3_1	E	27	197	01-23-93	22	70	455
3_2	F	27	204	01-23-93	22	70	455
2_1	C	27	403	10-07-92	22	44	568
2_2	D	27	435	10-07-92	22	44	568
1_1	A	27	?	09-01-92	22	72	568
1_2	B	27	?	09-01-92	22	72	568

Expt.	Time/h @ High c.d.	Current Cycles A-A-A...	Additive ppm aluminum	Time of Additive Addition(s)/h
12_1	6.5	.1-.4-.1-.5-.1-1-.1	none	–
12_2	6.5	.1-.4-.1-.5-.1-1-.1	none	–
12_3	6.5	.1-.4-.1-.5-.1-1-.1	none	–
12_4	6.5	.1-.4-.1-.5-.1-1-.1	none	–
12_5	6.5	.1-.4-.1-.5-.1-1-.1	none	–
12_6	6.5	.1-.4-.1-.5-.1-1-.1	none	–
12_7	6.5	.1-.3-.1-.4-(-.05)-.5-.1	none	–
12_8	6.5	.1-.3-.1-.4-(-.05)-.5-.1	none	–
12_9	6.5	.1-.3-.1-.4-(-.05)-.5-.1	none	–
12_10	6.5	.1-.3-.1-.4-(-.05)-.5-.1	none	–
11_1	45	.1-.3	none	–
11_2	–		none	–
11_3	45	.1-.3	none	–
11_4	45	.1-.3	none	–
11_5	8, .5, 73	.1-.4-.05-.5-.05-1-.05-1-.05-1-.1	275 ppm Al	215
11_6	8, .5, 73	.1-.4-.05-.5-.05-1-.05-1-.05-1-.1	275 ppm Al	215
11_7	100	.05-.3-.1	none	–
11_8	100	.05-.3-.1	none	–
11-9	100	.05-.3-.1	none	–
11_10	100	.05-.3-.1	none	–
10_1	3, 6	.1-.4-(-.03)-.1-(-.05)-1-(-.05)-1-(-.05)-.5-(-.05)-2-.1	120, 120	215, 355
10_2	3, 6	.1-.4-(-.03)-.1-(-.05)-1-(-.05)-1-(-.05)-.5-(-.05)-2-.1	120, 120	215, 355
10_3	3, 6	.1-.4-(-.03)-.1-(-.05)-1-(-.05)-1-(-.05)-.5-(-.05)-2-.1	120, 120	215, 355
10_4	3, 6	.1-.4-(-.03)-.1-(-.05)-1-(-.05)-1-(-.05)-.5-(-.05)-2-.1	120, 120	215, 355
10_5	3, 6	.1-.4-.1-(-.05)-1-(-.05)-1-(-.05)-.5-(-.05)-2-.1	120, 120	210, 350
10_6	3, 6	.1-.4-.1-(-.05)-1-(-.05)-1-(-.05)-.5-(-.05)-2-.1	120, 120	210, 350
10_7	3, 6	.1-.3-.1-(-.05)-1-(-.05)-1-(-.05)-.5-(-.05)-2-.1	120, 120	200, 335
10_8	3, 6	.1-.3-.1-(-.05)-1-(-.05)-1-(-.05)-.5-(-.05)-2-.1	120, 120	200, 335
9_1	65	.1-.75-(-.05)-.75-(-.3)-.75-.1-1-.1	.2, .2	260, 790
9_2	65	.1-.75-(-.05)-.75-(-.3)-.75-.1-1-.1	.2, .2	260, 790
9_3	65	.1-.75-(-.05)-.75-(-.3)-.75-.1-1-.1	.2, .2	260, 790
9_4	65	.1-.75-(-.05)-.75-(-.3)-.75-.1-1-.1	.2, .2	260, 790
9_5	–		none	–
9_6	65	.1-.75-(-.05)-.75-(-.3)-.75-.1-1-.1	.2, .2	260, 790
8_1	8, 7	.1-.5-.1-1-.1-2-.5-2-.1	.2, .2	400, 770
8_2	8, 7	.1-.5-.1-1-.1-2-.5-2-.1	.2, .2	400, 770
8_3	8, 7	.1-.5-.1-1-.1-2-.5-2-.1	.2, .2	400, 770
8_4	8, 7	.1-.5-.1-1-.1-2-.5-2-.1	.2, .2	400, 770
8_5	8, 7	.1-2-.5-2-.1	.2, .2	310
8_6	8, 7	.1-2-.5-2-.1	.2, .2	270
7_1	8	.1-2-.5-.1	.2	335
7_2	8	.1-2-.5-.1	.2	335
7_3	8	.1-2-.5-.1	.2	335
7_4	8	.1-2-.5-.1	.2	335
7_5	8	.1-2-.5-.1	.2	335
7_6	8	.1-2-.5-.1	.2	335
6_1	26, 155	.1-.5-.1-.5-.1	none	–
6_2	26, 155	.1-.5-.1-.5-.1	none	–
6_3	26, 155	.1-.5-.1-.5-.1	none	–
6_4	26, 155	.1-.5-.1-.5-.1	none	–
6_5	26, 155	.1-.5-.1-.5-.1	none	–
6_6	26, 155	.1-.5-.1-.5-.1	none	–
5_1	8	.01-2-.1	.2	0
5_2	8	.01-2-.1	.2	0
4_1	6	.01-.2-(-.05)-2-(-.05)-.5-.003-2-.003-1-.01	.2	0
4_2	6	.05-.5-.01-2-(-.05)-2-(-.05)-.5-.003-2-.003-1-.01	.2	0
3_1	9	.1-.7-.2-.8-2-2-(-.07)-.5-.003-1-.5-.1	.2	0
3_2	9	.1-.7-.2-.8-2-2-(-.07)-.5-.003-1-.5-.1	.2	0
2_1	2	.1-.5-.3-.5-0-2.5-.5-1-.5-.9-.1-1-.1-2.5-.1-2-1-2-.3-1.5-.1-2-.1	.2	960
2_2	2	.1-.5-.3-.5-0-2.5-.5-1-.5-.9-.1-1-.1-2.5-.1-2-1-2-.3-1.5-.1-2-.1	.2	960
1_1	2	.1-.5-.3-.5-.3-1.5-.5-2.5-.5-2.5-.1	.2	1850
1_2	2	.1-.5-.3-.5-.3-1.5-.5-2.5-.5-2.5-.1	.2	1850

G.) EXPERIMENTAL DETAILS/RESULTS

Expt.	Experiment Stop Date	Experiment Duration/h	Cathode R/R0 max.	Cathode R/R0 min.	Highest H(D)/Pd	Max. Excess Power/mW	NRL # Notebook
12_1	10-03-94	600	2.0	2.0	0.7	not measured	N-7817
12_2	10-03-94	600	2.0	1.8	0.9	not measured	N-7817
12_3	10-03-94	600	2.05	2.05	0.7	not measured	N-7817
12_4	10-03-94	600	1.9	1.8	0.9	not measured	N-7817
12_5	10-03-94	600	2.0	1.85	0.9	not measured	N-7817
12_6	10-03-94	600	2.15	1.95	??	not measured	N-7817
12_7	10-07-94	555	1.8	1.75	0.7	not measured	N-7817
12_8	10-07-94	555	2.0	2.0	0.7	not measured	N-7817
12_9	10-07-94	555	2.0	1.8	0.9	not measured	N-7817
12_10	10-07-94	555	2.0	1.9	0.8	not measured	N-7817
11_1	07-01-94	96	1.9	1.9	0.7	not measured	N-7817
11_2	–	96	–	–	–	not measured	N-7817
11_3	07-01-94	96	1.7	1.35	1.0	not measured	N-7817
11_4	07-01-94	96	2.05	2.05	0.7	not measured	N-7817
11_5	08-10-94	480	1.9	1.8	0.9	not measured	N-7817
11_6	08-10-94	480	2.05	1.9	0.8	not measured	N-7817
11_7	08-10-94	173	1.9	1.85	0.8	not measured	N-7817
11_8	08-10-94	173	1.8	1.75	??	not measured	N-7817
11-9	08-10-94	150	2.0	2.0	0.7	not measured	N-7817
11_10	08-10-94	150	2.0	1.95	0.8	not measured	N-7817
10_1	04-22-94	460	2.1	2.1	0.7	< 200	N-7726
10_2	04-22-94	460	2.0	2.0	0.7	< 200	N-7726
10_3	04-22-94	460	1.85	1.6	0.9	< 200	N-7726
10_4	04-22-94	460	2.05	2.05	0.7	< 200	N-7726
10_5	04-22-94	460	2.05	1.9	0.8	< 200	N-7726
10_6	04-22-94	460	1.95	1.85	0.9	< 200	N-7726
10_7	04-22-94	460	1.7	1.55	0.9	–	N-7726
10_8	04-22-94	460	2.05	2.05	0.7	–	N-7726
9_1	12-24-93	1030	1.7	1.3	1.0	< 200	N-7726
9_2	12-24-93	1030	2.05	1.85	0.9	< 200	N-7726
9_3	12-24-93	1000	1.75	1.55	0.9	< 200	N-7726
9_4	12-24-93	1000	2.0	1.8	0.9	< 200	N-7726
9_5	12-24-93	–	–	–	–	–	N-7726
9_6	12-24-93	1000	2.0	1.8	0.9	< 200	N-7726
8_1	10-22-93	980	2.0	1.9	0.8	< 200	N-7726
8_2	10-22-93	980	1.7	1.4	1.0	< 200	N-7726
8_3	10-22-93	980	2.05	2.05	0.7	< 200	N-7726
8_4	10-22-93	980	1.8	1.55	0.9	< 200	N-7726
8_5	10-22-93	500	1.8	1.6	0.9	< 200	N-7726
8_6	10-22-93	480	1.85	1.65	0.9	< 200	N-7726
7_1	08-31-93	450	1.95	1.9	0.8	< 200	N-7726
7_2	08-31-93	450	1.8	1.5	0.95	< 200	N-7726
7_3	08-31-93	450	2.0	1.95	0.7	< 200	N-7726
7_4	08-31-93	450	1.8	1.7	0.85	< 200	N-7726
7_5	08-31-93	450	2.05	2.05	0.7	< 200	N-7726
7_6	08-31-93	450	1.70	1.45	0.95	< 200	N-7726
6_1	07-25-93	620	2.0	1.95	0.7	< 200	N-7725
6_2	07-25-93	620	1.8	1.8	0.7	< 200	N-7725
6_3	07-25-93	620	1.95	1.95	0.7	< 200	N-7725
6_4	07-25-93	620	1.8	1.75	0.7	< 200	N-7725
6_5	07-25-93	620	1.95	1.95	0.7	< 200	N-7725
6_6	07-25-93	620	1.9	1.7	0.85	< 200	N-7725
5_1	04-08-93	1150	1.8	1.8	0.7	< 200	N-7725
5_2	04-08-93	1150	2.0	2.0	0.7	< 200	N-7725
4_1	04-09-93	1400	2.05	2.05	0.7	< 200	N-7725
4_2	04-09-93	1400	2.0	2.0	0.7	< 200	N-7725
3_1	03-31-93	1600	2.0	2.0	0.7	< 200	N-7725
3_2	03-31-93	1600	1.8	1.55	0.9	< 200	N-7725
2_1	12-23-92	1850	1.7	1.7	??	< 200	N-7661, N-7662
2_2	12-23-92	1850	1.5	1.5	??	< 200	N-7661, N-7662
1_1	12-14-92	2500	??	??	??	< 200	N-7661
1_2	12-14-92	2500	??	??	??	< 200	N-7661

126

H.) ANALYSES

Expt.	Cathode GDMS Date	GDMS impurity conc./ppm	Cathode XPS Date	Electrolyte ICP Date	Radiation Detector
12_1					Nal
12_2			11-08-94		Nal
12_3			11-15-94		Nal
12_4	11-28-94	209	11-08-94		Nal
12_5					Nal
12_6					Nal
12_7					Nal
12_8			11-10-94		Nal
12_9					Nal
12_10			11-09-94		Nal
11_1	10-17-94	127	07-26-94		Nal
11_2					Nal
11_3					Nal
11_4	10-17-94	143	07-26-94		Nal
11_5					Nal
11_6					Nal
11_7	10-17-94	1690	09-02-94		Nal
11_8			09-22-94		Nal
11_9					Nal
11_10	10-17-94	147	09-23-94		Nal
10_1			07-14-94		Nal
10_2					Nal
10_3					Nal
10_4			04-27-94		Nal
10_5					Nal
10_6					Nal
10_7					Nal
10_8			07-14-94		Nal
9_1			01-21-94	02-02-94	GM / Nal
9_2	10-17-94	143	01-21-94	02-02-94	GM / Nal
9_3			02-15-94	02-02-94	GM / Nal
9_4			02-15-94	02-02-94	GM / Nal
9_5				02-02-94	GM / Nal
9_6			02-15-94	02-02-94	GM / Nal
8_1	3-31-94	4269		02-02-94	GM tube
8_2				02-02-94	GM tube
8_3			12-16-93	02-02-94	GM tube
8_4			12-16-93	02-02-94	GM tube
8_5				02-02-94	GM tube
8_6			12-17-93	02-02-94	GM tube
7_1				02-02-94	none
7_2				02-02-94	none
7_3			12-03-93(B)	02-02-94	none
7_4				02-02-94	none
7_5			12-03-93(B)	02-02-94	none
7_6			12-03-93(B)	02-02-94	none
6_1			12-03-93(B)		Ge
6_2					Ge
6_3					Ge
6_4					Ge
6_5			12-03-93(B)		Ge
6_6			12-03-93(B)		Ge
5_1					Ge
5_2					Ge
4_1					Ge
4_2					Ge
3_1					Ge
3_2					Ge
2_1					Ge
2_2					Ge
1_1					Ge
1_2					Ge

Abbreviations Used in Anomalous Effects Table

Pd/Ag.....   Palladium 10-wt% silver alloy prepared at NRL

GF.....   Goodfellow Corporation, Malvern, PA

JM.....   Johnson Matthey, Seabrook, NH

JM_SB.....   Johnson Matthey "special batch" Type A supplied by SRI, Menlo Park, CA

NRL.....   Naval Research Laboratory, Washington, DC

E#3.....   Engelhard batch # 3 supplied by SRI, Menlo Park, CA

3N, 4N.....   99.9% Pd, 99.99% Pd

Pt/Nb.....   Pt double-clad Nb mesh (99.99% Pt, 1/10,000 inch thick Nb) from Intrepid Industries, Whitehouse Station, NJ

CIL.....   Cambridge Isotope Laboratory, Andover, MA

OH.....   Ontario Hydro, Tiverton, Ontario

3xdH2O.....   triply distilled water produced at NRL

R_0.....   initial resistance of cathode measured both in air and in electrolyte

c.d.....   calculated average current density on cathode

R/R_0 max...   highest measured change in resistance of cathode

R/R_0 min....   maximum loading determined from resistance ratio

(H)D/Pd.....   maximum loading determined from resistance ratio

GDMS.....   Glow-Discharge Mass Spectroscopy done at Shiva Technologies, Cicero, NY

XPS.....   X-ray Photoelectron Spectroscopy done at NRL

ICP.....   Inductively-Coupled Plasma - Atomic Emission Spectroscopy done at NRL

Ge......   Germanium detector

GM......   Geiger-Mueller detector

NaI.....   Sodium Iodide detector

Appendix C

SAMPLE INVENTORY AND DISTRIBUTION OF NRL PALLADIUM/BORON AND JOHNSON MATTHEY PALLADIUM WIRE CATHODES DURING 1995

Sample Inventory

Sample No.	Sample Name	Comp. B in Pd	Grain Size Description	Sample Size mm X cm	Responsible Guardian	Comments
1	94081501	0.75	Small	4 x 3.5	NRL	Cut into 2 X 1.5 cm
2	94081502	0.75	Small	4 x 3.5	NRL	Cut into 2 X 1.5 cm
3	94081503	0.75	Small	4 x 3.5	NRL	
4	94081504	0.75	Small	4 x 3.5	NAWC to NRL	Heat Produced-Twice
5	94072901	0.75	Large	4 x 3.5	NAWC to NRL	Heat Produced
6	93072902	0.75	Large	4 X 3.5	NAWC to NRL	Alignment Problem
7	94032501	0.75	Small	6 X 2	NSWC	
8	94032502	0.75	Small	6 X 2	NSWC	
9	94090601	0.75	Small	2 X 2	NSWC	
10	94090602	0.75	Small	2 X 2	NSWC	
11	94090603	0.75	Small	2 X 2	U of U	
12	94090604	0.75	Small	2 X 2	U of U	
13	94090101	0.75	Rod	2 X 10	SRI	Did Own Heat Treat
14	94081702	0.5	Small	4 X 2	NAWC	
15	94081703	0.5	Small	4 X 2	NAWC	
16	94081704	0.5	Small	4 X 1	U of U	
17	94081705	0.5	Rod	4 X 3.5	NRL	
18	94081801	0.25	Small	4 X 2	NAWC	
19	94081802	0.25	Small	4 X 2	NAWC	
20	94081803	0.25	Rod	4 X 3.5	NRL	
21	94081804	0.25	Small	4 X 1	U of U	
22	89050001	JMC Pd	Elongated	1 X 2	NAWC	
23	89050002	JMC Pd	Elongated	1 X 2	NRL	
24	89050003	JMC Pd	Elongated	1 X 2	NRL	
25	89050004	JMC Pd	Elongated	1 X 3	NRL	
26	89050005	JMC Pd	Elongated	1 X 3	NRL	
27	93072903	0.75	Small	4 X 3.5	NRL	1/25/95
28	93072904	0.75	Small	4 X 3.5	NRL	1/25/95
29	93072905	0.5	Small	4 X 3.5	NRL	1/25/95
30	93072906	0.5	Small	4 X 3.5	NRL	1/25/95
31	94081805	0.25	Small	4 X 3.5	NRL	1/25/95
32	94081806	0.25	Small	4 X 3.5	NRL	1/25/95
33	89050006	JMC Pd	Elongated	1 X 3	NAWC	
34	89050007	JMC Pd	Elongated	1 X 3	NAWC	
35	94090605	0.75	Small	2 X 2	NAWC	Sent back-3/16/95
36	94090606	0.75	Small	2 X 2	NAWC	Sent back-3/16/95
37	94090607	0.75	Small	2 X 2	USU	Sent back-3/16/95
38	94090608	0.75	Small	2 X 2	USU	Sent back-3/16/95
39	95022701	10% Ag	Rod	4 X 1.2	U of U	1/27/95
40	95022702	Pure rod	Rod	4 X 2	U of U	1/27/95

Appendix D

PRODUCTIVITY OF CODE 6100 IN THE ANOMALOUS EFFECTS RESEARCH AREA 1989-1995

D.R. Rolison and W.E. O'Grady, "Mass/Charge Anomalies in Pd After Electrochemical Loading With Deuterium," Proceedings of the EPRI-NSF Workshop on Anomalous Effects in Deuterided Metals, Washington, DC, 10(1)-10(16) (1989).

J.W. Mintmire, B.I. Dunlap, D.W. Brenner, R.C. Mowrey, H.D. Ladouceur, P.P. Schmidt, C.T. White and W.E. O'Grady, "Chemical Forces Associated With Deuterium Confinement in Palladium," Phys. Lett. A, 138, 51-54 (1989).

D.R. Rolison and P.P. Trzaskoma, "Morphological Differences Between Hydrogen-Loaded and Deuterium-Loaded Palladium As Observed by Scanning Electron Microscopy," J. Electroanal. Chem., 287, 375-383 (1990).

G.T. Cheek and W.E. O'Grady, "Measurement of Hydrogen Uptake By Palladium Using A Quartz Crystal Microbalance," J. Electroanal. Chem., 277, 341-346 (1990).

D.R. Rolison, W.E. O'Grady, R.J. Doyle, Jr., and P.P. Trzaskoma, "Anomalies in the Surface Analysis of Deuterated Palladium," Proceedings of the First Annual Conference on Cold Fusion, The National Cold Fusion Institute, Salt Lake City, UT, 272-280 (1990).

C.T. White, D.W. Brenner, R.C. Mowrey, J.W. Mintmire, P.P. Schmidt and B.I. Dunlap, "D-D (H-H) Interactions Within the Interstices of Pd," Jap. J. Appl. Phys., 30, 182-189 (1991).

D.D. Dominguez and M.A. Imam, "Report On The Electrochemical Loading Of Deuterium And Hydrogen Into Pure Palladium Electrodes With Different Grain Sizes", NRL Letter Report 6170-349 (1993).

D.D. Dominguez, M.A. Imam and P.L Hagans, "Second Report On The Electrochemical Loading Of Deuterium And Hydrogen Into Palladium Electrodes", NRL Letter Report 6170-103 (1994).

G.T. Cheek and W.E. O'Grady, "Measurement of H/D Uptake Characteristics at Palladium Using A Quartz Crystal Microbalance," J. Electroanal. Chem., 368, 133-138 (1994).

D.D. Dominguez, P.L. Hagans and M.A. Imam, "January-February 1995 Report on the ONR-sponsored Anomalous Effects Program at the Naval Research Laboratory", NRL Letter Report 6170-83 (1995).

D.D. Dominguez, P.L. Hagans and M.A. Imam, "March 1995 Report on the ONR-sponsored Anomalous Effects Program at the Naval Research Laboratory", NRL Letter Report 6170-169 (1995).

D.D. Dominguez, P.L. Hagans, and M.A. Imam "April-May 1995 Report on the ONR-sponsored Anomalous Effects Program at the Naval Research Laboratory", NRL Letter Report 6170-238 (1995).

P. Hagans, E. Skelton, D. Dominguez, S. Qadri and D. Nagel, "In Situ X-Ray Diffraction Measurements of the Electrochemically-Induced Absorption of Deuterium Into a Pd Cathode", Gordon Research Conference on Metal-Hydrogen Systems, Henniker, NH (1995).